

Genome sequence of *Gossypium anomalum* facilitates interspecific introgression breeding

Zhenzhen Xu^{1,5}, Jiedan Chen^{2,5}, Shan Meng^{1,5}, Peng Xu¹, Caijiao Zhai¹, Fang Huang¹, Qi Guo¹, Liang Zhao¹, Yonggang Quan³, Yixin Shangguan¹, Zhuang Meng⁴, Tian Wen³, Ya Zhang⁴, Xianggui Zhang¹, Jun Zhao¹, Jianwen Xu¹, Jianguang Liu¹, Jin Gao¹, Wanchao Ni¹, Xianglong Chen¹, Wei Ji^{1,4}, Nanyi Wang¹, Xiaoxi Lu^{1,4}, Shihong Wang³, Kai Wang^{4,*}, Tianzhen Zhang^{2,*} and Xinlian Shen^{1,*}

¹Key Laboratory of Cotton and Rapeseed (Nanjing), Ministry of Agriculture and Rural Affairs, the Institute of Industrial Crops, Jiangsu Academy of Agricultural Sciences, Nanjing, China

²Institute of Crop Science, Plant Precision Breeding Academy, Zhejiang Provincial Key Laboratory of Crop Genetic Resources, College of Agriculture and Biotechnology, Zhejiang University, Hangzhou, China

³JOIN HOPE SEEDS Co., Ltd., Changji, China

⁴Key Laboratory of Genetics, Breeding and Multiple Utilization of Crops (MOE), Fujian Agriculture and Forestry University, Fuzhou, China

⁵These authors contributed equally to this article.

*Correspondence: Kai Wang (kwang5@126.com), Tianzhen Zhang (cotton@zju.edu.cn), Xinlian Shen (xlshen68@126.com)

<https://doi.org/10.1016/j.xplc.2022.100350>

ABSTRACT

Crop wild relatives are an important reservoir of natural biodiversity. However, incorporating wild genetic diversity into breeding programs is often hampered by reproductive barriers and a lack of accurate genomic information. We assembled a high-quality, accurately centromere-anchored genome of *Gossypium anomalum*, a stress-tolerant wild cotton species. We provided a strategy to discover and transfer agronomically valuable genes from wild diploid species to tetraploid cotton cultivars. With a (*Gossypium hirsutum* × *G. anomalum*)² hexaploid as a bridge parent, we developed a set of 74 diploid chromosome segment substitution lines (CSSLs) of the wild cotton species *G. anomalum* in the *G. hirsutum* background. This set of CSSLs included 70 homozygous substitutions and four heterozygous substitutions, and it collectively contained about 72.22% of the *G. anomalum* genome. Twenty-four quantitative trait loci associated with plant height, yield, and fiber qualities were detected on 15 substitution segments. Integrating the reference genome with agronomic trait evaluation of the CSSLs enabled location and cloning of two *G. anomalum* genes that encode peroxiredoxin and putative callose synthase 8, respectively, conferring drought tolerance and improving fiber strength. We have demonstrated the power of a high-quality wild-species reference genome for identifying agronomically valuable alleles to facilitate interspecific introgression breeding in crops.

Keywords: wild diploid species, *Gossypium anomalum*, genome, chromosome segment substitution lines, drought tolerance, fiber strength

Xu Z., Chen J., Meng S., Xu P., Zhai C., Huang F., Guo Q., Zhao L., Quan Y., Shangguan Y., Meng Z., Wen T., Zhang Y., Zhang X., Zhao J., Xu J., Liu J., Gao J., Ni W., Chen X., Ji W., Wang N., Lu X., Wang S., Wang K., Zhang T., and Shen X. (2022). Genome sequence of *Gossypium anomalum* facilitates interspecific introgression breeding. *Plant Comm.* **3**, 100350.

INTRODUCTION

The world is expected to reach a projected population of 9.8 billion in 2050 and 11.2 billion in 2100 (www.un.org), but increases in crop yields are not keeping pace with the concomitant growing demand. The narrow genetic base of modern crops has resulted in a yield plateau from crop breeding (Tanksley and McCouch, 1997). Crop wild relatives represent both raw material for breeding and a valuable source of diversity that can

be used to improve the adaptation and agricultural performance of modern crop cultivars. However, the key challenge in using wild diversity is overcoming inherent difficulties in distant hybridization such as cross-incompatibility

Published by the Plant Communications Shanghai Editorial Office in association with Cell Press, an imprint of Elsevier Inc., on behalf of CSPB and CEMPS, CAS.

Category	<i>G. anomalum</i>	<i>G. anomalum</i> (Grover et al., 2021)
Sequenced genome size (bp)	1 208 248 306	1 193 340 424
Anchored chromosome size (bp)	1 198 670 087	1 191 544 213
Percentage of anchoring (%)	99.21	99.85
Contig N50 (Mb)	7.78	10.8
Scaffold N50 (bp)	99 188 525	97 682 888
GC content (%)	34.25	34.27
Complete BUSCOs (%)	99.01	97.1
Number of annotated genes	42 752	37 830
Percentage of TEs (%)	62.59	47.90

Table 1. Summary of the final genome assembly and annotation for *G. anomalum*

and the sterility of F_1 hybrids (Zhang and Batley, 2020). Another obstacle is the dual lack of efficient introgression strategies and genomic information, which greatly hinders the wide use of wild species in breeding programs. Genome assemblies are expected to provide increased opportunities for revealing wild-species-derived genetic variation (Bredeson et al., 2016) and introducing disease resistance (Szymanski et al., 2020; Wang et al., 2020), plant architecture for high yield (Stein et al., 2018; Tian et al., 2019; Mamidi et al., 2020), and quality (Szymanski et al., 2020) into cultivated varieties. It is now possible to rapidly discover and clone agronomic genes from crop wild relatives and engineer them into domesticated varieties with the help of their reference genome. Therefore, wild relatives of modern crops can be a rich resource to mine for useful variants lost during domestication (Stein et al., 2018; Hake and Richardson, 2019).

Gossypium anomalum (B_1B_1 , $2n = 2x = 26$), a stress-tolerant diploid wild *Gossypium* species, grows widely in arid to extremely arid parts of the southern Sahara, from the Sudan to the upper reaches of the Baraka River valley in Eritrea (Silow, 1941). It offers a rich source of breeding potential for desirable traits such as good fiber quality, immunity to certain bacterial diseases, resistance to insect pests, tolerance of water deficit, and cytoplasmic male sterility (Mehetre, 2010; Newaskar et al., 2013). Here, we assembled a high-quality, accurately centromere-anchored genome of *G. anomalum* and developed a set of 74 chromosome segment substitution lines (CSSLs) of *G. anomalum* in the *G. hirsutum* background. This genome resource enabled the discovery of genes for drought tolerance and high fiber quality (Supplemental Figure 1). This wild-species genome assembly and CSSL development will aid our understanding of the extent of hybridization between wild and domesticated populations and of wild relative diversity, and it will allow the identification of genomic regions for additional introgression breeding to improve domesticated cotton.

RESULTS

Assembly, annotation, and evolution of the *G. anomalum* genome

We generated 82.68 Gb ($\sim 64\times$) of high-quality long reads using the PacBio SMART platform (Supplemental Table 1). After correction using 132.61 Gb ($\sim 103\times$) of Illumina paired-end

data, the PacBio long reads were assembled into 611 contigs that captured 1.20 Gb of the *G. anomalum* genome, 363 of which were too short (total length 9.35 Mb) to be then validated and scaffolded using BioNano optical maps (Supplemental Tables 1–3). A total of 249 816 916 valid high-throughput chromosome conformation capture (Hi-C) reads were used to categorize, order, and orient these scaffolds (Supplemental Figure 2; Supplemental Tables 2 and 4). The final assembly comprised 364 scaffolds (N50 = 99.19 Mb), spanning 1.21 Gb and accounting for $\sim 93.66\%$ of the estimated genome (total size 1.29 Gb based on K-mer distribution analysis and 1.35 Gb by flow-cytometry analysis), 351 of which were short scaffolds (total length 9.58 Mb) and 13 were super-scaffolds representing the complete set of *G. anomalum* pseudo-chromosomes and comprising 99.21% of the total assembled sequence (Table 1, Supplemental Figure 3, and Supplemental Tables 2, 5, and 6).

Significant correlation was observed between the linkage and physical maps (Zhai et al., 2015) (Supplemental Figure 4). The assembly's completeness in genic regions was supported by the identification of 2303 (99.01%) of the 2326 BUSCO groups (Simão et al., 2015) and 242 (97.58%) of the 248 core eukaryotic genes in the CEGMA v2.5 database (Parra et al., 2007) (Supplemental Tables 7 and 8). Evaluation of assembly continuity on the basis of repeat sequences yielded a long terminal repeat (LTR) Assembly Index (LAI) value (Ou et al., 2018) of 15.71. The Illumina short-read data and transcripts derived from RNA sequencing (RNA-seq) of various tissues were aligned to the genome with mapping ratios of 97.25% and 88.65% (>500 bp), respectively (Supplemental Tables 9 and 10). Assembly of centromeric regions was evaluated by chromatin immunoprecipitation and sequencing (ChIP-seq) using cotton CenH3 antibodies (Bi et al., 2020) (Supplemental Figure 5A–5C). Unique prominent ChIP-seq peaks were observed from each chromosome assembly, ranging from 0.96 to 1.89 Mb in length (Figure 1A and Supplemental Figure 5D).

A total of 42 752 high-confidence protein-coding gene models were predicted in *G. anomalum* (Figure 1A, Table 1, and Supplemental Table 11), similar to previous predictions of published diploid *Gossypium* species (Paterson et al., 2012; Wang et al., 2012b; Li et al., 2014; Du et al., 2018; Udall et al., 2019a; Cai et al., 2020; Grover et al., 2020; Huang et al., 2020). Approximately 97.29% of the genes identified in *G. anomalum* were annotated in the Swiss-Prot, NR, KEGG, InterPro, Gene

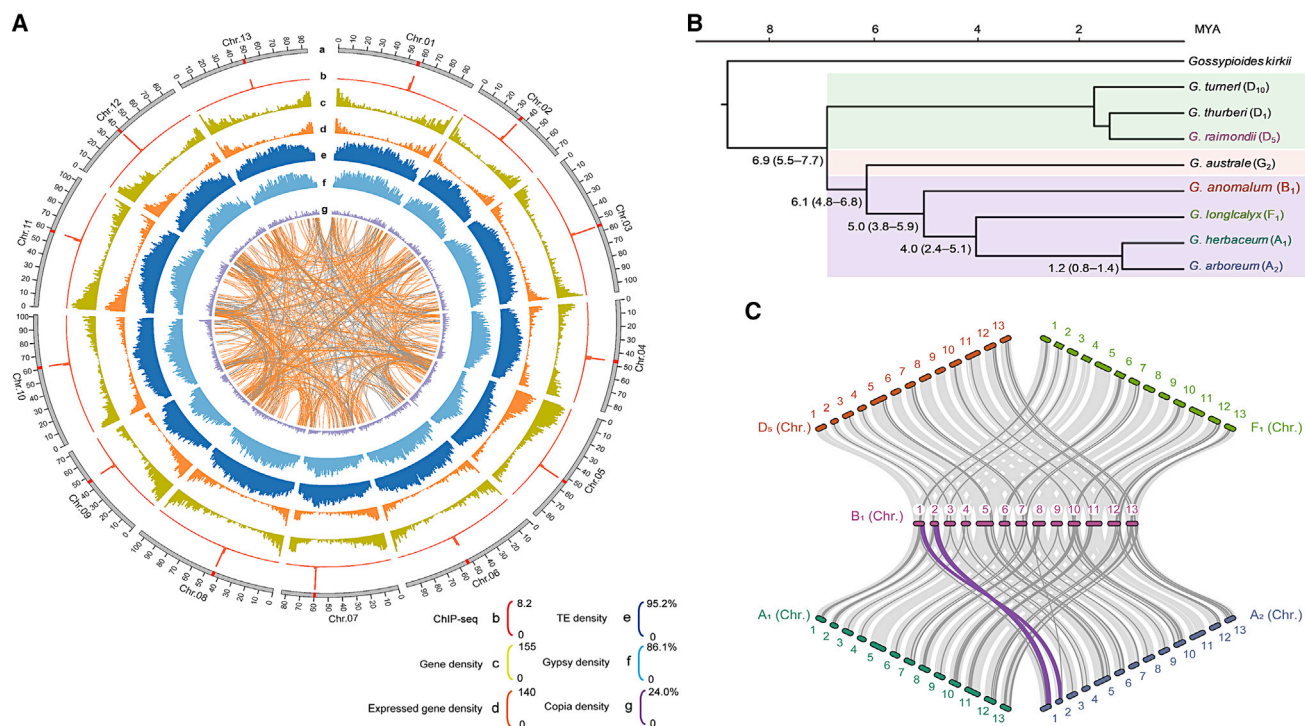


Figure 1. Overview and evolution of the *G. anomalum* genome.

(A) Chromosomal characterization of the *G. anomalum* genome. a, centromere distribution in each chromosome; b, centromere on each chromosome by CenH3 ChIP-seq mapping; c, gene density in each chromosome; d, genes expressed in at least one tissue (root, stem, leaf, and flower); e, f, g, transposable element (TE), *Gypsy*, and *Copia* retrotransposon density, respectively, on each chromosome. The inner lines show syntenic blocks among the 13 chromosomes.

(B) Phylogenetic analysis of eight diploid cotton species and *Gossypioides kirkii*.

(C) Analysis of synteny among diploid cotton genomes. Light gray indicates syntenic regions, dark gray indicates inversions, and purple indicates translocations.

Ontology (GO), or Pfam database (Supplemental Table 12). In addition, 262 microRNAs (miRNAs), 1085 tRNAs, 774 rRNAs, and 6064 small nuclear RNAs (snRNAs) were predicted in *G. anomalum* (Supplemental Table 13). Transposable elements (TEs) comprising a total of 756.28 Mb accounted for 62.59% of the total genome (Figure 1A, Table 1, and Supplemental Table 14). Compared with the published *G. anomalum* genome (Grover et al., 2021), our assembled genome had a little larger genome size and scaffold N50, more annotated genes, a larger percentage of TEs, slightly higher complete BUSCO ratio, and 13 anchored centromeres but a similar anchoring percentage, GC content, and CEGMA ratio, a lower contig N50, and more contigs (Table 1, Supplemental Figure 5, and Supplemental Tables 6–8).

From the molecular phylogenetic tree, *G. anomalum* and its close relatives *G. longicalyx* (F₁) (Grover et al., 2020), *G. herbaceum* (A₁) (Huang et al., 2020), and *G. arboreum* (A₂) (Du et al., 2018) were estimated to have diverged ~5.0 (3.8–5.9) million years ago (MYA); likewise, the divergence time for *G. anomalum* and *G. australe* (G₂) (Cai et al., 2020) was determined to be ~6.1 (4.8–6.8) MYA. In addition, their common ancestor diverged from *G. turneri* (D₁₀) (Udall et al., 2019a), *G. thurberi* (D₁) (Grover et al., 2019), and *G. raimondii* (D₅) (Udall et al., 2019a) at around ~6.9 (5.5–7.7) MYA (Figure 1B). The LTR activity of *G. anomalum* increased

continuously from 8.0 MYA until about 0.5 MYA, and it apparently had higher LTR retrotransposition activity than *G. raimondii* (D₅) (Udall et al., 2019a) but lower activity than *G. herbaceum* (A₁) (Huang et al., 2020), *G. arboreum* (A₂) (Du et al., 2018), and *G. australe* (G₂) (Cai et al., 2020) (Supplemental Figure 6). This finding is consistent with the species' different genome sizes (Hawkins et al., 2006).

In one-to-one matching of syntenic blocks, approximately 86.88% of the *G. anomalum* genome matched with 89.99% of the *G. raimondii* (D₅) genome (Udall et al., 2019a), 89.51% with 87.21% of *G. longicalyx* (F₁) (Grover et al., 2020), 80.41% with 72.11% of *G. herbaceum* (A₁) (Huang et al., 2020), 77.42% with 69.49% of *G. arboreum* (A₂) (Du et al., 2018), and 65.21% with 64.63% of *G. australe* (G₂) (Cai et al., 2020) (Figure 1C and Supplemental Figure 7). These results suggest that the overall collinearities of *G. anomalum* with *G. raimondii* (D₅) and *G. longicalyx* (F₁) are more conserved than those with other species. There were at least 13 inversion events spanning a total of 85.65 Mb that occurred across nine chromosomes (Chr.02–05, 07, and 10–13) between *G. anomalum* and *G. raimondii* (D₅) (Udall et al., 2019a), (Figure 1C and Supplemental Table 15). A much greater degree of chromosomal rearrangement, 129.78 Mb, 184.77 Mb, 153.10 Mb, and 146.49 Mb, was detected between *G. anomalum* and *G. longicalyx* (F₁) (Grover et al., 2020), *G. herbaceum* (A₁) (Huang et al., 2020), *G.*

arborescens (A_2) (Du et al., 2018), and *G. australe* (G_2) (Cai et al., 2020), respectively (Figure 1C, Supplemental Figure 7, and Supplemental Table 15).

Development of the CSSL population

To transfer valuable genes that control important agronomic traits from *G. anomalum* into *G. hirsutum*, a fertile hexaploid hybrid (AADDDB)₁ was successfully developed by first crossing *G. hirsutum* cv. 86-1 × *G. anomalum* and then inducing chromosome doubling (Zhang et al., 2014). This hexaploid was further backcrossed with *G. hirsutum* cv. Su8289 to develop the CSSL population (Supplemental Figure 8). The major problem in developing a cotton wild relative CSSL population is the selection of recombinants, which occur at low frequency. In the BC₂F₁ segregation generation, 50 recombination types from 357 recombination events were identified among 384 BC₂F₁ individuals, and the recombination events occurred only between *G. anomalum* and the A_t genome of *G. hirsutum* (Zhai et al., 2015). In the present study, only 36 recombination types produced viable BC₃F₁ seeds. To recover any of the missing donor segments and obtain as many recombination types as possible, alien addition lines of 13 *G. anomalum* chromosomes were also backcrossed to Su8289 in the BC₂F₁ and BC₃F₁ generations. Marker-assisted selection (MAS) was conducted in each proceeding generation (Supplemental Table 16). A summary of population sizes during five successive generations during the establishment of the CSSL population is provided in Supplemental Table 17.

In the BC₃F₁ generation, 40 recombination types were obtained from 4331 BC₃F₁ individuals. Compared with BC₂F₁, nine new recombination types were identified on five chromosomes, and five recombination types were lost during the backcross process on the other five chromosomes (Supplemental Table 18). In the BC₄F₁ generation, 56 recombination types were obtained from 8540 BC₄F₁ individuals. Compared with BC₃F₁, 18 new recombination types were detected on eight chromosomes, and two recombination types were lost on Chr.04 (Supplemental Table 18). In the BC₄F₂ generation, 51 recombination types, including 45 homozygous genotypes and six heterozygous genotypes, were obtained from 4543 BC₄F₂ individuals. Compared with BC₄F₁, five new recombination types were detected on Chr.06, Chr.09, and Chr.11 (Supplemental Table 18), and 10 recombination types on 6 chromosomes were lost in BC₄F₂. We assumed that some homozygous genotypes had low gamete or zygote viability. In the BC₄F₃ generation, homozygous candidate substitution lines were investigated again to confirm the homozygous exotic genotype of each line; in the BC₄F₃ and BC₄F₄ generations, heterozygous substitution lines were further analyzed to identify homozygous substitution segments. A total of 53 recombination types, including 47 homozygous substitutions and 6 heterozygous substitutions, were obtained from 1533 BC₄F₃ individuals. Compared with BC₄F₂, two new recombination types were detected on Chr.05 and Chr.11 (Supplemental Table 18).

In the BC₄F₄ generation, all recombination types were subjected to a whole-genome survey with 230 markers evenly distributed across the *G. anomalum* genome. A total of 74 CSSLs were obtained, including 70 homozygous substitutions and four heterozygous substitutions. These four heterozygous CSSLs remain in the

final CSSL set, as they are expected to be of further use in fine mapping significant quantitative trait locus (QTL) regions. Genome-wide scanning enabled us to detect an additional 21 substitution lines, most of which carry more than one introgression segment in addition to the target introgression (Supplemental Table 18).

Among the 74 CSSLs numbered from CSSL1 to CSSL74, 41, 26, and 7 CSSLs had one, two, and three substitution segments of the donor parents, respectively (Supplemental Table 19). CSSL24 on Chr.03 and Chr.08, CSSL37 on Chr.05, CSSL43 on Chr.06, and CSSL51 on Chr.09 still carried heterozygous substitution segments even when they were selfed two or three times. The cover length of substitution segments among different CSSLs ranged from 4.75 cM (CSSL17) to 267.45 cM (CSSL43), with an average of 72.09 cM. The total cover length was 1668.69 cM, and the coverage rate was about 72.22% of the *G. anomalum* genome (Figure 2A and Supplemental Table 20). Uneven distribution among the 13 chromosomes was observed: Chr.01 and Chr.11 of *G. anomalum* were completely represented by 20 and 28 different CSSLs, respectively, whereas Chr.03 and Chr.07 were only represented by one CSSL, and Chr.10 had the lowest coverage of only 17.89%. The distribution of all the substitution segments among the CSSL population is shown in Figure 2A and 2B.

To verify the accuracy of introgression segment identifications using simple sequence repeat (SSR) markers, six CSSLs were resequenced and verified for the presence of corresponding *G. anomalum* segments (Figure 2C and 2D, Supplemental Figure 9, and Supplemental Table 21). Four of these six CSSLs (CSSL44, CSSL50, CSSL56, and CSSL63) were further confirmed by fluorescence *in situ* hybridization (FISH) using *G. anomalum*-specific oligo-FISH probes. FISH signals from corresponding *G. anomalum* chromosomes were detected, and signal coverage was consistent with the results of SSR and resequencing (Figure 2E and Supplemental Figure 10).

Agronomically valuable QTLs identified in *G. anomalum*

A total of nine quantitative traits, including plant height (PH), three yield traits (boll seed index [SI], boll weight [BW], and lint percentage [LP]), and five fiber quality traits (fiber length [FL], fiber strength [FS], micronaire [MIC], fiber uniformity [FU], and fiber elongation [FE]), were investigated in four environments (Supplemental Table 22). The genetic coefficient of variation (GCV) of the nine traits ranged from 0.60% (FU in E3) to 17.21% (BW in E4), indicating that various degrees of genetic variation existed in all of the traits. The relatively low GCVs were related to the relatively high genetic background recovery rate of Su8289. The heritability of traits ranged from 35.91% (FE in Joint) to 98.49% (MIC in E4). The mean values of most traits were similar to those of the recurrent parent, indicating that transgressive segregation occurred in both positive and negative directions in the CSSL population. Therefore, CSSLs with significant differences from Su8289 could be found at both sides for most traits in Supplemental Figure 11, and these CSSLs might carry elite genes from *G. anomalum*.

Twenty-four QTLs were detected on 15 substitution segments of six chromosomes (Supplemental Table 23). The total cover length

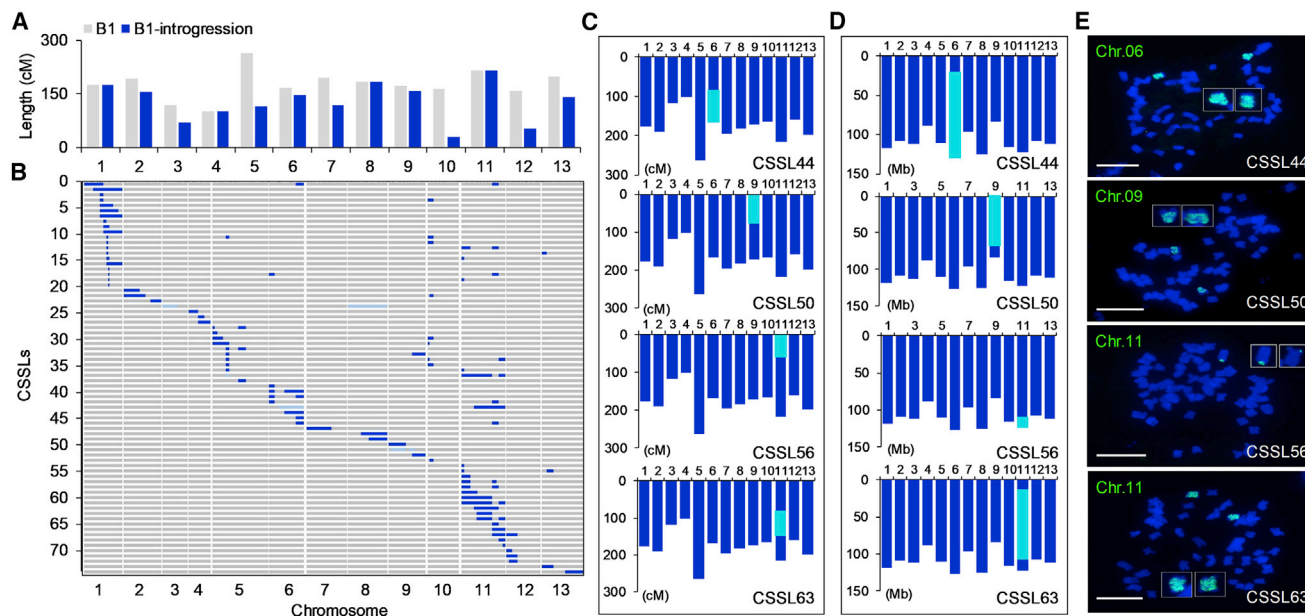


Figure 2. Characterization of the CSSL population derived from *G. anomalum* and introgression segments identified in CSSL44, CSSL50, CSSL56, and CSSL63 based on SSR markers, resequencing, and FISH experiments.

(A) Genome coverage of substitution segments in the CSSL population.

(B) Chromosomal distribution of introgression segments identified from the 74 CSSLs and genome coverage of substitution segments in the CSSL population. Gray represents the genotype of the recurrent parent Su8289, blue represents the genotype of the donor parent *G. anomalum*, and light blue represents heterozygous regions. On the vertical axis are the 74 CSSLs, arranged from top to bottom, and on the horizontal axis are the 13 chromosomes of the *G. hirsutum* A₁ genome, arranged from left to right.

(C–E) Introgression segments identified by SSR markers **(C)**, resequencing **(D)**, and FISH experiments **(E)**. Introgression segments are indicated by light-blue boxes. Scale bars, 10 μ m.

of the 15 segments was 402.25 cM, accounting for 24.11% of the total cover length of all the substitution segments. Of these 24 QTLs, four were associated with PH, seven with yield traits (four with BW and three with LP), and 13 with fiber quality traits (three with FL, three with FS, two with MIC, two with FU, and three with FE) (Supplemental Table 23). Some QTLs were located on the same substituted segments; for example, four different QTLs (*qBW11-1*, *qLP11-2*, *qFL11*, and *qFU11*) all mapped to the interval NAU3234–NAU2877 on Chr.11, and two QTLs (*qBW01* and *qFL01-2*) were both located on the same interval as the linked marker JAAS0392 on Chr.01 (Supplemental Table 23). Of the 24 QTLs, 13 for 7 traits (PH, LP, FL, FS, MIC, FU, and FE) were identified as valuable loci involving 12 different substitution segments on Chr.01, Chr.04, Chr.05, and Chr.11. Two valuable QTLs, *qFL01-1* and *qFE01*, were located on a single *G. anomalum* segment on Chr.01, indicating that this segment could increase FL and elongation simultaneously (Supplemental Table 23).

Causal gene conferring drought tolerance in *G. anomalum*

Through the transfer of genomic fragments associated with distinct agronomic traits into cultivars in CSSLs, it is possible to rapidly discover and clone agronomic genes from crop wild relatives that have been sequenced. *G. anomalum* is distinctly characterized by its extreme drought tolerance due to adaptation to an extremely arid environment (Figure 3A); accordingly, we attempted to identify *G. ANOMALUM DROUGHT TOLERANCE*

(*GADT*) gene(s) from the CSSLs by combining substitution mapping, expression profiling analyses, and functional validation by virus-induced gene silencing (VIGS). Drought tolerance of all CSSLs was assessed using 20% polyethylene glycol (PEG) treatment, and three introgression lines (CSSL29, CSSL30, and CSSL31) showed tolerance to PEG stress at the seedling stage (Figure 3B; Supplemental Figure 12A and 12B). Interestingly, these three CSSLs carried overlapping substitution segments on Chr.05 anchored by SSR markers JAAS6365 and JAAS5604. Moreover, another introgression line, CSSL28, harbored a *G. anomalum* segment anchored by JAAS6365–JAAS0803 that also overlapped with the interval anchored by JAAS6365 and JAAS5604. PEG treatment demonstrated that CSSL28 was drought sensitive (Supplemental Figure 12C). These results indicate that one or more genes involved in drought tolerance were located in the JAAS0803–JAAS5604 interval (Chr.05: 1 415 831 bp to 2 878 211 bp) (Supplemental Figure 12D). This interval of the *G. anomalum* genome contained 192 genes.

To exploit genes in the JAAS0803–JAAS5604 interval involved in drought tolerance, a global analysis of transcriptome dynamics was performed to compare CSSL29 and its recurrent parent Su8289, both grown under 20% PEG stress conditions (Supplemental Table 24). Twenty genes in the interval were upregulated in CSSL29 relative to Su8289 under PEG stress at any time point (6, 12, 24, and 72 h) (Supplemental Table 25). Upon integrating these upregulated genes with functional annotations of their *Arabidopsis* orthologs, nine genes were validated by qRT–PCR and their functional relevance further

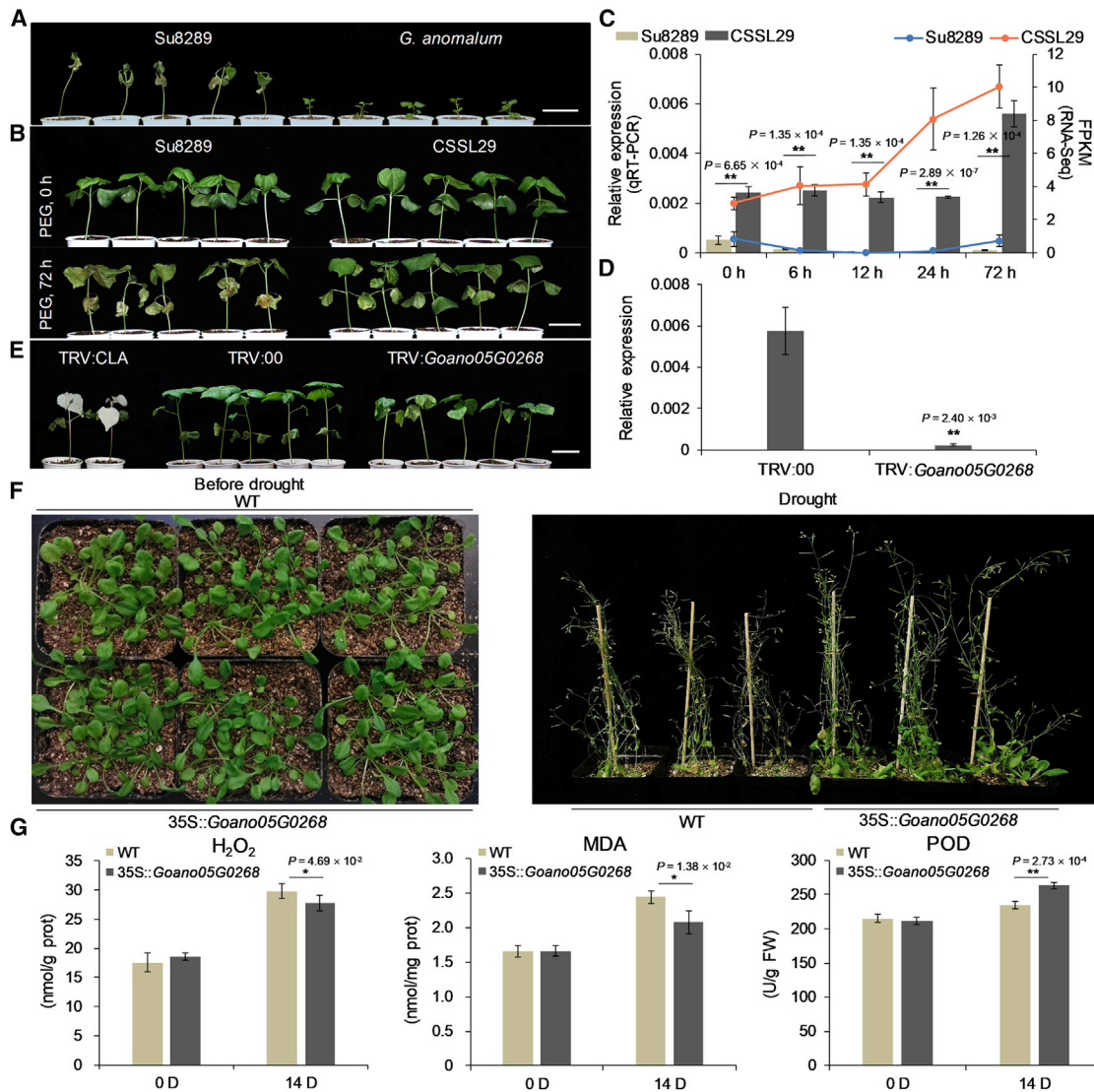


Figure 3. Drought tolerance of CSSL29, functional verification of *Goano05G0268* by VIGS in CSSL29, and ectopic expression in *Arabidopsis*.

(A) Phenotypic comparison of Su8289 and *G. anomalum* in response to water deficit. Scale bar, 5 cm.
 (B) Phenotypic comparison of Su8289 and CSSL29 in response to drought stress using 20% PEG treatment. Photographs were taken at 0 and 72 h after PEG treatment. Scale bar, 5 cm.
 (C) Expression level of *Goano05G0268* in Su8289 and CSSL29 under PEG stress at 0, 6, 12, 24, and 72 h. The left y axis shows the relative expression according to qRT-PCR, and the right y axis shows the FPKM (fragments per kilobase per million mapped reads) value obtained from RNA-seq data. $**P < 0.01$, Student's *t*-test.
 (D) Transcript levels of *Goano05G0268* in leaves from CSSL29 plants infected with pTRV2 and pTRV2-*Goano05G0268* under PEG stress at 72 h, evaluated by qRT-PCR. $**P < 0.01$, Student's *t*-test.
 (E) Phenotypes of CSSL29 plants infected with pTRV2, pTRV2-*Goano05G0268*, and pTRV2-*CLA*. Scale bar, 5 cm.
 (F) Phenotypic comparison of *Arabidopsis* EE and WT seedlings after 25 days of drought stress.
 (G) Endogenous H_2O_2 content, MDA content, and POD activity of *Arabidopsis* EE and WT lines before and after 14 days of drought stress. $**P < 0.01$, Student's *t*-test.

confirmed by VIGS (Figure 3C, 3D, and 3E; Supplemental Figures 13 and 14; Supplemental Tables 26 and 27). The expression level of nine genes in VIGS-silenced plants at 72 h of PEG stress was much lower than that in control plants (Figure 3D; Supplemental Figure 14). Plants in which the peroxiredoxin gene *Goano05G0268* was silenced were more sensitive to PEG stress at 72 h than TRV:00 plants, whereas plants in which any of the other eight genes were silenced

showed no significant sensitivity to PEG stress (Figure 3E; Supplemental Figure 14). Hydrogen peroxide (H_2O_2) and malondialdehyde (MDA) content and peroxidase (POD) activity were measured in TRV:00 and TRV:*Goano05G0268* cotton plants under PEG stress at 0 and 72 h. *Goano05G0268*-silenced plants had higher ($P < 0.01$) H_2O_2 and MDA content but lower ($P < 0.01$) POD activity than TRV:00 plants under PEG stress at 72 h (Supplemental Figure 15).

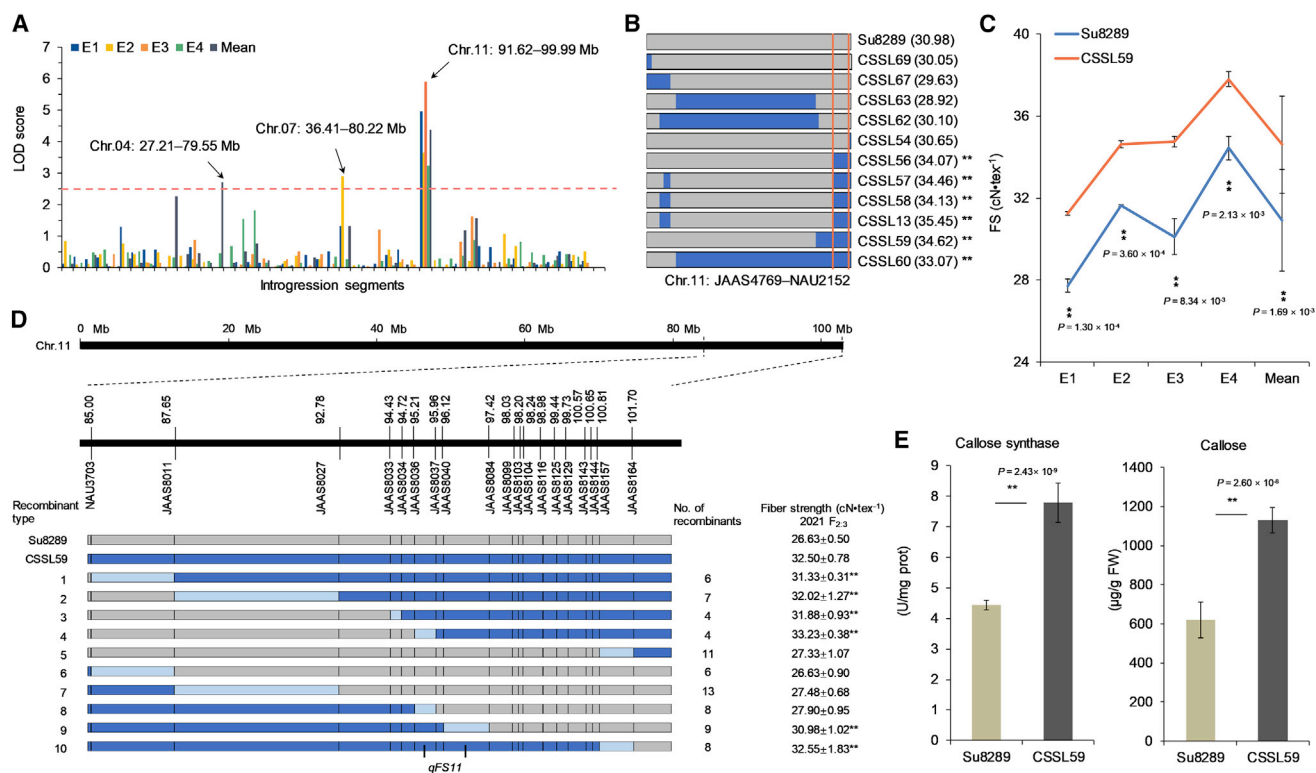


Figure 4. Identification of valuable substitution segment associated with fiber strength and characterization of the candidate gene on Chr.11 of *G. anomalum*.

(A) QTL distribution for the fiber strength trait in multiple environments. The x axis represents all introgression segments and the y axis the logarithm of odds (LOD) score; the dashed line indicates the threshold value of 2.5, and the physical locations of QTLs are denoted by arrows.

(B) Graphical genotypes of SSR interval for fiber strength on Chr.11 and the phenotype of corresponding CSSLs. The orange line indicates the *G. anomalum* locus *qFS11* mapped to the interval of JAAS4769–NAU2152 on Chr.11.

(C) Fiber strength phenotypic values of Su8289 and CSSL59 in multiple environments. ** $P < 0.01$, Student's *t*-test.

(D) Graphical genotypes and fiber strength values of Su8289, CSSL59, and 76 recombinants from the F_{2:3} population. Gray portions represent the genotype of Su8289, blue portions represent the genotype of CSSL59, and light blue represents regions where crossover has occurred. The table on the right indicates mean fiber strength values for the recombinant classes collected from Hainan Island. ** $P < 0.01$, Student's *t*-test.

(E) Callose synthase activity and callose content in fibers from CSSL59 and Su8289 at 20 DPA. ** $P < 0.01$, Student's *t*-test.

Ectopic expression of *Goano05G0268* modulates drought response in *Arabidopsis* (Figure 3F and 3G; Supplemental Figure 16). Three ectopic expression (EE) transgenic lines of *Goano05G0268* grown on Murashige and Skoog (MS) medium with 200 and 250 mM mannitol had longer roots ($P < 0.05$) than wild-type (WT) lines (Supplemental Figure 16B and 16C). These lines had relatively lower ($P < 0.01$) H₂O₂ and MDA content but higher ($P < 0.01$) POD activity than WT lines to modulate drought-tolerant phenotypes (Figure 3F and 3G). *Goano05G0268* encodes a peroxiredoxin protein, which participates in protection against oxidative damage and plays a role in plant responses to drought stress (Rey et al., 2005; Dietz, 2007; Hernández et al., 2012; Marquez-García et al., 2015; AbdElgawad et al., 2020). Therefore, *Goano05G0268* may be involved in drought response and might play an important role in drought-adapted evolution.

The *Goano05G0268* gene in CSSL29 and its orthologous gene *GH_A05G0249* (Hu et al., 2019) (*GhGADT*) in Su8289 were isolated by PCR amplification (Supplemental Table 28). Sequence analysis revealed that the Su8289-derived *GhGADT* contained one deletion (408 bp), three insertions (2549 bp, 159 bp, and 2 bp) in the second intron, and 11 SNPs within exons

1, 2, and 3 (Supplemental Figure 17), leading to the conclusion that this gene likely became pseudogenized in Su8289 over the course of evolution. The *Goano05G0268* gene in *G. anomalum* was also aligned with its orthologs in other allotetraploid cotton species, such as *G. hirsutum* L. acc. TM-1 (Wang et al., 2019), *G. barbadense* L. cv. Hai7124 (Hu et al., 2019), *G. barbadense* L. accession 3-79 (Wang et al., 2019), *G. tomentosum* (Chen et al., 2020), *G. mustelinum* (Chen et al., 2020), and *G. darwinii* (Chen et al., 2020). The results were similar to those of the alignment of *G. anomalum* and Su8289, that is, *Goano05G0268* orthologs in these allotetraploid cotton species contained a ~2500-bp insertion and other small deletions and insertions in the second intron and different numbers of SNPs within exons 1, 2, and 3 (Supplemental Figure 18 and Supplemental Table 29).

Candidate gene for improved fiber strength in *G. anomalum*

Among the two elite QTLs identified as associated with FS, the *G. anomalum* locus *qFS11* mapped to the JAAS4769–NAU2152 interval on Chr.11 was consistently detected across all four

environments (Figure 4A and Supplemental Table 30). Six CSSLs carrying the overlapping segment (CSSL13, CSSL56, CSSL57, CSSL58, CSSL59, and CSSL60) all showed significantly ($P < 0.01$) greater FS values than the recurrent parent Su8289; CSSLs lacking that segment showed no significant difference from Su8289, indicating a tight association between the introgression segment and greater FS (Figure 4B and 4C; Supplemental Figure 19). To mine the *G. ANOMALUM FIBER STRENGTH* (*GAFS*) gene, we performed fine mapping of *qFS11* in an $F_{2:3}$ population constructed from CSSL59 × Su8289 using data collected at Hainan Island in 2021. Substitution mapping narrowed down *qFS11* to the 1.19-Mb interval of JAAS8037–JAAS8040, which contained 49 candidate genes (Figure 4D and Supplemental Table 31). We then conducted a transcriptomic analysis of fibers from CSSL59, CSSL13, and Su8289 at 20 days post anthesis (DPA) (Supplemental Table 32), when the fiber elongates and the secondary cell wall (SCW) thickens. Twelve genes located in the *qFS11* interval JAAS8037–JAAS8040 showed upregulated expression in fibers from CSSL59 and CSSL13 relative to those from Su8289 (Supplemental Table 33).

Of those 12 genes, nine contained probable function-altering variations relative to their homologs in *G. hirsutum*, whether from transcript splicing, frameshift, gain of stop codon, or loss of stop codon (Supplemental Table 34). These nine genes were verified by qRT-PCR (Supplemental Figure 19 and Supplemental Table 35). Among them, one gene, *Goano11G3883* encoding *PUTATIVE CALLOSE SYNTHASE 8 PROTEIN (PCSY8P)*, was significantly upregulated at 20 DPA in CSSL13, CSSL56, CSSL57, CSSL58, CSSL59, and CSSL60, all of which carried the same substituted segment JAAS4769–NAU2152 (Supplemental Figure 20). The orthologous gene *GH_A11G3315* in *G. hirsutum* (Hu et al., 2019) contains two deletions (2 bp and 13 bp) within exon 30 that result in a frameshift (Supplemental Figure 21A). The protein encoded by *GH_A11G3315* has five amino acids deleted from the *Glucan synthase* domain (Supplemental Figure 21B). We amplified the partial sequence of this gene containing structural variation from CSSL59 and Su8289 and confirmed their sequence differences (Supplemental Figure 22 and Supplemental Table 36).

The SCW thickening stage, characterized by the synthesis and accumulation of cellulose, is a key period that determines FS (Meinert and Delmer, 1977; Hsieh et al., 2000; Kim and Triplett, 2001). *PCSY8P* is involved in the biosynthesis of callose ((1 → 3)-β-D-glucan), an intermediate in cellulose biosynthesis (Meier et al., 1981; Brown et al., 1996; Salnikov et al., 2003; Ruan et al., 2004). Callose synthase activity and relative callose content were significantly higher ($P < 0.01$) in CSSL59 than in Su8289 (Figure 4E). Therefore, *Goano11G3883* appears to be a candidate for the *GAFS* gene that improves FS. The *GAFS* gene may have been pseudogenized in the A subgenome chromosome of *G. hirsutum* during evolution.

DISCUSSION

High-quality assembly of a wild-species genome will greatly facilitate interspecific introgression breeding

It is well known that wild relatives of modern crops are rich resources to mine for useful variants lost during domestication (Hake and Richardson, 2019). Obtaining a high-quality reference genome is an essential step in understanding the evolution, origin,

and domestication of wild and cultivated species and enables the best utilization of genetic resources and the improvement of agronomic traits in modern plant breeding (Stein et al., 2018; Mamidi et al., 2020; Szymanski et al., 2020). In this study, we assembled a high-quality genome of *G. anomalum* based on PacBio Illumina, BioNano, and Hi-C technology. The quality of our assembly and the recently published genome of *G. anomalum* (Grover et al., 2021) are comparable, as we used similar approaches (PacBio + Illumina + BioNano + Hi-C for our assembly, PacBio + Hi-C for Grover et al., 2021) for genome sequencing and assembly. The different results may arise from differences in analytical methods and criteria. The two genomes can complement each other in reference and utility value for the cotton community.

During the domestication and improvement of cultivated species, particularly during the formation of allopolyploid species, some agronomic genes lose their function or become defunctionalized because of genome shock; these can be recovered by transferring the original functional gene from a crop wild relative into domesticated stock. However, interspecific hybridization between cultivated species and wild species from the tertiary gene pool is often challenging, hampered by reproductive barriers and a lack of genomic information (Wendel et al., 2010). Here, we have developed a strategy to transfer elite genes from a wild diploid cotton species to tetraploid cultivars by developing CSSLs, performing transcriptome and sequence variation analysis, and identifying causal genes integrated with the reference genome. We report that introgressive *G. anomalum* genes encoding peroxidase and putative callose synthase 8 can confer drought tolerance and improve FS in upland cotton. Such transfers of original functional genes from wild or progenitor species into *G. hirsutum* along with the corresponding agronomic trait, such as FS, will be very important and useful in interspecific introgression breeding to improve yield and quality.

Development of a first set of CSSLs derived from a diploid wild species and their application in cotton breeding

In previous reports, the tetraploid wild species *G. tomentosum* (AADD)₃, *G. mustelinum* (AADD)₄, and *G. darwinii* (AADD)₅, were used as donor parents to create CSSLs (Wang et al., 2012a; Chandhani et al., 2017; Keerio et al., 2018). There are no previous reports on creating a CSSL library with a diploid wild cotton species as a donor parent owing to crossability inhibition and limited recombination between chromosomes of wild and cultivated plants. In this study, a fertile hexaploid hybrid (AADDDB)₁ developed in our previous studies was further backcrossed three times with *G. hirsutum* cv. Su8289 and selfed three times. MAS was applied in every generation. Finally, a set of 74 CSSLs in the *G. hirsutum* background were developed. This *G. anomalum* CSSL population is comparable with those developed for other crop species with regard to the “quality” of introgression lines, e.g., relatively high exotic genome coverage (72.22%) and a high grade of pureness (41 out of 74 lines possess a single exotic introgression segment). These lines will be powerful materials for QTL identification, fine mapping, map-based cloning, and ultimately breeding utilization.

Cotton breeders have long recognized that low-performing wild cotton species can contribute agronomically favorable alleles.

Successful examples of utilizing cotton wild species in cotton-breeding history include the use of *G. harknessii* (D₂₋₂) as the source of cytoplasmic male sterility (Meyer, 1973), the use of *G. thurberi* (D₁) to improve fiber quality (Culp and Harrell, 1973; Culp et al., 1979), and the use of *G. aridum* (D₄) to provide resistance to reniform nematode (Sacks and Robinson, 2009). In this study, agronomically positive QTL alleles from *G. anomalum* were identified for drought tolerance, fiber quality (e.g., FL, FS), and yield traits (LP), despite *G. anomalum* having short seed hairiness. Linkage drag is one of the main factors that affect the utilization of wild species in breeding programs. We observed that exotic chromosome fragments were associated with deleterious effects on some traits such as BW and LP. For example, 28 of 74 CSSLs showed significantly lower BW than the recurrent parent Su8289 (Supplemental Figure 11). Linkage drag between fiber quality and yield traits was observed for *G. anomalum* loci on Chr.01 and Chr.11 (Supplemental Table 23). However, CSSL17 contained a positive FL QTL at a small introgression fragment of Chr.01 and showed no detectable negative effects on BW and LP, indicating that further genetic dissection of the target region could break linkage drag. Disruption of deleterious linkages and reduction of pleiotropic effects could be achieved by fine mapping of target QTL regions or editing negative genes using CRISPR technology.

METHODS

Plant materials

Highly homozygous *G. anomalum* plants were cultivated at Lishui Plant Experiment Station, Jiangsu Academy of Agricultural Sciences (JAAS), China. Young leaves from a single plant were harvested and frozen immediately in liquid nitrogen for extraction of genomic DNA.

PacBio sequencing

An improved cetyltrimethylammonium bromide (CTAB) method was used to extract the genomic DNA of *G. anomalum*. Size selection was carried out on more than 5 µg of sheared and concentrated DNA by the BluePippin system. Approximately 40-kb SMRTbell libraries were prepared according to the protocol released by PacBio. A total of 14 single-molecule, real-time (SMRT) cells were run on the PacBio Sequel system, and 82.75 Gb of polymerase reads were produced.

Illumina sequencing

A total of 1.5 µg of *G. anomalum* genomic DNA was used as input material for sample preparation. Sequencing libraries were generated using the TruSeq Nano DNA HT Sample Preparation Kit (Illumina, USA) following the manufacturer's recommendations; index codes were added in order to attribute sequences to each sample. DNA samples were fragmented by sonication to sizes of 230 bp, 350 bp, and 500 bp, and the fragments were end-polished, A-tailed, and ligated with the full-length adapter for Illumina sequencing with further PCR amplification. PCR products were purified (AMPure XP system), and libraries were analyzed for size distribution and quantification with an Agilent 2100 Bioanalyzer and real-time PCR, respectively. The libraries were sequenced on an Illumina HiSeq platform, producing 46.80 Gb, 41.38 Gb, and 44.92 Gb of raw data, respectively, for each fragment size.

De novo assembly

The *G. anomalum* PacBio data were first corrected by the Fast Alignment and CONsensus (Falcon) sense method (option correctedErrorRate = 0.025). High-quality pre-assembled reads were then used for genome as-

sembly via Falcon using the Overlap-Layout-Consensus algorithm. Quiver software was used to compute the genomic consensus and to call variants relative to the reference. The resulting contigs were then used to map the Illumina short reads with BWA (version 0.7.15-r1140) (Li and Durbin, 2009) and were polished using Pilon (version 1.22) with default parameters (Walker et al., 2014).

Genome assembly improvement with BioNano optical maps

A highly homozygous *G. anomalum* plant was cultivated in a greenhouse at the JAAS. Young leaves were collected after 4 days of dark treatment. High-molecular-weight DNA was isolated and labeled according to the BioNano protocol with the single-stranded nicking endonuclease Nt.BssSI (Lam et al., 2012). After labeling and staining, the complete genome-specific marker library was constructed and loaded onto the Loading Saphyr array. The stretched DNA molecules were imaged on a BioNano Irys system, and the raw image data were converted into bnx files. After filtering on the Label SNR filter (threshold: 3.5–20), molecule length (more than 150 kb), and label density, a total of 291.88 Gb of single-molecule data were produced. High-quality labeled single molecules were pairwise aligned, clustered, and assembled into contigs according to the BioNano assembly pipeline (Lam et al., 2012; Cao et al., 2014), yielding a physical map with a total length of 1.29 Gb. Hybrid scaffolding was performed with the assembled PacBio contigs and BioNano optical maps using BioNano Solve. To detect the best matches and potential reciprocal scaffolding of each dataset, BioNano genome nick-based maps were compared with *in silico* nick maps of the genome sequence. If any sites conflicted between the genome sequence and optical maps, both were broken at those sites and reassembled using Hybrid Scaffold software.

Hi-C library construction and chromosome assembly

Hi-C library construction for *G. anomalum* was performed according to the Hi-C procedure (Servant et al., 2015). The Hi-C library was controlled for quality and sequenced on an Illumina HiSeq X Ten sequencer. After filtering, we obtained 249 816 916 valid read pairs for the high-quality assembly of *G. anomalum*. The 396 assembled scaffolds were separately broken into fragments with an average length of 50 kb, and valid Hi-C read pairs were mapped to these fragments using BWA (Li and Durbin, 2009). Uniquely mapped reads were retained and used for assembly with LACHESIS (Burton et al., 2013). Any two fragments that showed inconsistent connections with information from the raw scaffolds were checked manually, and these corrected scaffolds were then assembled by LACHESIS. Finally, 364 scaffolds with a total length of 1.21 Gb were anchored, and 13 super-scaffolds (99.19%) were oriented to the respective 13 high-quality groups of *G. anomalum*.

The completeness of the genome assembly was evaluated using the Benchmarking Universal Single-Copy Orthologs (BUSCO) dataset (Simão et al., 2015) and the Core Eukaryotic Genes Mapping Approach (CEGMA) version 2.5 with default settings (Parra et al., 2007). The LAI was used to evaluate the continuity of repeat element sequences throughout the assembly (Ou et al., 2018). In addition, assembly accuracy and completeness were also supported by alignment via BLAT of Illumina short-read data and transcripts derived from RNA-seq of different tissues (Kent, 2002).

Identification of centromeric regions by CenH3 ChIP

ChIP experiments were performed according to a published protocol (Nagaki et al., 2004). A total of 47.8 and 22.9 million CenH3 ChIP-seq and genomic control reads (150 bp) were generated, respectively, 17.8 and 2.8 million of which were mapped to unique sites in the *G. anomalum* genome assembly using Bowtie 2. Read density was calculated for each genomic window by dividing the total number of uniquely mapped reads by the total number of mapped nucleotides. The density of ChIP-seq reads in each window was normalized using the density of input reads. CenH3 domains were detected with SICER version 1.1 (Zang et al., 2009) using the following parameters: 200-bp windows, required fold

change (ChIP/control) ≥ 5 and false discovery rate (FDR) < 0.01 , and allowed gaps of 400 bp.

Repeat sequence and non-coding RNA prediction

A *de novo* TE library was first constructed using LTR_FINDER (Xu and Wang, 2007), RepeatScout (Price et al., 2005), and PILER-DF (Edgar and Myers, 2005). TEs were then identified with RepeatMasker (version 4.0.6) (Chen, 2004) run against the *de novo* TE library and the Repbase database (version 20.01) (Jurka et al., 2005). Tandem Repeats Finder was used to search for tandem repeats in the genome (Benson, 1999). The tRNAscan-SE program was used to predict tRNA fragments, and INFERNAL was used against the Rfam database (release 9.1) to identify rRNA, miRNA, and snRNA fragments (Griffiths-Jones et al., 2005). All intact LTR-retrotransposons (LTRs) in cotton genome species were used to calculate the insertion time using the formula $\text{time} = K_s/2r$, where K_s is the synonymous substitutions per synonymous site and r is the rate of nucleotide substitution (which was set to 7×10^{-9}) (Li et al., 2014).

Protein-coding gene prediction

De novo, homology-based, and RNA-seq-based predictions were used to annotate protein-coding genes in the *G. anomalum* genome. *De novo* prediction used the programs AUGUSTUS (version 3.0.2) (Stanke and Waack, 2003), GENSCAN (version 1.0) (Burge and Karlin, 1997), geneid (version 1.3) (Blanco et al., 2007), GlimmerHMM (version 3.0.2) (Majoros et al., 2004), and SNAP (Korf, 2004). For identification by homology, protein sequences from six plant species—*Arabidopsis thaliana* (Arabidopsis Genome Initiative, 2000), *G. arboreum* (CRI) (Du et al., 2018), *G. hirsutum* (NAU) (Zhang et al., 2015), *G. raimondii* (JGI) (Paterson et al., 2012), *Populus trichocarpa* (Tuskan et al., 2006), and *Theobroma cacao* (Argout et al., 2011)—were aligned against the repeat-masked *G. anomalum* genome using tblastn (E-value $\leq 1e-5$). BLAT (Kent, 2002) and GeneWise (version 2.4.1) (Birney et al., 2004) were used to predict gene models based on the aligned sequences. Finally, RNA-seq-based predictions were made on the basis of two methods for assembling the data into unique transcript sequences: mapping the RNA-seq data to the *G. anomalum* genome using TopHat (version 2.0.8) and cufflinks (version 2.1.1), and using Trinity to assemble the RNA-seq data followed by PASA to model the gene structures (Haas et al., 2003). Consensus gene models were generated by merging the *de novo* predictions, protein alignments, and transcript data using EVIDENCEModeler (EVM) (Haas et al., 2008). Finally, the gene models generated by EVM were adjusted using PASA based on the transcript assembly, yielding 42 752 predicted protein-coding genes.

Functional annotation of protein-coding genes was performed according to the best BLAST hit by BLASTP (E-value $\leq 1e-5$) against Swiss-Prot (Boeckmann et al., 2003), Pfam, and NCBI non-redundant (NR) protein databases. Motifs and domains were annotated by searching against InterPro (version 29.0) (Zdobnov and Apweiler, 2001). GO terms (Ashburner et al., 2000) for each gene were obtained from the corresponding InterPro description. Pathways in which the protein-coding genes might be involved were assigned by performing BLAST searches (McGinnis and Madden, 2004) against the KEGG database (release 53) (Kanehisa and Goto, 2000) (E-value $\leq 1e-5$). In all, 41 592 protein-coding genes were annotated, accounting for 96.5% of the predicted genes.

Phylogenetic tree construction and gene synteny analysis

We identified single-copy gene families using the OrthoFinder package based on protein sequences of eight diploid cotton species and *Gossypioideis kirkii* (Udall et al., 2019b). The corresponding CDS sequences of proteins from single-copy gene families were extracted and aligned using MAFF with default parameters (Rozewicki et al., 2019). The alignments were then concatenated into a super matrix, which was used for phylogenetic tree reconstruction via maximum-likelihood methods implemented in RAxML with a GTRGAMMA substitution model (Stamatakis, 2014). Divergence times among these species

were estimated using the MCMCTree program (Yang, 1997). The collinearity between cotton species was estimated using the MCSANX package (Wang et al., 2012c).

Development and molecular characterization of the CSSL population

From the BC₂F₁ generation produced in 2013, recombinants carrying as few substitution segments as possible were selected to make successive backcrosses with Su8289 to produce the BC₄F₁ generation in 2015. In parallel, to obtain as many recombination types as possible, alien addition lines of 13 *G. anomalum* chromosomes were also backcrossed with the BC₂F₁ and BC₃F₁ generations. The BC₄F₁ plants were subsequently selfed three times to achieve stable and homozygous recombinant lines.

To efficiently monitor *G. anomalum* substitution segments and reduce labor cost as much as possible, 130 *G. anomalum*-specific markers (7–14 markers per chromosome) were used to track the target substitution segments (marker names listed in Supplemental Table 37) in each generation. These markers were selected as being near the recombination breakpoints in the BC₂F₁ generation and represented genomic regions delimited by specific recombination events. MAS for foreground selection was used to confirm the presence of target substitution segments in each generation. In the BC₄F₃ generation, homozygous candidate substitution lines were investigated again to confirm the homozygous exotic genotype of each line and were then propagated until BC₄F₄ to obtain a sufficient number of seeds for phenotype studies.

In the BC₄F₄ generation, all recombination types were subjected to foreground and background genotyping with 230 markers evenly distributed across the *G. anomalum* genome. The size of the substitution segment in each finished CSSL was calculated, with the midpoint of two adjacent markers with different genotypes being considered the endpoint of a substitution segment (Young and Tanksley, 1989). Graphical genotype analysis was performed using GGT 2.0 software (van Berloo, 2008).

All generations except BC₄F₃ were planted at the Experiment Station for Plant Science (JAAS), Nanjing, China (N31°36' E119°10'); BC₄F₃ plants were grown at Nanbin Farm, Sanya, China (N18°21' E109°10').

SSR marker analysis

Genomic DNA was extracted from fresh leaves using a modified CTAB method for cotton. PCR reactions were performed using a Applied Biosystems 2720 thermal cycler (Thermo Fisher Scientific, MA, USA) in a 10- μ L volume containing 7.5 μ L of PCR Master Mix (1 \times , TsingKe Biotech, Beijing, China), 0.5 μ L of each primer (100 μ M), and 1.5 μ L of DNA template (20 ng). For the collection of genotypic data, banding patterns were marked as follows: the same band type as *G. hirsutum* was marked as “1;” the same band type as *G. anomalum* was marked as “2;” the same band type as the F₁ was marked as “3;” and missing and unclear band types were marked as “0.”

Resequencing of CSSLs and Su8289 and identification of SNPs

Leaves from six CSSLs (CSSL29, CSSL44, CSSL50, CSSL56, CSSL59, and CSSL63) and Su8289 were collected from the Lishui Plant Experiment Station, JAAS, China. DNA was extracted from leaves using an improved CTAB method, and at least 1.5 μ g of DNA was used for library construction via the TruSeq Library Construction Kit with an insert size of about 350 bp. All libraries were sequenced on the Illumina HiSeq platform with genome coverage of at least 50 \times for Su8289, 30 \times for CSSL63, and 10 \times for other CSSLs (Supplemental Table 21). After trimming of low-quality bases using Trimmomatic (version 0.32), the clean data were mapped to the A subgenome of *G. hirsutum* TM-1 using BWA (Li and Durbin, 2009). All uniquely mapped reads were extracted and SNP identification performed using GATK (version 3.1.1) (McKenna et al., 2010) and SAMtools (version 0.1.19) (Li et al., 2009).

Development of *G. anomalum* chromosome type-specific oligo-FISH probes and FISH

Oligo-FISH probes were designed using Chorus2 based on a previously published pipeline (Albert et al., 2019). In brief, single-copy oligos (45 nt) were generated from Chr.06, Chr.09, and Chr.11 of *G. anomalum* with the parameters of chorus “-l 45 -homology 75 -step 5.” Repetitive oligos were then filtered using *G. anomalum* genomic sequence data. In total, 117 685, 117 287, and 156 457 oligos were generated from *G. anomalum* Chr.06, Chr.09, and Chr.11, respectively. To distinguish *G. anomalum* Chr.06, Chr.09, and Chr.11 in CSSL lines, we developed oligo probes specific to *G. anomalum* following a previously published protocol (do Vale Martins et al., 2019). Oligos from *G. anomalum* Chr.06, Chr.09, and Chr.11 were first mapped to the *G. hirsutum* reference genome and then classified into three sets on the basis of that mapping: oligos that were identical to *G. hirsutum*, oligos that were completely different (PAV oligos), and oligos that contained mismatches and/or indels (SNP oligos). Finally, all PAV oligos and SNP oligos were selected as haplotype-specific oligo-FISH probes for *G. anomalum*. This process yielded 266 PAV and 8 861 SNP oligos, 314 PAV and 7 185 SNP oligos, and 259 PAV and 10 597 SNP oligos for *G. anomalum* Chr.06, Chr.09, and Chr.11, respectively. All oligos were synthesized by MYcroarray (Ann Arbor, MI, USA).

FISH was performed as previously described with several modifications (Meng et al., 2020). Mitotic chromosome spreads were prepared using root tips, and slides with good metaphase chromosomes were selected for the FISH experiment. After hybridization, chromosomes were counterstained with 4',6-diamidino-2-phenylindole (DAPI; Vector Laboratories, USA), and the signal was detected directly under an Olympus BX63 fluorescence microscope. Chromosome and FISH signals were captured using cellSens Dimension 1.9 software with an Olympus DP80 CCD camera. Final image adjustments were performed using Adobe Photoshop CC software.

Phenotypic identification of the CSSL population

The CSSL population and Su8289 were planted in a completely randomized block design with three replications at the Experiment Station for Plant Science (JAAS), Nanjing, China in 2017 (designated E1), 2018 (E2), and 2019 (E4). In each environment, the seeds were first sown in plug trays to ensure good seedling emergence and growth rate. Seedlings were transplanted to the field after 30 days, with one row per replication and 10 plants per row. Plants were separated by 50 cm and rows by 100 cm. Su8289 was planted among every tenth row and used as a boundary. The lines were also planted in a completely randomized block design with four replications at the National Crop Seeding Farm, Kuerle, China (N41°50' E85°48') in 2018 (E3). In this environment, the seeds were sown directly on mulch film with one row per replication and 30 plants per row. The rows were 4 m in length with 40 cm between rows. Field management was carried out according to the local cotton production management model in each environment.

PH was measured as the length from the cotyledon node to the apical bud at maturity in environments E1 and E2, and the average of 10 plants per row was taken as the corresponding phenotypic value. Thirty mature cotton bolls, fully open and from the interior middle of the plants, were selected to investigate BW, LP, and SI in E1, E2, E3, and E4 (SI was determined only in E2 and E3). Approximately 15 g of lint from each sample was used for quality testing of FL, FS, MIC, FU, and FE at the Supervision, Inspection and Test Center of Cotton Quality, Ministry of Agriculture and Rural Affairs, Anyang, China.

Descriptive analysis of phenotypes was performed using PROC MEANS in SAS/STAT version 9.1.2 (SAS Institute, NC, USA).

Identification of substitution segments associated with agronomic traits

A likelihood ratio test based on stepwise regression (RSTEP-LRT) in QTL IciMapping 4.1 (Li et al., 2007) was used to detect associations between

substitution segments and traits in each environment with the statistical threshold of LOD (likelihood of odds) >2.5. RSTEP-LRT is suitable for QTL mapping in a non-idealized CSSL population in which each line carries two or more segments from the donor parent. The stepwise regression was used to select the most important segments for the trait of interest, and the likelihood ratio test was used to calculate the LOD score of each chromosome segment (Wang et al., 2006). The QTL designations begin with “q” followed by abbreviations of trait name, chromosome name, and serial number.

Fine mapping of the genes for fiber strength

The hybridization of CSSL59 × Su8289 was performed in 2019. The F₁ seeds were planted and self-pollinated in Hainan Island. The F₂ population of 2168 individuals was grown at Lishui Plant Experiment Station, JAAS, China in 2020. Nineteen polymorphic SSR markers were used to genotype all the F₂ plants, and 81 recombinants were identified (Supplemental Table 31). The seeds of recombinants in the F₂ population were harvested separately, and these seeds of each F₂ individual generated F_{2:3} families, which were planted in Hainan Island. The fiber quality of homozygous recombinants in the F_{2:3} families was tested at the Supervision, Inspection and Test Center of Cotton Quality, Ministry of Agriculture and Rural Affairs, Anyang, China.

Transcriptome analysis

For the drought tolerance test, CSSL29 and Su8289 were germinated in soil and then irrigated with 20% PEG6000 solution at the seedling stage (14 days after germination). Leaves were collected at 0, 6, 12, 24, and 72 h after PEG treatment. Fiber samples at 20 DPA were collected from CSSL13, CSSL59, and Su8289. Three biological replicates of total RNA for each sample were extracted using a plant RNA purification kit (Omega, Beijing, China) following the manufacturer's instructions. Libraries were constructed using the Illumina TruSeq Stranded RNA Library Preparation Kit and then sequenced on an Illumina HiSeq platform (150 bp paired-end). We used the DESeq2 package (<http://www.bioconductor.org/packages/release/bioc/html/DESeq2.html>) to identify genes that were differentially expressed across samples or groups. We defined genes as significantly differentially expressed when comparison yielded a fold change ≥ 2 and an FDR < 0.05.

Quantitative RT-PCR analysis

To estimate the validity of RNA-seq technology for expression profile analysis and screen the candidate genes involved in PEG stress and fiber development, total RNA was extracted from leaves at 0, 6, 12, 24, and 72 h after PEG treatment and from fiber samples at 20 DPA and then reverse transcribed into cDNA. Endogenous cotton *histone-3* (AF024716) was used as an internal standard to normalize the total amount of cDNA in each reaction. Gene-specific primers corresponding to the candidate genes were designed with Beacon Designer software (Supplemental Tables 26 and 35). The qRT-PCR experiment was conducted using the TB Green Premix Ex Taq (Tli RNaseH Plus) kit (TaKaRa), and three biological replicates of all reactions were run on a QuantStudio 5 Real-Time PCR System. Relative transcript levels were computed using the 2^{-ΔCt} method, where ΔCt is the difference in Ct values between the control *histone-3* gene (AF024716) products and the target gene products.

Virus-induced gene-silencing assay

For knockdown of *Goano05G0164*, *Goano05G0170*, *Goano05G0207*, *Goano05G0222*, *Goano05G0235*, *Goano05G0236*, *Goano05G0268*, *Goano05G0301*, and *Goano05G0319*, approximately 300-bp fragments of these genes were PCR-amplified from CSSL29 cDNA. The primers used are given in Supplemental Table 27. The resulting PCR products were recombined into pTRV2 to produce VIGS vectors, after which pTRV1 and recombinant pTRV2 vectors were separately introduced into *Agrobacterium* strain GV3101 by means of electroporation (Bio-Rad, Hercules, CA, USA); bacteria harboring each vector were then mixed by equal volume and incubated for 3 h at 28°C. Infiltration of CSSL29

seedlings with mature cotyledons but without a visible true leaf (7 days after germination) was then performed by inserting the combined *Agrobacterium* suspension into the cotyledons via a syringe. The plants were grown at 23°C with a 16 h/8 h (light/dark) cycle and a relative humidity of 60%. VIGS effectiveness was assessed by generating a TRV:GbCLA construct using the *G. anomalum* *CLA1* gene as described previously. The VIGS experiments were repeated at least three times with more than five plants in each repeat.

Drought stress tolerance assays in *Arabidopsis*

We used the floral dip method (Clough and Bent, 1998) to generate EE lines of *Goano05G0268* in *Arabidopsis* and selected the positive lines on MS basal salt mixture medium with 50 mg/l kanamycin. The positive lines were further confirmed by PCR amplification (Supplemental Figure 16A). Three EE (T₁ generation) and WT lines were grown on MS medium containing 0, 200, and 250 mM mannitol. The root length was measured after 8 days. To assess drought stress during seedling development, the WT and EE lines (T₀ generation) were well watered for 21 days and then treated without supplemental water in the soil to place the plants under drought stress. After 25 days, all of the WT plants wilted and lost vitality owing to severe drought stress, whereas most EE plants remained alive (Figure 3F).

Determination of physiological and biochemical indexes

Callose content (Keppler and Novacky, 1987) and callose synthase activity in fibers of CSSL59 and Su8289 at 20 DPA were measured using the aniline blue staining method. POD activity and H₂O₂ and MDA content in TRV:00 and TRV:Goano05G0268 cotton plants under PEG stress and in EE and WT lines of *Arabidopsis* under drought stress were measured with assay kits (JianCheng, Nanjing, China).

SUPPLEMENTAL INFORMATION

Supplemental information is available at *Plant Communications Online*.

ACCESSION NUMBERS

The *G. anomalum* genome assembly and annotation data are available at <https://www.cottongen.org/>. All raw sequencing data generated in the current study are deposited in the BioProject database of NCBI and the National Genomics Data Center under accession numbers PRJNA697836 and PRJCA004607, respectively. PacBio, Illumina paired-end, Hi-C, and ChIP-seq data of *G. anomalum* have been deposited in the Sequence Read Archive (SRA) under accession numbers SRR19241842–SRR19241849, SRR19241851–SRR19241856, SRR19241861, SRR19241872, SRR19241876–SRR19241877, SRR19241883, SRR19241894, SRR19241902, SRR19241905, SRR19241916–SRR19241917, and SRR192426739. The BioNano file ID is SUPPF_0000004289. All of the RNA-seq data are available at the SRA under accession numbers SRR19241840–SRR19241841, SRR19241850, SRR19241857–SRR19241860, SRR19241862–SRR19241871, SRR19241873–SRR19241875, SRR19241879–SRR19241882, SRR19241884–SRR19241893, SRR19241895, SRR19241903–SRR19241904, and SRR19241906–SRR19241915. The resequencing data for CSSLs and Su8289 are available under at the SRA under accession numbers SRR19261769, SRR19241896–SRR19241897, SRR19241899–SRR19241901, and SRR19241878.

FUNDING

National Natural Science Foundation of China (31471545, 32171986, 32100494, and 32070544), Jiangsu Agricultural Science and Technology Innovation Fund (CX (20) 3139), and Leading Innovative and Entrepreneur Team Introduction Program of Zhejiang (2019R01002).

AUTHOR CONTRIBUTIONS

X.S. conceptualized the project. X.S., T.Z., K.W., Z.X., J.C., and S.M. conceived and designed the project. Z.X., S.M., P.X., C.Z., and F.H. constructed the CSSL population. Z.X. and S.M. collected the plant materials and prepared DNA and RNA for Illumina and PacBio SMRT sequencing.

Z.X., S.M., and J.C. performed genome assembly and annotation. S.M. and Z.X. analyzed the BioNano and Hi-C data. J.C. analyzed the genome evolution of *G. anomalum* and identified SNPs in CSSL and Su8289. Z.M. and Y.Z. identified centromeric regions by CenH3 ChIP-seq mapping. X.S., Z.X., S.M., Y.Q., T.W., X.Z., J.L., J.G., W.N., X.C., and S.W. performed the field experiments and identified the phenotypes of the CSSL population. Z.X., S.M., and Y.S. performed fine mapping of genes for fiber strength. Z.X., S.M., Q.G., L.Z., Y.S., J.Z., J.X., W.J., N.W., and X.L. analyzed genes related to fiber development and drought stress. J.C., Z.X., and S.M. carried out data submission. Z.X., X.S., T.Z., S.M., and K.W. wrote the manuscript. All authors read and approved the final manuscript.

ACKNOWLEDGMENTS

No conflict of interest declared.

Received: January 11, 2022

Revised: June 1, 2022

Accepted: June 17, 2022

Published: June 22, 2022

REFERENCES

- AbdElgawad, H., Avramova, V., Baggerman, G., Van Raemdonck, G., Valkenburg, D., Van Ostade, X., Guisez, Y., Prinsen, E., Asard, H., Van den Ende, W., et al. (2020). Starch biosynthesis contributes to the maintenance of photosynthesis and leaf growth under drought stress in maize. *Plant Cell Environ.* **43**:2254–2271. <https://doi.org/10.1111/pce.13813>.
- Albert, P.S., Zhang, T., Semrau, K., Rouillard, J.M., Kao, Y.H., Wang, C.J.R., Danilova, T.V., Jiang, J.M., and Birchler, J.A. (2019). Whole-chromosome paints in maize reveal rearrangements, nuclear domains, and chromosomal relationships. *Proc. Natl. Acad. Sci. USA* **116**:1679–1685. <https://doi.org/10.1073/pnas.1813957116>.
- Arabidopsis Genome Initiative. (2000). Analysis of the genome sequence of the flowering plant *Arabidopsis thaliana*. *Nature* **408**:796–815. <https://doi.org/10.1038/35048692>.
- Argout, X., Salse, J., Aury, J.M., Guiltinan, M.J., Droc, G., Gouzy, J., Allegre, M., Chaparro, C., Legavre, T., Maximova, S.N., et al. (2011). The genome of *Theobroma cacao*. *Nat. Genet.* **43**:101–108. <https://doi.org/10.1038/ng.736>.
- Ashburner, M., Ball, C.A., Blake, J.A., Botstein, D., Butler, H., Cherry, J.M., Davis, A.P., Dolinski, K., Dwight, S.S., Eppig, J.T., et al. (2000). Gene Ontology: tool for the unification of biology. *Nat. Genet.* **25**:25–29. <https://doi.org/10.1038/75556>.
- Benson, G. (1999). Tandem repeats finder: a program to analyze DNA sequences. *Nucleic Acids Res.* **27**:573–580. <https://doi.org/10.1093/Nar/27.2.573>.
- Bi, Y., Zhao, Q., Yan, W., Li, M., Liu, Y., Cheng, C., Zhang, L., Yu, X., Li, J., Qian, C., et al. (2020). Flexible chromosome painting based on multiplex PCR of oligonucleotides and its application for comparative chromosome analyses in *Cucumis*. *Plant J.* **102**:178–186. <https://doi.org/10.1111/tpj.14600>.
- Birney, E., Clamp, M., and Durbin, R. (2004). GeneWise and genomewise. *Genome Res.* **14**:988–995. <https://doi.org/10.1101/gr.1865504>.
- Blanco, E., Parra, G., and Guigó, R. (2007). Using geneid to identify genes. *Curr. Protoc. Bioinformatics* **Chapter 4**:Unit 4.3. <https://doi.org/10.1002/0471250953.bi0403s18>.
- Boeckmann, B., Bairoch, A., Apweiler, R., Blatter, M.C., Estreicher, A., Gasteiger, E., Martin, M.J., Michoud, K., O'Donovan, C., Phan, I., et al. (2003). The SWISS-PROT protein knowledgebase and its supplement TrEMBL in 2003. *Nucleic Acids Res.* **31**:365–370. <https://doi.org/10.1093/nar/gkg095>.
- Bredeson, J.V., Lyons, J.B., Prochnik, S.E., Wu, G.A., Ha, C.M., Edsinger-Gonzales, E., Grimwood, J., Schmutz, J., Rabbi, I.Y., Egesi, C., et al.

- (2016). Sequencing wild and cultivated cassava and related species reveals extensive interspecific hybridization and genetic diversity. *Nat. Biotechnol.* **34**:562–570. <https://doi.org/10.1038/nbt.3535>.
- Brown, R.M., Saxena, I.M., and Kudlicka, K.** (1996). Cellulose biosynthesis in higher plants. *Trends Plant Sci.* **1**:149–156. [https://doi.org/10.1016/S1360-1385\(96\)80050-1](https://doi.org/10.1016/S1360-1385(96)80050-1).
- Burge, C., and Karlin, S.** (1997). Prediction of complete gene structures in human genomic DNA. *J. Mol. Biol.* **268**:78–94. <https://doi.org/10.1006/jmbi.1997.0951>.
- Burton, J.N., Adey, A., Patwardhan, R.P., Qiu, R., Kitzman, J.O., and Shendure, J.** (2013). Chromosome-scale scaffolding of *de novo* genome assemblies based on chromatin interactions. *Nat. Biotechnol.* **31**:1119–1125. <https://doi.org/10.1038/nbt.2727>.
- Cai, Y., Cai, X., Wang, Q., Wang, P., Zhang, Y., Cai, C., Xu, Y., Wang, K., Zhou, Z., Wang, C., et al.** (2020). Genome sequencing of the Australian wild diploid species *Gossypium australe* highlights disease resistance and delayed gland morphogenesis. *Plant Biotechnol. J.* **18**:814–828. <https://doi.org/10.1111/pbi.13249>.
- Cao, H., Hastie, A.R., Cao, D., Lam, E.T., Sun, Y., Huang, H., Liu, X., Lin, L., Andrews, W., Chan, S., et al.** (2014). Rapid detection of structural variation in a human genome using nanochannel-based genome mapping technology. *GigaScience* **3**:34. <https://doi.org/10.1186/2047-217X-3-34>.
- Chandnani, R., Wang, B., Draye, X., Rainville, L.K., Auckland, S., Zhuang, Z., Lubbers, E.L., May, O.L., Chee, P.W., and Paterson, A.H.** (2017). Segregation distortion and genome-wide digenic interactions affect transmission of introgressed chromatin from wild cotton species. *Theor. Appl. Genet.* **130**:2219–2230. <https://doi.org/10.1007/s00122-017-2952-y>.
- Chen, Z.J., Sreedasyam, A., Ando, A., Song, Q.X., De Santiago, L.M., Hulse-Kemp, A.M., Ding, M.Q., Ye, W.X., Kirkbride, R.C., Jenkins, J., et al.** (2020). Genomic diversifications of five *Gossypium* allopolyploid species and their impact on cotton improvement. *Nat. Genet.* **52**:525–533. <https://doi.org/10.1038/s41588-020-0614-5>.
- Chen, N.** (2004). Using RepeatMasker to identify repetitive elements in genomic sequences. *Curr. Protoc. Bioinformatics* **Chapter 4**, Unit 4.10. <https://doi.org/10.1002/0471250953.bi0410s05>.
- Clough, S.J., and Bent, A.F.** (1998). Floral dip: a simplified method for *Agrobacterium*-mediated transformation of *Arabidopsis thaliana*. *Plant J.* **16**:735–743. <https://doi.org/10.1046/j.1365-313x.1998.00343.x>.
- Culp, T.W., and Harrell, D.C.** (1973). Breeding methods for improving yield and fiber quality of upland cotton (*Gossypium hirsutum* L.). *Crop Sci.* **13**:686–689. <https://doi.org/10.2135/cropsci1973.0011183X001300060030x>.
- Culp, T.W., Harrell, D.C., and Kerr, T.** (1979). Some genetic implications in the transfer of high fiber strength genes to upland cotton. *Crop Sci.* **19**:481–484. <https://doi.org/10.2135/cropsci1979.0011183X001900040013x>.
- Dietz, K.J.** (2007). The dual function of plant peroxiredoxins in antioxidant defence and redox signaling. In *Peroxioredoxin Systems*, L. Flohé and J.R. Harris, eds. (Springer), pp. 267–294.
- do Vale Martins, L., Yu, F., Zhao, H., Dennison, T., Lauter, N., Wang, H., Deng, Z., Thompson, A., Semrau, K., Rouillard, J.M., et al.** (2019). Meiotic crossovers characterized by haplotype-specific chromosome painting in maize. *Nat. Commun.* **10**:4604. <https://doi.org/10.1038/s41467-019-12646-z>.
- Du, X., Huang, G., He, S., Yang, Z., Sun, G., Ma, X., Li, N., Zhang, X., Sun, J., Liu, M., et al.** (2018). Resequencing of 243 diploid cotton accessions based on an updated A genome identifies the genetic basis of key agronomic traits. *Nat. Genet.* **50**:796–802. <https://doi.org/10.1038/s41588-018-0116-x>.
- Edgar, R.C., and Myers, E.W.** (2005). PILER: identification and classification of genomic repeats. *Bioinformatics* **21**:i152–i158. <https://doi.org/10.1093/bioinformatics/bti1003>.
- Griffiths-Jones, S., Moxon, S., Marshall, M., Khanna, A., Eddy, S.R., and Bateman, A.** (2005). Rfam: annotating non-coding RNAs in complete genomes. *Nucleic Acids Res.* **33**:D121–D124. <https://doi.org/10.1093/nar/gki081>.
- Grover, C.E., Arick, M.A., II, Thrash, A., Conover, J.L., Sanders, W.S., Peterson, D.G., Frelichowski, J.E., Scheffler, J.A., Scheffler, B.E., and Wendel, J.F.** (2019). Insights into the evolution of the New World diploid cottons (*Gossypium*, subgenus *Houzingenia*) based on genome sequencing. *Genome Biol. Evol.* **11**:53–71. <https://doi.org/10.1093/gbe/evy256>.
- Grover, C.E., Pan, M., Yuan, D., Arick, M.A., Hu, G., Brase, L., Stelly, D.M., Lu, Z., Schmitz, R.J., Peterson, D.G., et al.** (2020). The *Gossypium longicalyx* genome as a resource for cotton breeding and evolution. *G3 (Bethesda)* **10**:1457–1467. <https://doi.org/10.1534/g3.120.401050>.
- Grover, C.E., Yuan, D., Arick, M.A., Miller, E.R., Hu, G., Peterson, D.G., Wendel, J.F., and Udall, J.A.** (2021). The *Gossypium anomalum* genome as a resource for cotton improvement and evolutionary analysis of hybrid incompatibility. *G3 (Bethesda)* **11**:jkab319. <https://doi.org/10.1093/g3journal/jkab319>.
- Haas, B.J., Delcher, A.L., Mount, S.M., Wortman, J.R., Smith, R.K., Hannick, L.I., Maiti, R., Ronning, C.M., Rusch, D.B., Town, C.D., et al.** (2003). Improving the *Arabidopsis* genome annotation using maximal transcript alignment assemblies. *Nucleic Acids Res.* **31**:5654–5666. <https://doi.org/10.1093/nar/gkg770>.
- Haas, B.J., Salzberg, S.L., Zhu, W., Pertea, M., Allen, J.E., Orvis, J., White, O., Buell, C.R., and Wortman, J.R.** (2008). Automated eukaryotic gene structure annotation using EVIDENCEModeler and the Program to Assemble Spliced Alignments. *Genome Biol.* **9**:R7. <https://doi.org/10.1186/gb-2008-9-1-r7>.
- Hake, S., and Richardson, A.** (2019). Using wild relatives to improve maize. *Science* **365**:640–641. <https://doi.org/10.1126/science.aay5299>.
- Hawkins, J.S., Kim, H., Nason, J.D., Wing, R.A., and Wendel, J.F.** (2006). Differential lineage-specific amplification of transposable elements is responsible for genome size variation in *Gossypium*. *Genome Res.* **16**:1252–1261. <https://doi.org/10.1101/gr.5282906>.
- Hernández, I., Cela, J., Alegre, L., and Munné-Bosch, S.** (2012). Antioxidant defenses against drought stress. In *Plant Responses to Drought Stress*, R. Aroca, ed. (Springer), pp. 231–258.
- Hsieh, Y.L., Hu, X.P., and Wang, A.J.** (2000). Single fiber strength variations of developing cotton fibers - strength and structure of *G. hirsutum* and *G. barbedense*. *Textil. Res. J.* **70**:682–690. <https://doi.org/10.1177/004051750007000805>.
- Hu, Y., Chen, J., Fang, L., Zhang, Z., Ma, W., Niu, Y., Ju, L., Deng, J., Zhao, T., Lian, J., et al.** (2019). *Gossypium barbadense* and *Gossypium hirsutum* genomes provide insights into the origin and evolution of allotetraploid cotton. *Nat. Genet.* **51**:739–748. <https://doi.org/10.1038/s41588-019-0371-5>.
- Huang, G., Wu, Z., Percy, R.G., Bai, M., Li, Y., Frelichowski, J.E., Hu, J., Wang, K., Yu, J.Z., and Zhu, Y.** (2020). Genome sequence of *Gossypium herbaceum* and genome updates of *Gossypium arboreum* and *Gossypium hirsutum* provide insights into cotton A-genome evolution. *Nat. Genet.* **52**:516–524. <https://doi.org/10.1038/s41588-020-0607-4>.
- Jurka, J., Kapitonov, V.V., Pavlicek, A., Klonowski, P., Kohany, O., and Walichewicz, J.** (2005). Repbase update, a database of eukaryotic repetitive elements. *Cytogenet. Genome Res.* **110**:462–467. <https://doi.org/10.1159/000084979>.

- Kanehisa, M., and Goto, S.** (2000). KEGG: kyoto encyclopedia of genes and genomes. *Nucleic Acids Res.* **28**:27–30. <https://doi.org/10.1093/Nar/28.1.27>.
- Keerio, A.A., Shen, C., Nie, Y., Ahmed, M.M., Zhang, X., and Lin, Z.** (2018). QTL mapping for fiber quality and yield traits based on introgression lines derived from *Gossypium hirsutum* × *G. tomentosum*. *Int. J. Mol. Sci.* **19**:243. <https://doi.org/10.3390/ijms19010243>.
- Kent, W.J.** (2002). BLAT—The BLAST-like alignment tool. *Genome Res.* **12**:656–664. <https://doi.org/10.1101/gr.229202>.
- Keppler, L.D., and Novacky, A.** (1987). The initiation of membrane lipid-peroxidation during bacteria-induced hypersensitive reaction. *Physiol. Mol. Plant Pathol.* **30**:233–245. [https://doi.org/10.1016/0885-5765\(87\)90037-3](https://doi.org/10.1016/0885-5765(87)90037-3).
- Kim, H.J., and Triplett, B.A.** (2001). Cotton fiber growth in planta and in vitro. models for plant cell elongation and cell wall biogenesis. *Plant Physiol.* **127**:1361–1366. <https://doi.org/10.1104/pp.010724>.
- Korf, I.** (2004). Gene finding in novel genomes. *BMC Bioinform.* **5**:59. <https://doi.org/10.1186/1471-2105-5-59>.
- Lam, E.T., Hastie, A., Lin, C., Ehrlich, D., Das, S.K., Austin, M.D., Deshpande, P., Cao, H., Nagarajan, N., Xiao, M., et al.** (2012). Genome mapping on nanochannel arrays for structural variation analysis and sequence assembly. *Nat. Biotechnol.* **30**:771–776. <https://doi.org/10.1038/nbt.2303>.
- Li, F., Fan, G., Wang, K., Sun, F., Yuan, Y., Song, G., Li, Q., Ma, Z., Lu, C., Zou, C., et al.** (2014). Genome sequence of the cultivated cotton *Gossypium arboreum*. *Nat. Genet.* **46**:567–572. <https://doi.org/10.1038/ng.2987>.
- Li, H., and Durbin, R.** (2009). Fast and accurate short read alignment with Burrows-Wheeler transform. *Bioinformatics* **25**:1754–1760. <https://doi.org/10.1093/bioinformatics/btp324>.
- Li, H., Handsaker, B., Wysoker, A., Fennell, T., Ruan, J., Homer, N., Marth, G., Abecasis, G., Durbin, R., and Genome Project Data Processing, S.** (2009). The sequence alignment/map format and SAMtools. *Bioinformatics* **25**:2078–2079. <https://doi.org/10.1093/bioinformatics/btp352>.
- Li, H., Ye, G., and Wang, J.** (2007). A modified algorithm for the improvement of composite interval mapping. *Genetics* **175**:361–374. <https://doi.org/10.1534/genetics.106.066811>.
- Majoros, W.H., Pertea, M., and Salzberg, S.L.** (2004). TigrScan and GlimmerHMM: two open source *ab initio* eukaryotic gene-finders. *Bioinformatics* **20**:2878–2879. <https://doi.org/10.1093/bioinformatics/bth315>.
- Mamidi, S., Healey, A., Huang, P., Grimwood, J., Jenkins, J., Barry, K., Sreedasyam, A., Shu, S., Lovell, J.T., Feldman, M., et al.** (2020). A genome resource for green millet *Setaria viridis* enables discovery of agronomically valuable loci. *Nat. Biotechnol.* **38**:1203–1210. <https://doi.org/10.1038/s41587-020-0681-2>.
- Marquez-Garcia, B., Shaw, D., Cooper, J.W., Karpinska, B., Quain, M.D., Makgopa, E.M., Kunert, K., and Foyer, C.H.** (2015). Redox markers for drought-induced nodule senescence, a process occurring after drought-induced senescence of the lowest leaves in soybean (*Glycine max*). *Ann. Bot.* **116**:497–510. <https://doi.org/10.1093/aob/mcv030>.
- McGinnis, S., and Madden, T.L.** (2004). BLAST: at the core of a powerful and diverse set of sequence analysis tools. *Nucleic Acids Res.* **32**:W20–W25. <https://doi.org/10.1093/nar/gkh435>.
- McKenna, A., Hanna, M., Banks, E., Sivachenko, A., Cibulskis, K., Kernysky, A., Garimella, K., Altshuler, D., Gabriel, S., Daly, M., et al.** (2010). The Genome Analysis Toolkit: a MapReduce framework for analyzing next-generation DNA sequencing data. *Genome Res.* **20**:1297–1303. <https://doi.org/10.1101/gr.107524.110>.
- Mehetre, S.S.** (2010). Wild *Gossypium anomalum*: a unique source of fibre fineness and strength. *Curr. Sci.* **5**:e11405. <https://doi.org/10.1371/journal.pone.0011405>.
- Meier, H., Buchs, L., Buchala, A.J., and Homewood, T.** (1981). (1 → 3)-β-D-Glucan (callose) is a probable intermediate in biosynthesis of cellulose of cotton fibres. *Nature* **289**:821–822. <https://doi.org/10.1038/289821a0>.
- Meinert, M.C., and Delmer, D.P.** (1977). Changes in biochemical composition of the cell wall of the cotton fiber during development. *Plant Physiol.* **59**:1088–1097. <https://doi.org/10.1104/pp.59.6.1088>.
- Meng, Z., Han, J., Lin, Y., Zhao, Y., Lin, Q., Ma, X., Wang, J., Zhang, M., Zhang, L., Yang, Q., et al.** (2020). Characterization of a *Saccharum spontaneum* with a basic chromosome number of x = 10 provides new insights on genome evolution in genus *Saccharum*. *Theor. Appl. Genet.* **133**:187–199. <https://doi.org/10.1007/s00122-019-03450-w>.
- Meyer, V.G.** (1973). Fertility-restorer genes for cytoplasmic male sterility from *Gossypium harknessii*. In *Proceedings of Beltwide Cotton Production Research Conference*.
- Nagaki, K., Cheng, Z., Ouyang, S., Talbert, P.B., Kim, M., Jones, K.M., Henikoff, S., Buell, C.R., and Jiang, J.** (2004). Sequencing of a rice centromere uncovers active genes. *Nat. Genet.* **36**:138–145. <https://doi.org/10.1038/ng1289>.
- Newaskar, G.S., Chimote, V.P., Mehetre, S.S., and Jadhav, A.S.** (2013). Interspecific hybridization in *Gossypium* L.: characterization of progenies with different ploidy-confirmed multigenomic backgrounds. *Plant Breed.* **132**:211–216. <https://doi.org/10.1111/pbr.12031>.
- Ou, S., Chen, J., and Jiang, N.** (2018). Assessing genome assembly quality using the LTR Assembly Index (LAI). *Nucleic Acids Res.* **46**:e126. <https://doi.org/10.1093/nar/gky730>.
- Parra, G., Bradnam, K., and Korf, I.** (2007). CEGMA: a pipeline to accurately annotate core genes in eukaryotic genomes. *Bioinformatics* **23**:1061–1067. <https://doi.org/10.1093/bioinformatics/btm071>.
- Paterson, A.H., Wendel, J.F., Gundlach, H., Guo, H., Jenkins, J., Jin, D., Llewellyn, D., Showmaker, K.C., Shu, S.Q., Udall, J., et al.** (2012). Repeated polyploidization of *Gossypium* genomes and the evolution of spinnable cotton fibres. *Nature* **492**:423–427. <https://doi.org/10.1038/nature11798>.
- Price, A.L., Jones, N.C., and Pevzner, P.A.** (2005). *De novo* identification of repeat families in large genomes. *Bioinformatics* **21**:i351–i358. <https://doi.org/10.1093/bioinformatics/bti1018>.
- Rey, P., Cuiné, S., Eymery, F., Garin, J., Court, M., Jacquot, J.P., Rouhier, N., and Broin, M.** (2005). Analysis of the proteins targeted by CDSP32, a plastidic thioredoxin participating in oxidative stress responses. *Plant J.* **41**:31–42. <https://doi.org/10.1111/j.1365-313X.2004.02271.x>.
- Rozewicki, J., Li, S., Amada, K.M., Standley, D.M., and Katoh, K.** (2019). MAFFT-DASH: integrated protein sequence and structural alignment. *Nucleic Acids Res.* **47**:W5–W10. <https://doi.org/10.1093/nar/gkz342>.
- Ruan, Y.L., Xu, S.M., White, R., and Furbank, R.T.** (2004). Genotypic and developmental evidence for the role of plasmodesmatal regulation in cotton fiber elongation mediated by callose turnover. *Plant Physiol.* **136**:4104–4113. <https://doi.org/10.1104/pp.104.051540>.
- Sacks, E.J., and Robinson, A.F.** (2009). Introgression of resistance to reniform nematode (*Rotylenchulus reniformis*) into upland cotton (*Gossypium hirsutum*) from *Gossypium arboreum* and a *G. hirsutum*/*Gossypium aridum* bridging line. *Field Crop. Res.* **112**:1–6. <https://doi.org/10.1016/j.fcr.2009.01.006>.
- Salnikov, V.V., Grimson, M.J., Seagull, R.W., and Haigler, C.H.** (2003). Localization of sucrose synthase and callose in freeze-substituted secondary-wall-stage cotton fibers. *Protoplasma* **221**:175–184. <https://doi.org/10.1007/s00709-002-0079-7>.

- Servant, N., Varoquaux, N., Lajoie, B.R., Viara, E., Chen, C.J., Vert, J.P., Heard, E., Dekker, J., and Barillot, E. (2015). HiC-Pro: an optimized and flexible pipeline for Hi-C data processing. *Genome Biol.* **16**:259. <https://doi.org/10.1186/S13059-015-0831-X>.
- Silow, R.A. (1941). The comparative genetics of *Gossypium anomalum* and the cultivated Asiatic cottons. *J. Genet.* **42**:259–358. <https://doi.org/10.1007/bf02982878>.
- Simão, F.A., Waterhouse, R.M., Ioannidis, P., Kriventseva, E.V., and Zdobnov, E.M. (2015). BUSCO: assessing genome assembly and annotation completeness with single-copy orthologs. *Bioinformatics* **31**:3210–3212. <https://doi.org/10.1093/bioinformatics/btv351>.
- Stamatakis, A. (2014). RAxML version 8: a tool for phylogenetic analysis and post-analysis of large phylogenies. *Bioinformatics* **30**:1312–1313. <https://doi.org/10.1093/bioinformatics/btu033>.
- Stanke, M., and Waack, S. (2003). Gene prediction with a hidden Markov model and a new intron submodel. *Bioinformatics* **19** (Suppl 2):ii215–ii225. <https://doi.org/10.1093/bioinformatics/btg1080>.
- Stein, J.C., Yu, Y., Copetti, D., Zwickl, D.J., Zhang, L., Zhang, C., Chougule, K., Gao, D., Iwata, A., Goicoechea, J.L., et al. (2018). Genomes of 13 domesticated and wild rice relatives highlight genetic conservation, turnover and innovation across the genus *Oryza*. *Nat. Genet.* **50**:285–296. <https://doi.org/10.1038/s41588-018-0040-0>.
- Szymański, J., Bocobza, S., Panda, S., Sonawane, P., Cárdenas, P.D., Lashbrooke, J., Kamble, A., Shahaf, N., Meir, S., Bovy, A., et al. (2020). Analysis of wild tomato introgression lines elucidates the genetic basis of transcriptome and metabolome variation underlying fruit traits and pathogen response. *Nat. Genet.* **52**:1111–1121. <https://doi.org/10.1038/s41588-020-0690-6>.
- Tanksley, S.D., and McCouch, S.R. (1997). Seed banks and molecular maps: unlocking genetic potential from the wild. *Science* **277**:1063–1066. <https://doi.org/10.1126/science.277.5329.1063>.
- Tian, J., Wang, C., Xia, J., Wu, L., Xu, G., Wu, W., Li, D., Qin, W., Han, X., Chen, Q., et al. (2019). Teosinte ligule allele narrows plant architecture and enhances high-density maize yields. *Science* **365**:658–664. <https://doi.org/10.1126/science.aax5482>.
- Tuskan, G.A., Difazio, S., Jansson, S., Bohlmann, J., Grigoriev, I., Hellsten, U., Putnam, N., Ralph, S., Rombauts, S., Salamov, A., et al. (2006). The genome of black cottonwood, *Populus trichocarpa* (Torr. & Gray). *Science* **313**:1596–1604. <https://doi.org/10.1126/science.1128691>.
- Udall, J.A., Long, E., Hanson, C., Yuan, D., Ramaraj, T., Conover, J.L., Gong, L., Arick, M.A., Grover, C.E., Peterson, D.G., et al. (2019a). *De novo* genome sequence assemblies of *Gossypium raimondii* and *Gossypium turneri*. *G3* (Bethesda) **9**:3079–3085. <https://doi.org/10.1534/g3.119.400392>.
- Udall, J.A., Long, E., Ramaraj, T., Conover, J.L., Yuan, D., Grover, C.E., Gong, L., Arick, M.A., 2nd, Masonbrink, R.E., Peterson, D.G., et al. (2019b). The genome sequence of *Gossypioides kirkii* illustrates a descending dysploidy in plants. *Front. Plant Sci.* **10**:1541. <https://doi.org/10.3389/fpls.2019.01541>.
- van Berloo, R. (2008). GGT 2.0: versatile software for visualization and analysis of genetic data. *J. Hered.* **99**:232–236. <https://doi.org/10.1093/jhered/esm109>.
- Walker, B.J., Abeel, T., Shea, T., Priest, M., Abouelliel, A., Sakthikumar, S., Cuomo, C.A., Zeng, Q.D., Wortman, J., Young, S.K., et al. (2014). Pilon: an integrated tool for comprehensive microbial variant detection and genome assembly improvement. *PLoS One* **9**:e112963. <https://doi.org/10.1371/journal.pone.0112963>.
- Wang, B., Nie, Y., Lin, Z., Zhang, X., Liu, J., and Bai, J. (2012a). Molecular diversity, genomic constitution, and QTL mapping of fiber quality by mapped SSRs in introgression lines derived from *Gossypium hirsutum* x *G. darwinii* Watt. *Theor. Appl. Genet.* **125**:1263–1274. <https://doi.org/10.1007/s00122-012-1911-x>.
- Wang, H., Sun, S., Ge, W., Zhao, L., Hou, B., Wang, K., Lyu, Z., Chen, L., Xu, S., Guo, J., et al. (2020). Horizontal gene transfer of *Fhb7* from fungus underlies *Fusarium* head blight resistance in wheat. *Science* **368**:eaba5435. <https://doi.org/10.1126/science.aba5435>.
- Wang, J., Wan, X., Crossa, J., Crouch, J., Weng, J., Zhai, H., and Wan, J. (2006). QTL mapping of grain length in rice (*Oryza sativa* L.) using chromosome segment substitution lines. *Genet. Res.* **88**:93–104. <https://doi.org/10.1017/s0016672306008408>.
- Wang, K., Wang, Z., Li, F., Ye, W., Wang, J., Song, G., Yue, Z., Cong, L., Shang, H., Zhu, S., et al. (2012b). The draft genome of a diploid cotton *Gossypium raimondii*. *Nat. Genet.* **44**:1098–1103. <https://doi.org/10.1038/ng.2371>.
- Wang, M., Tu, L., Yuan, D., Zhu, D., Shen, C., Li, J., Liu, F., Pei, L., Wang, P., Zhao, G., et al. (2019). Reference genome sequences of two cultivated allotetraploid cottons, *Gossypium hirsutum* and *Gossypium barbadense*. *Nat. Genet.* **51**:224–229. <https://doi.org/10.1038/s41588-018-0282-x>.
- Wang, Y., Tang, H., Debarry, J.D., Tan, X., Li, J., Wang, X., Lee, T.H., Jin, H., Marler, B., Guo, H., et al. (2012c). MCScanX: a toolkit for detection and evolutionary analysis of gene synteny and collinearity. *Nucleic Acids Res.* **40**:e49. <https://doi.org/10.1093/nar/gkr1293>.
- Wendel, J.F., Brubaker, C.L., and Seelanan, T. (2010). The origin and evolution of *Gossypium*. In *Physiology of Cotton*, J.M. Stewart, D.M. Oosterhuis, J.J. Heitholt, and J.R. Mauney, eds. (Springer), pp. 1–18.
- Xu, Z., and Wang, H. (2007). LTR_FINDER: an efficient tool for the prediction of full-length LTR retrotransposons. *Nucleic Acids Res.* **35**:W265–W268. <https://doi.org/10.1093/nar/gkm286>.
- Yang, Z. (1997). PAML: a program package for phylogenetic analysis by maximum likelihood. *Comput. Appl. Biosci.* **13**:555–556. <https://doi.org/10.1093/bioinformatics/13.5.555>.
- Young, N.D., and Tanksley, S.D. (1989). Restriction fragment length polymorphism maps and the concept of graphical genotypes. *Theor. Appl. Genet.* **77**:95–101. <https://doi.org/10.1007/Bf00292322>.
- Zang, C., Schones, D.E., Zeng, C., Cui, K., Zhao, K., and Peng, W. (2009). A clustering approach for identification of enriched domains from histone modification ChIP-Seq data. *Bioinformatics* **25**:1952–1958. <https://doi.org/10.1093/bioinformatics/btp340>.
- Zdobnov, E.M., and Apweiler, R. (2001). InterProScan—an integration platform for the signature-recognition methods in InterPro. *Bioinformatics* **17**:847–848. <https://doi.org/10.1093/bioinformatics/17.9.847>.
- Zhai, C., Xu, P., Zhang, X., Guo, Q., Zhang, X., Xu, Z., and Shen, X. (2015). Development of *Gossypium anomalum*-derived microsatellite markers and their use for genome-wide identification of recombination between the *G. anomalum* and *G. hirsutum* genomes. *Theor. Appl. Genet.* **128**:1531–1540. <https://doi.org/10.1007/s00122-015-2528-7>.
- Zhang, F., and Batley, J. (2020). Exploring the application of wild species for crop improvement in a changing climate. *Curr. Opin. Plant Biol.* **56**:218–222. <https://doi.org/10.1016/j.pbi.2019.12.013>.
- Zhang, T., Hu, Y., Jiang, W., Fang, L., Guan, X., Chen, J., Zhang, J., Sasaki, C.A., Scheffler, B.E., Stelly, D.M., et al. (2015). Sequencing of allotetraploid cotton (*Gossypium hirsutum* L. acc. TM-1) provides a resource for fiber improvement. *Nat. Biotechnol.* **33**:531–537. <https://doi.org/10.1038/nbt.3207>.
- Zhang, X., Zhai, C., He, L., Guo, Q., Zhang, X., Xu, P., Su, H., Gong, Y., Ni, W., and Shen, X. (2014). Morphological, cytological and molecular analyses of a synthetic hexaploid derived from an interspecific hybrid between *Gossypium hirsutum* and *Gossypium anomalum*. *Crop J.* **2**:272–277. <https://doi.org/10.1016/j.cj.2014.06.009>.

Supplemental information

Genome sequence of *Gossypium anomalum* facilitates interspecific introgression breeding

Zhenzhen Xu, Jiedan Chen, Shan Meng, Peng Xu, Caijiao Zhai, Fang Huang, Qi Guo, Liang Zhao, Yonggang Quan, Yixin Shangguan, Zhuang Meng, Tian Wen, Ya Zhang, Xianggui Zhang, Jun Zhao, Jianwen Xu, Jianguang Liu, Jin Gao, Wanchao Ni, Xianglong Chen, Wei Ji, Nanyi Wang, Xiaoxi Lu, Shihong Wang, Kai Wang, Tianzhen Zhang, and Xinlian Shen

Supporting Information

Genome sequence of *Gossypium anomalum* facilitates interspecific introgression breeding

Zhenzhen Xu^{1,5}, Jiedan Chen^{2,5}, Shan Meng^{1,5}, Peng Xu¹, Caijiao Zhai¹, Fang Huang¹, Qi Guo¹, Liang Zhao¹, Yonggang Quan³, Yixin Shangguan¹, Zhuang Meng⁴, Tian Wen³, Ya Zhang⁴, Xianggui Zhang¹, Jun Zhao¹, Jianwen Xu¹, Jianguang Liu¹, Jin Gao¹, Wanchao Ni¹, Xianglong Chen¹, Wei Ji^{1,4}, Nanyi Wang¹, Xiaoxi Lu^{1,4}, Shihong Wang³, Kai Wang^{4,*}, Tianzhen Zhang^{2,*}, Xinlian Shen^{1,*}

¹Key Laboratory of Cotton and Rapeseed (Nanjing), Ministry of Agriculture and Rural Affairs, the Institute of Industrial Crops, Jiangsu Academy of Agricultural Sciences, Nanjing, China

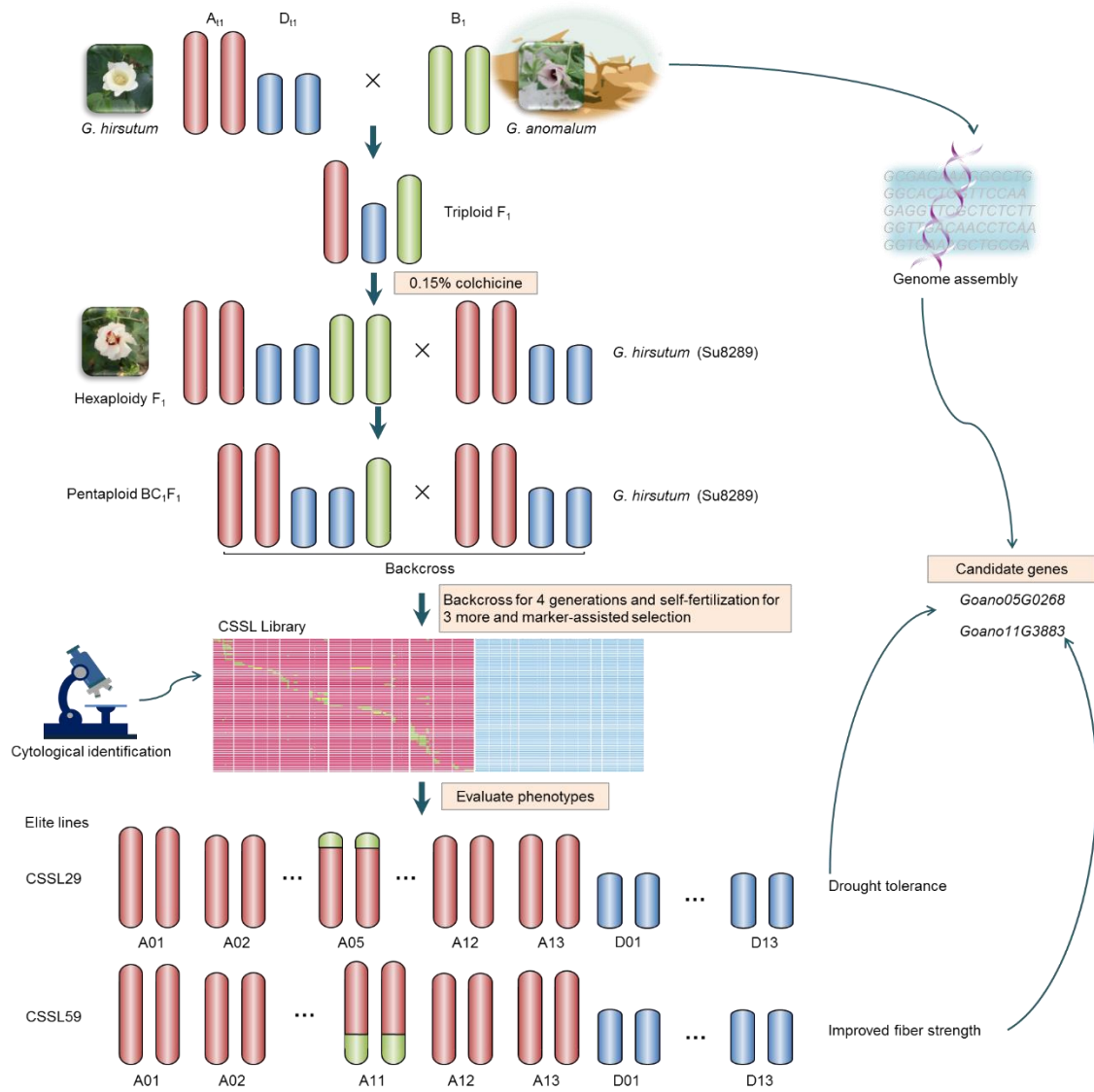
²Institute of Crop Science, Plant Precision Breeding Academy, Zhejiang Provincial Key Laboratory of Crop Genetic Resources, College of Agriculture and Biotechnology, Zhejiang University, Hangzhou, China

³JOIN HOPE SEEDS Co., Ltd., Changji, China

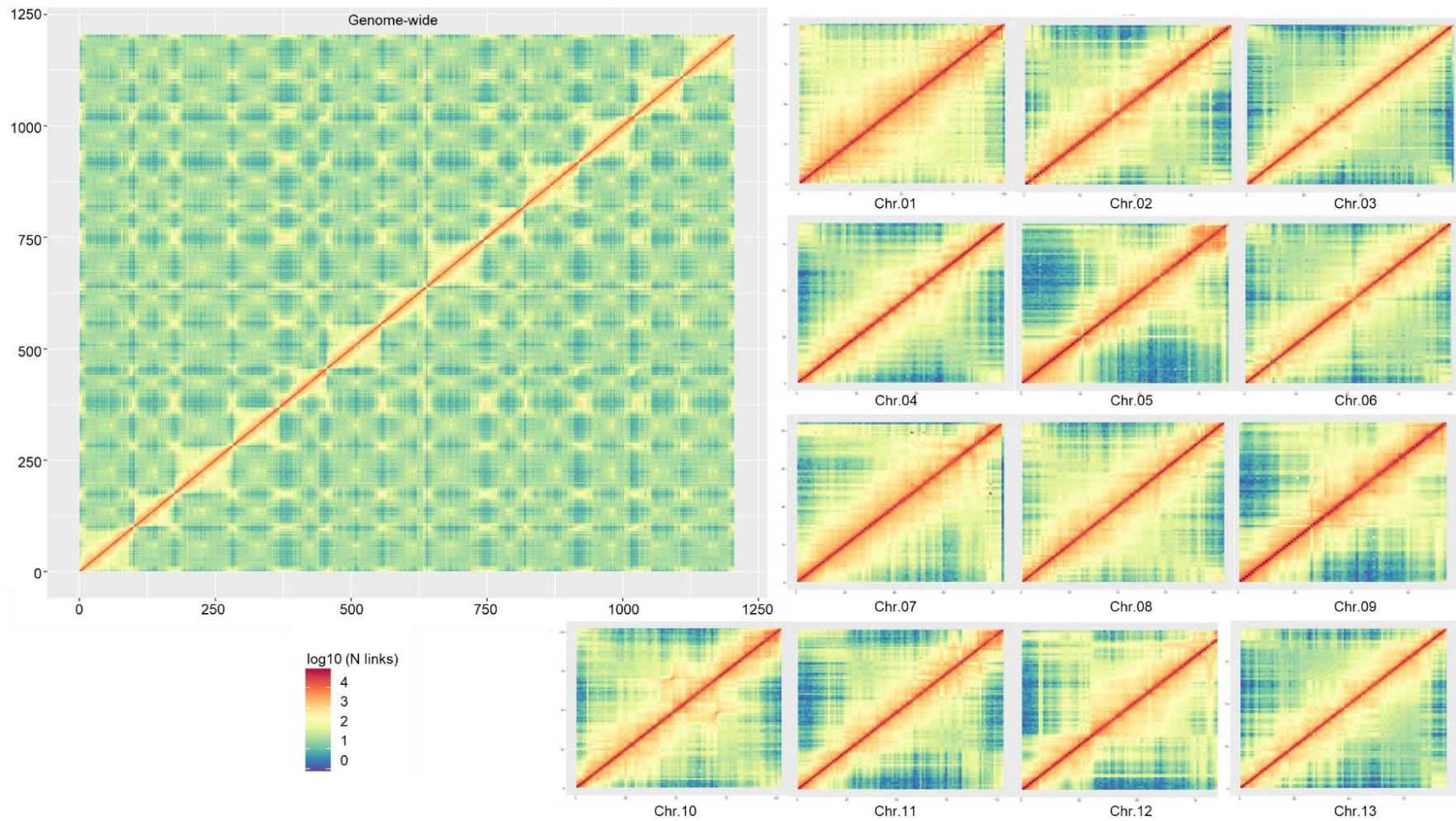
⁴Key Laboratory of Genetics, Breeding and Multiple Utilization of Crops (MOE), Fujian Agriculture and Forestry University, Fuzhou, China

⁵These authors contributed equally to this article.

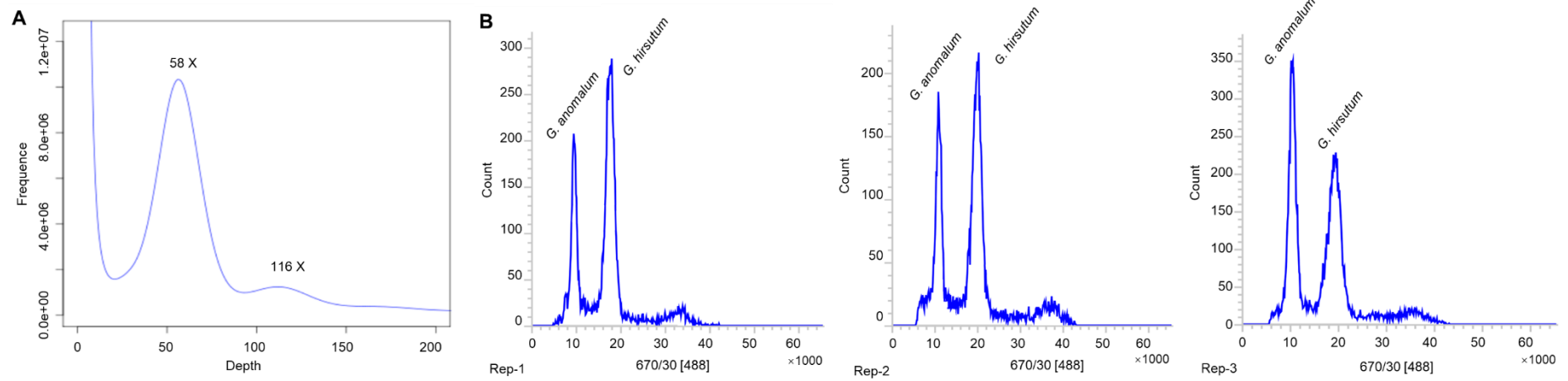
*Correspondence: Kai Wang (kwang5@126.com), Tianzhen Zhang (cotton@zju.edu.cn), Xinlian Shen (xlshen68@126.com)



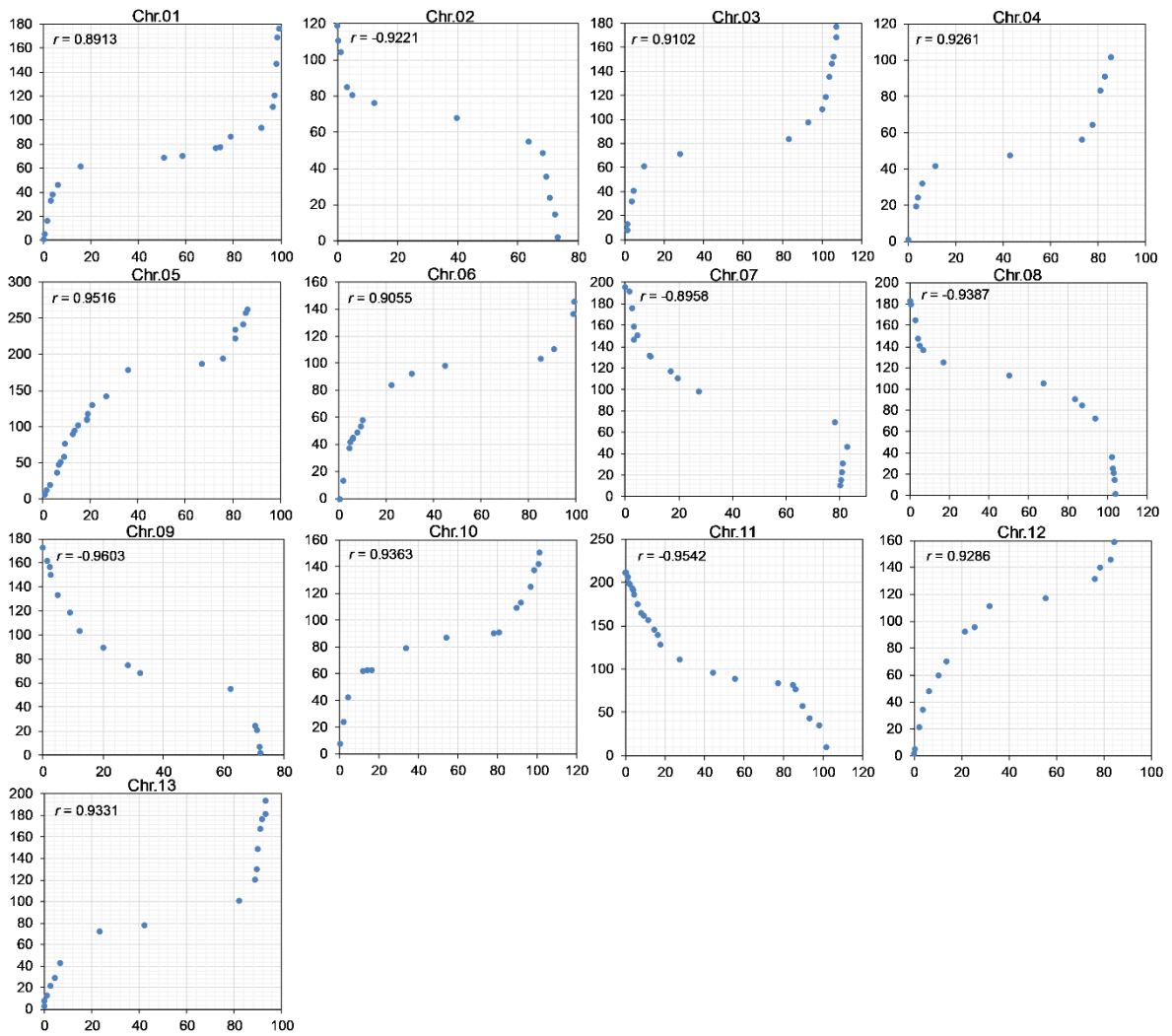
Supplemental Figure 1. Scheme for generating the CSSL population and rapidly discovering and cloning agronomic genes from *G. anomalum*.



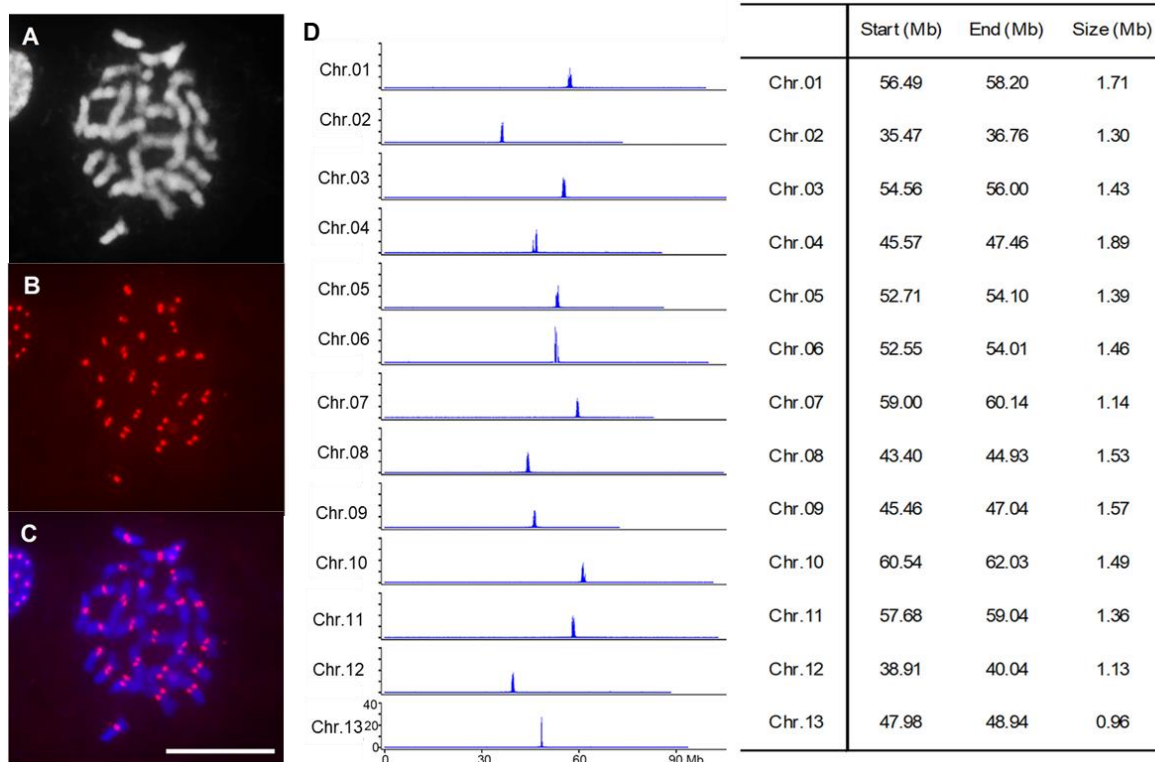
Supplemental Figure 2. Chromatin interaction frequency distribution of Hi-C links among chromosomes of *G. anomalum*. Strong signals (dark red dots) were distributed in diagonal lines, and this indicated that the scaffolds were accurately grouped and oriented on the pseudo-chromosomes.



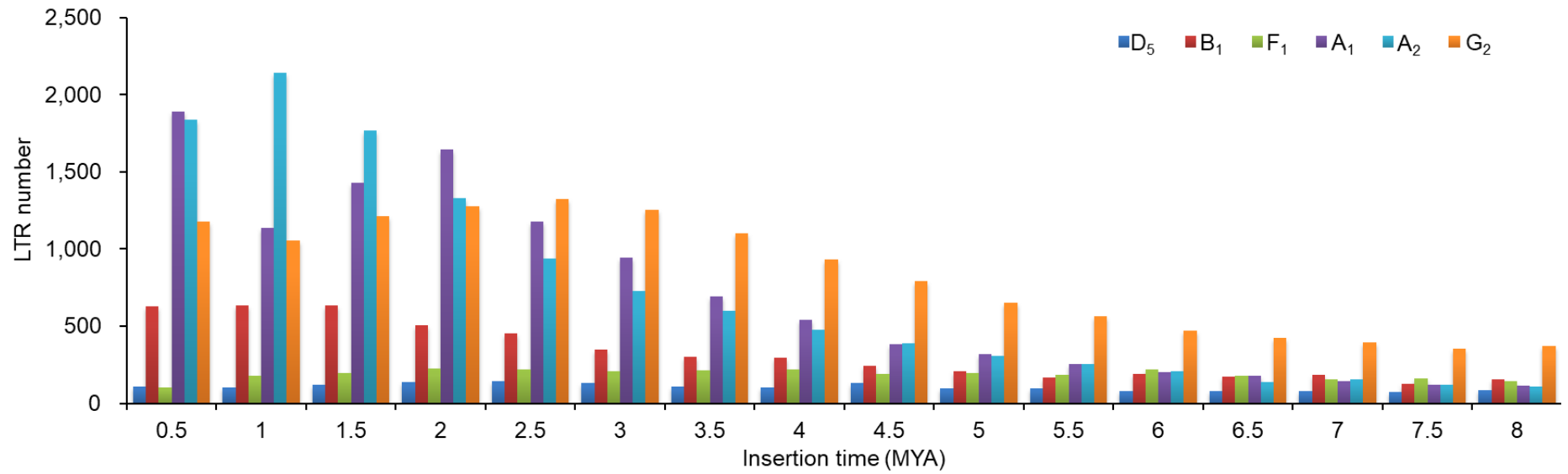
Supplemental Figure 3. (A) Distribution of sequencing depth and K-mer number frequency (K-mer = 17). (B) The schematic diagram of genome size determined by flow cytometry.



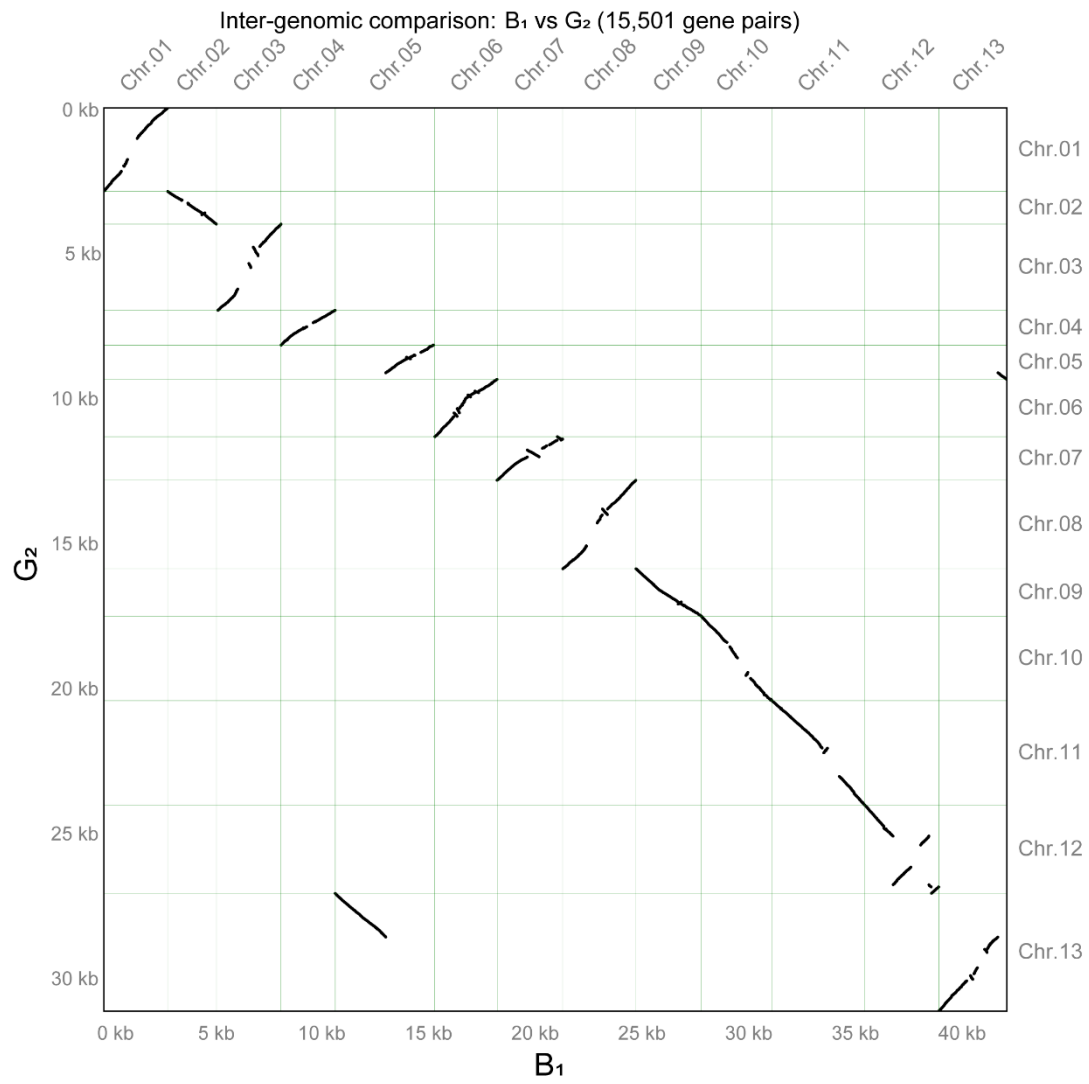
Supplemental Figure 4. Comparison of Hi-C directed chromosome assembly with genetic map in *G. anomalum*. The x-axes represent the physical positions in the assembled chromosomes (Mb) and the y-axes represent the genetic distance on the genetic map (cM). The r represents the correlation coefficient between the genetic and physical map distance.



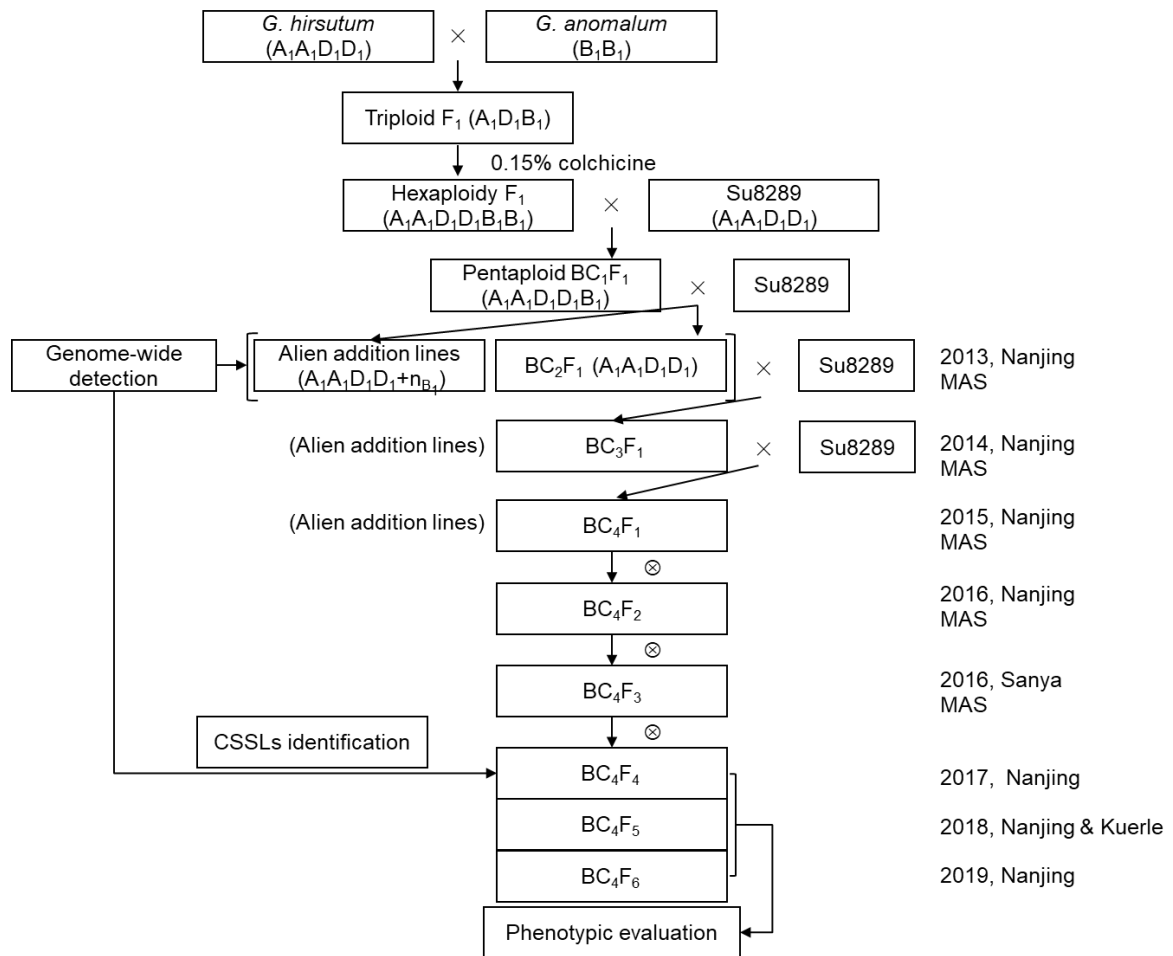
Supplemental Figure 5. Immunostaining using cotton anti-CenH3 antibodies in *G. anomalum*. Somatic metaphase chromosomes were stained with 4', 6-diamidino-2-phenylindole (DAPI) and showed in gray and blue in (A) and (C), respectively. Immunofluorescence signals (B) are visible at the primary constrictions of the chromosomes (C). Scale bar, 10 μ m. (D) The centromere distribution in each chromosome. Left panel, CenH3 binding region i.e. centromere on each chromosome by CenH3 ChIP-seq mapping. The x- and y-axes indicate the position on the chromosome and the read density, respectively. Read density was represented by the percentage of mapped unique reads of respective 10-kb window. Right panel, the list of the size and spanning regions of each centromere.



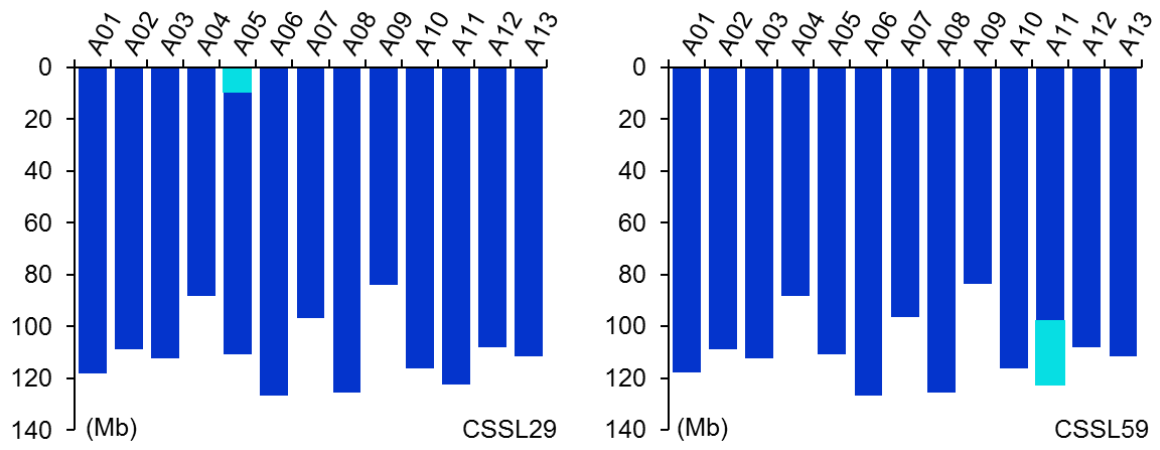
Supplemental Figure 6. Analysis of the LTR number and insertion time in D₅, B₁, F₁, A₁, A₂, and G₂ genome.



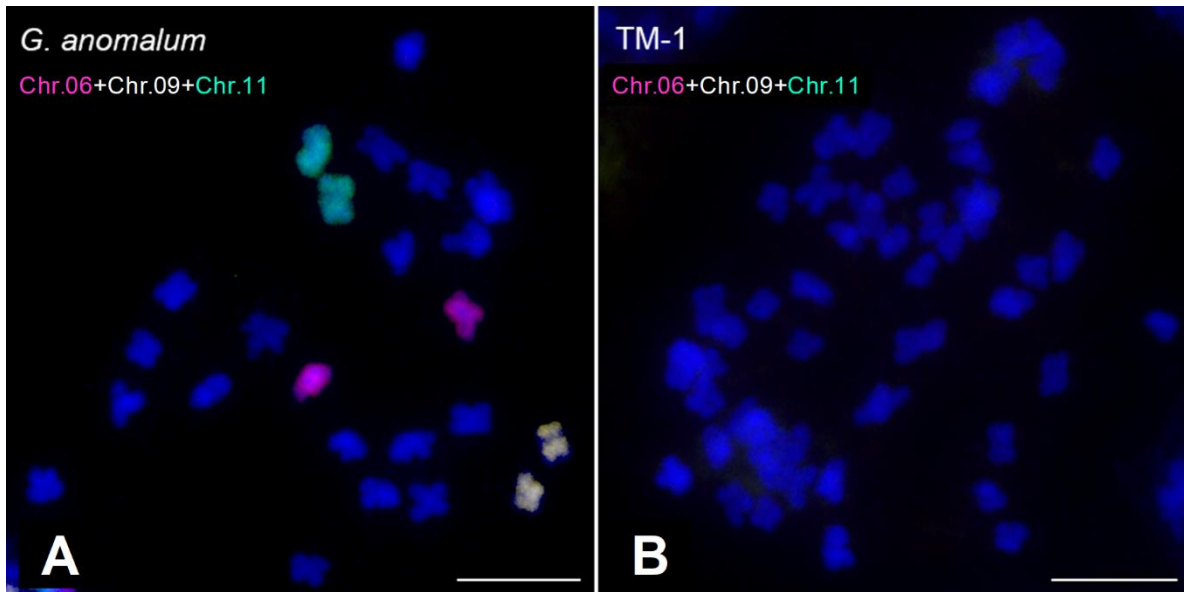
Supplemental Figure 7. Analysis of the synteny between *G. anomalum* and *G. austral* genome.



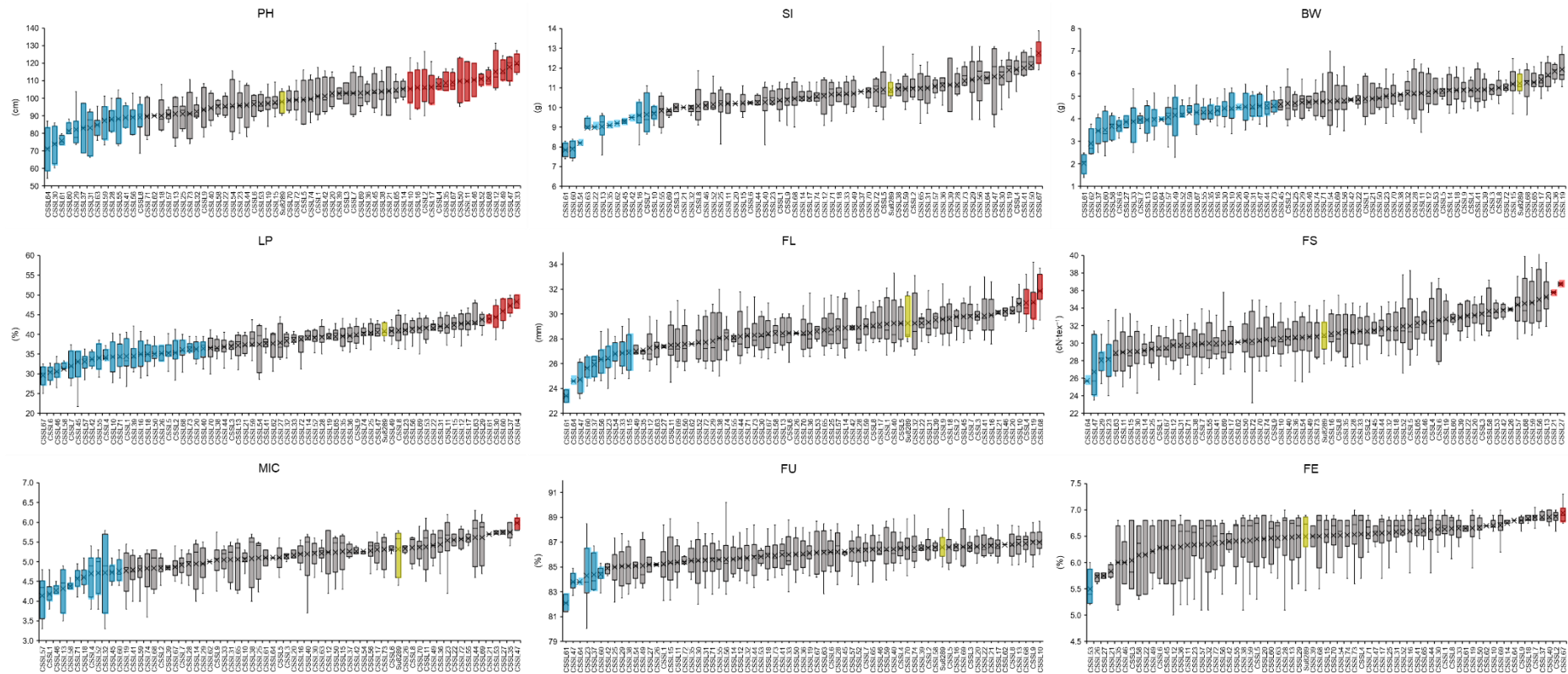
Supplemental Figure 8. Development of the CSSL population.



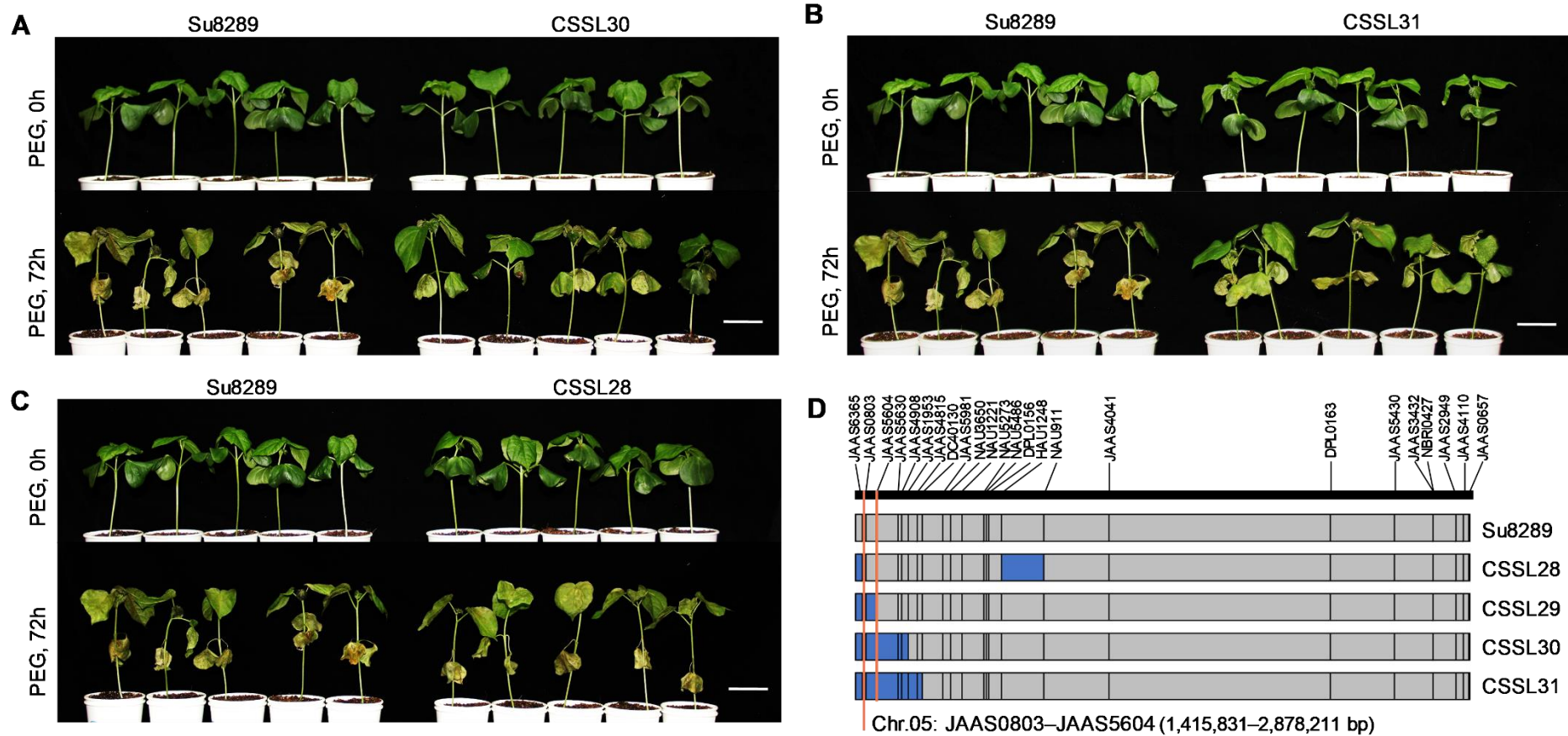
Supplemental Figure 9. Graphical genotype of CSSL29 and CSSL59 based on re-sequencing method. The introgression segments on A05 (from 0.02 Mb to 5.89 Mb) and A11 (from 104.49 Mb to 121.36 Mb) were shown by the light blue box, respectively.



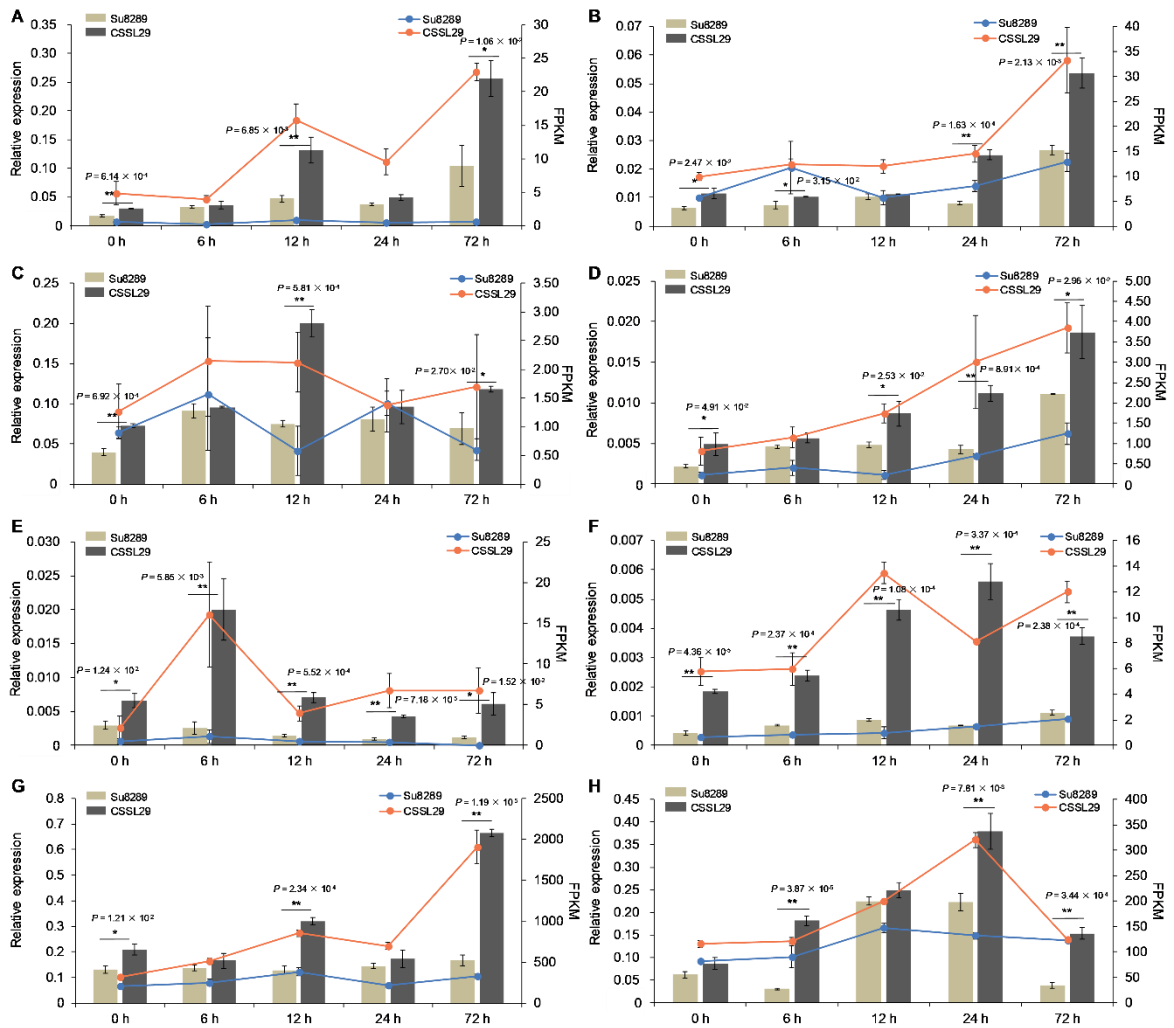
Supplemental Figure 10. FISH analyses using *G. anomalum*-specific oligo probes of chromosomes 6, 9, and 11. FISH image showing that *G. anomalum*-specific oligo probes of chromosomes 6, 9, and 11 were hybridized in the same mitotic metaphase cell of *G. anomalum* (A) and *G. hirsutum* TM-1 (B). The signals of the chromosomes 6, 9, and 11 probes are pseudocolored in magenta, white, and light blue, respectively. Scale bar, 10 μ m.



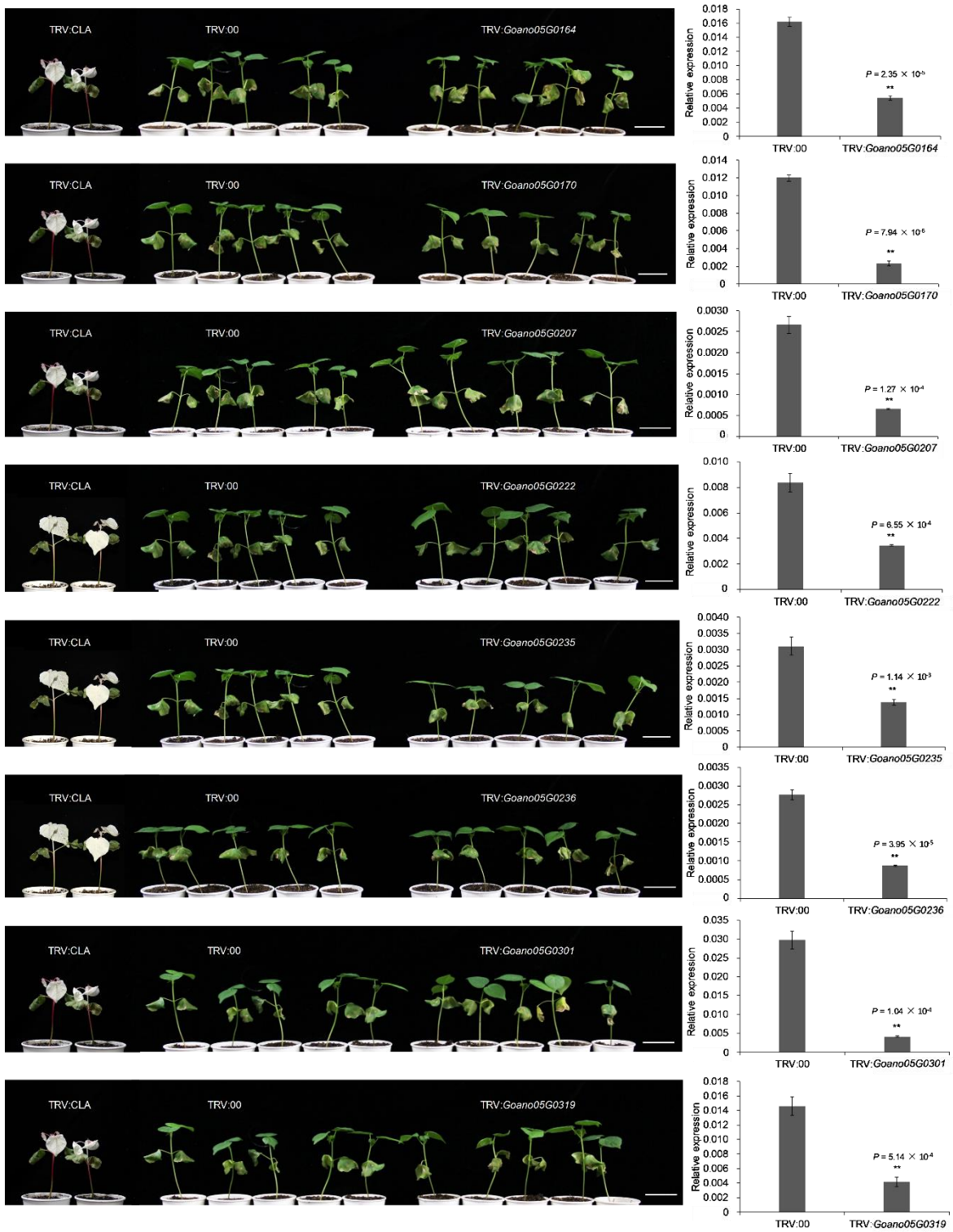
Supplemental Figure 11. Boxplots of phenotypic distribution of nine traits in the CSSL population. The horizontal axis indicates CSSL, and the vertical axis represents phenotypic value. The yellow graph represents the recurrent parent Su8289, the red graph indicates the CSSL with phenotypic value significantly higher ($P < 0.05$) than that of Su8289, while the blue graph indicates the CSSL with phenotypic value significantly lower ($P < 0.05$) than that of Su8289.



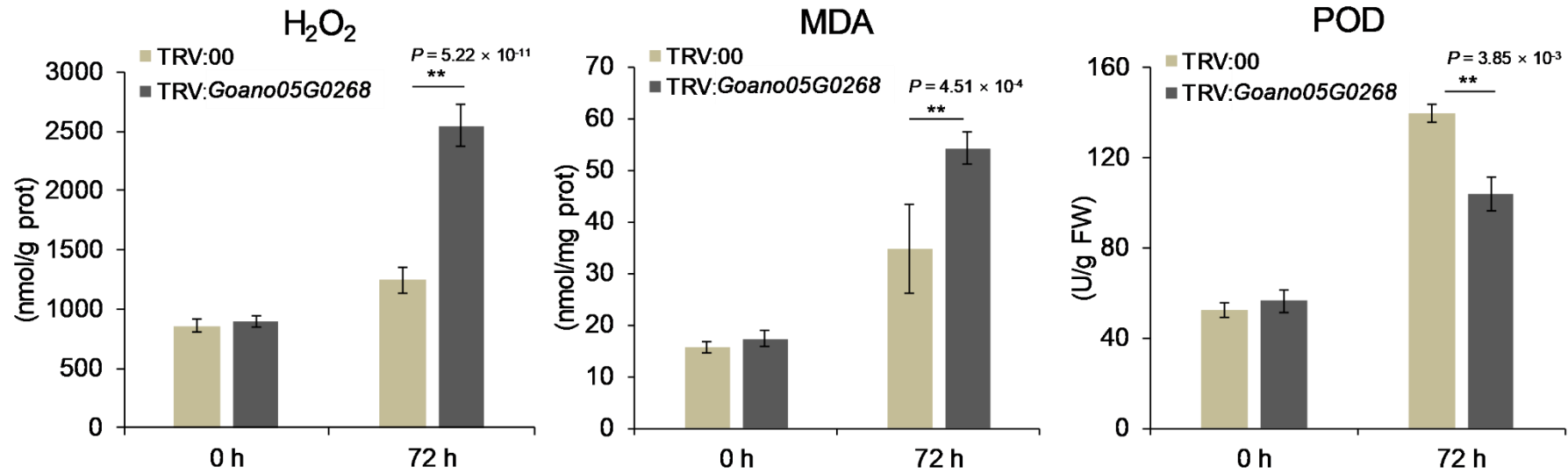
Supplemental Figure 12. Identification of valuable substitution segment associated with drought tolerance. (A, B, and C) Phenotypic comparison of CSSL30, CSSL31, CSSL28, and Su8289 cotton seedlings in response to drought stress in the form of PEG treatment. Photographs were taken at 0 h and 72 h after PEG treatment. Scale bars, 5 cm. (D) Graphical genotypes of SSR interval for drought stress on Chr.05.



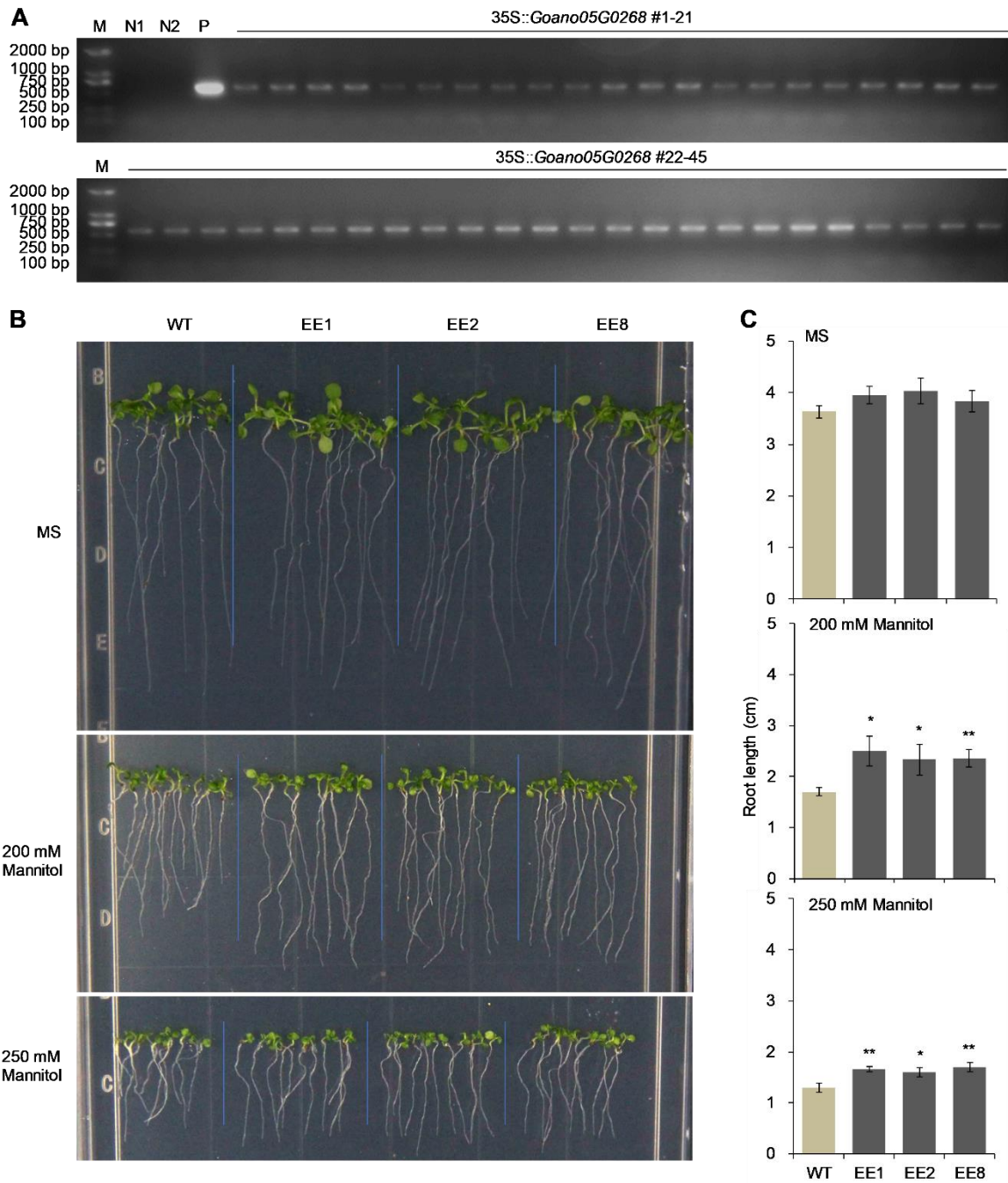
Supplemental Figure 13. Expression level of eight candidate genes under PEG stress in CSSL29 and Su8289. (A-H) Expression level of *Goano05G0164*, *Goano05G0170*, *Goano05G0207*, *Goano05G0222*, *Goano05G0235*, *Goano05G0236*, *Goano05G0301*, and *Goano05G0319* in CSSL29 and Su8289 under PEG stress at 0, 6, 12, 24, and 72 hours. The left y-axis shows the relative expression obtained from qRT-PCR, and the right y-axis shows the FPKM value obtained from RNA-Seq data. * $P < 0.05$, ** $P < 0.01$, Student's *t* test.



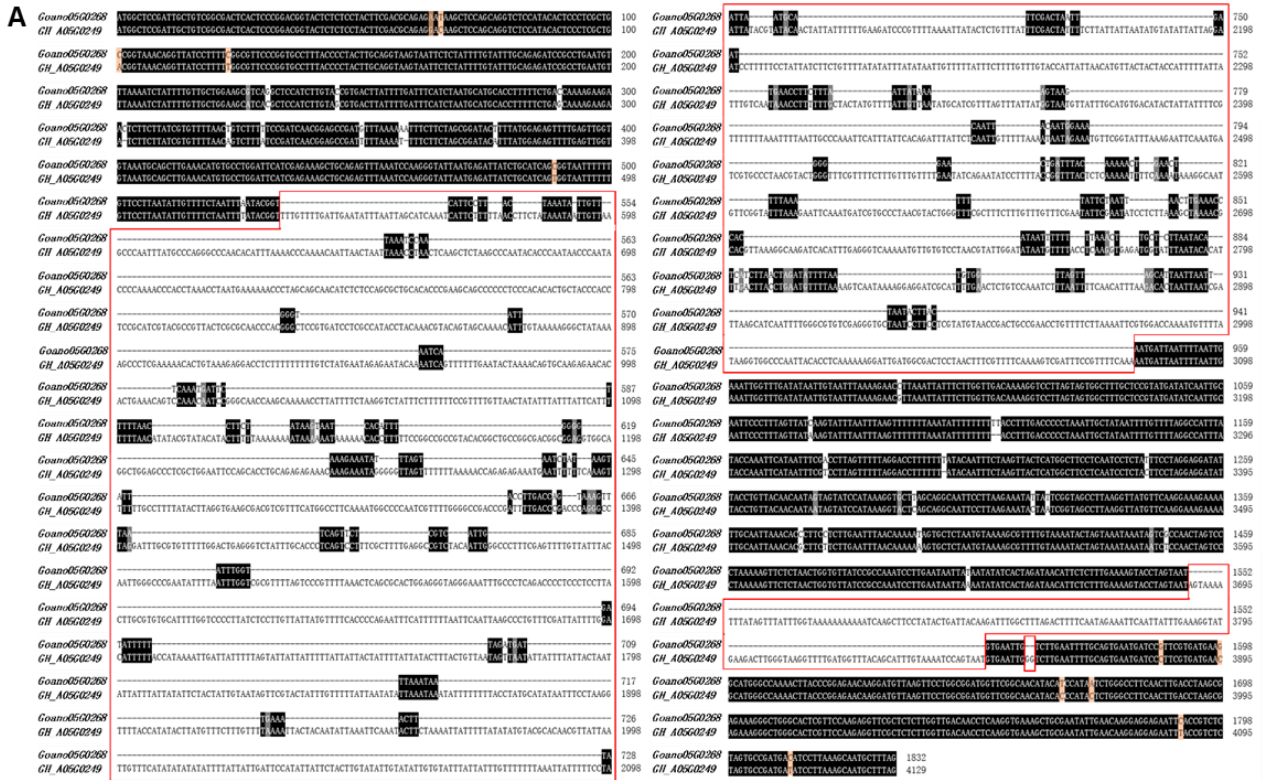
Supplemental Figure 14. Functional verification of eight candidate genes by VIGS. Scale bars, 5 cm. ** $P < 0.01$, Student's t test.



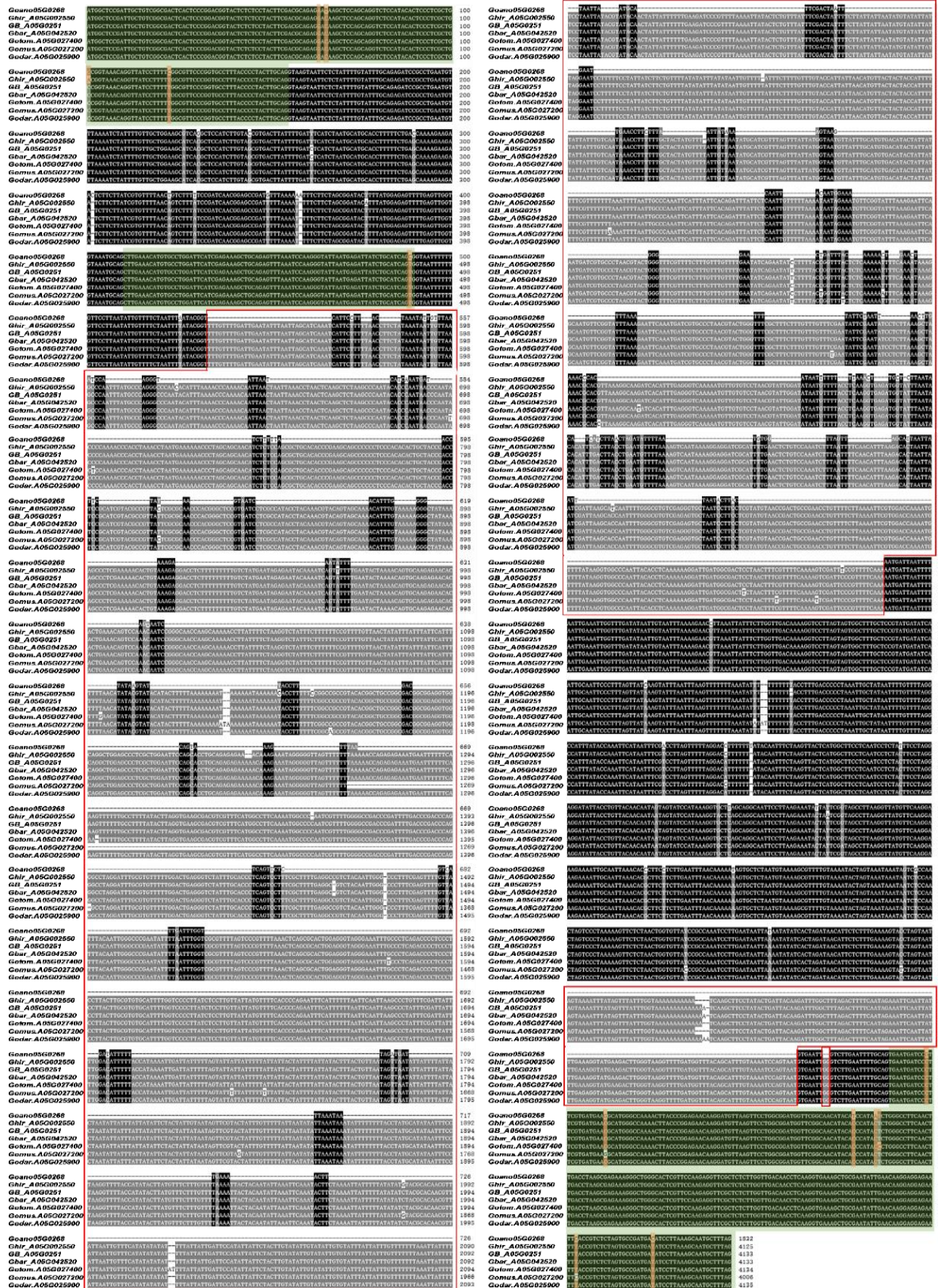
Supplemental Figure 15. Endogenous H₂O₂, MDA, and POD content in TRV:00 and TRV:Goano05G0268 cotton plants under PEG stress. ** $P < 0.01$, Student's t test.



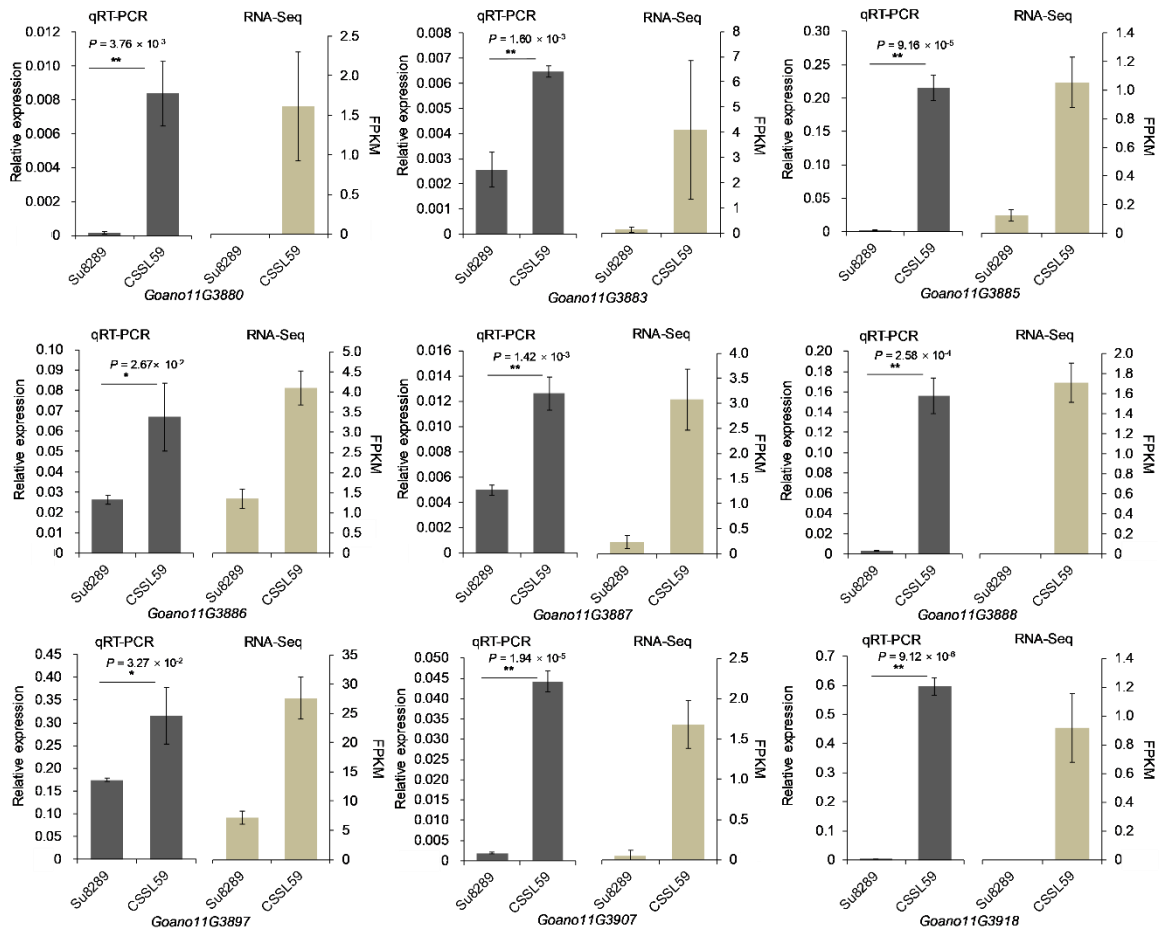
Supplemental Figure 16. Ectopic expression of *Goano05G0268* modulates drought response in *Arabidopsis*. **(A)** Identification of the EE transgenic lines by PCR amplification. M: DNA marker, N1: H₂O control, N2: WT, P: 35::Goano05G0268 plasmid. **(B and C)** Root elongation of seedlings grown on MS medium with 0, 200, and 250 mM mannitol after eight days. * $P < 0.05$, ** $P < 0.01$, Student's *t* test.



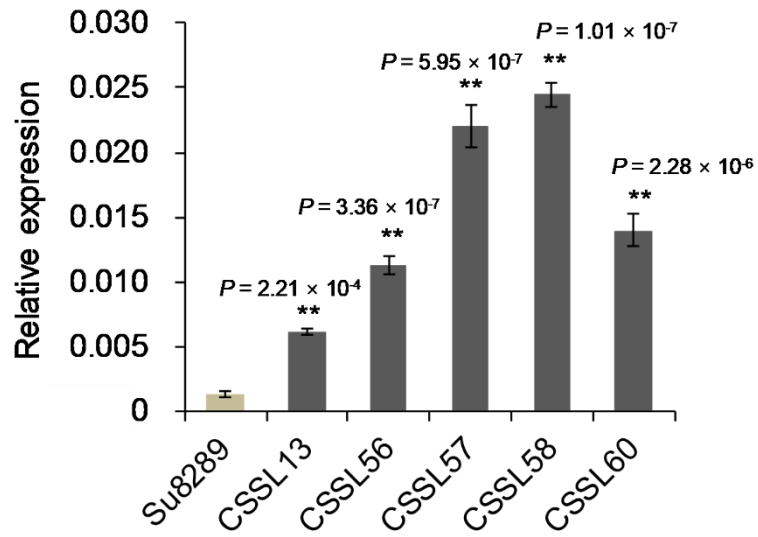
Supplemental Figure 17. (A and B) Structural variation of *Goano05G0268* and *GH_A05G0249* by PCR amplification in CSSL 29 and Su8289, respectively. Sequences highlighted in red boxes are structural variation sites (A). The blue lines represent structural variation sites in exons (B).



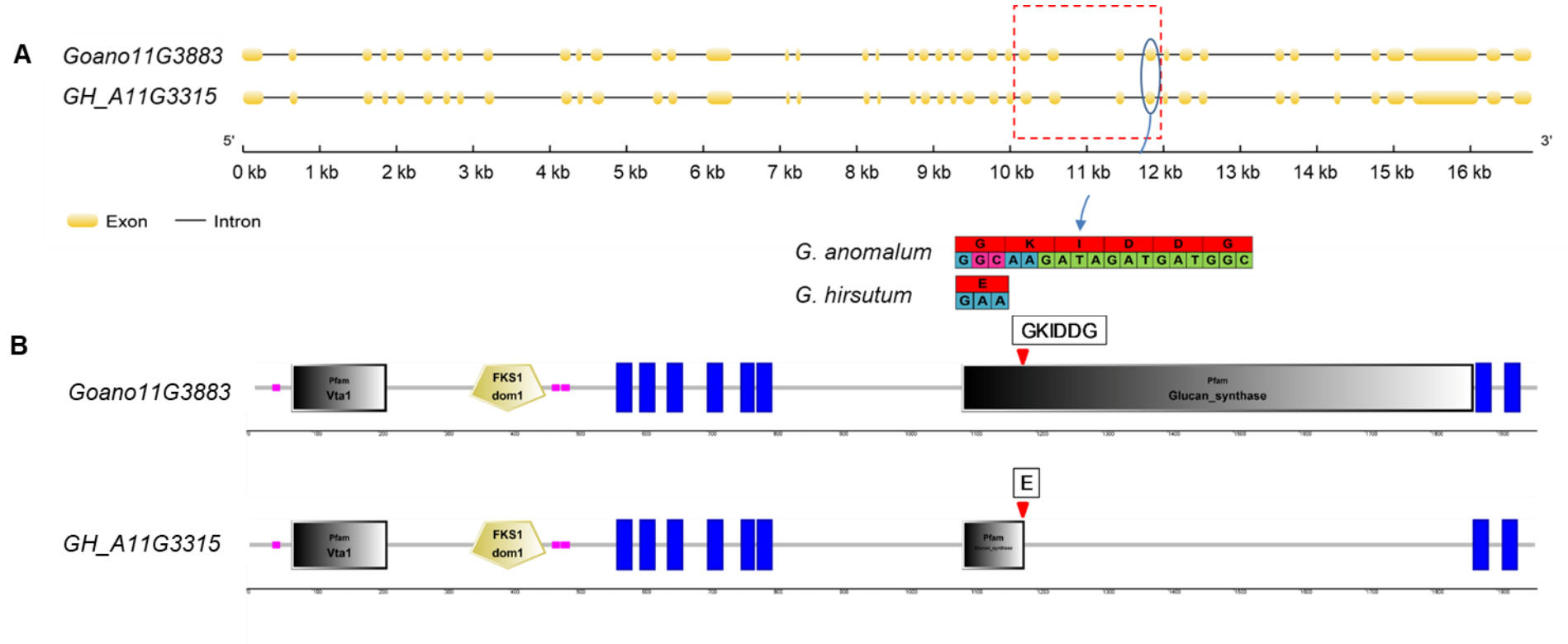
Supplemental Figure 18. Structural variation of *Goano05G0268* and its orthologous gene in *G. hirsutum* L. acc. TM-1, *G. barbadense* L. cv. Hai7124, *G. barbadense* L. accession 3-79, *G. tomentosum*, *G. mustelinum*, and *G. darwinii*, respectively. Sequences highlighted in red boxes are structural variation site.



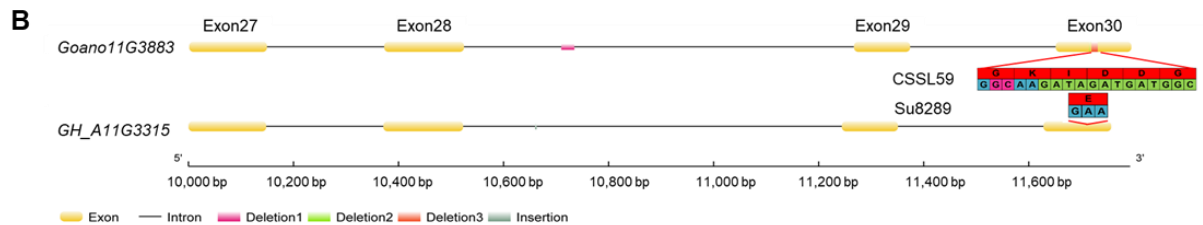
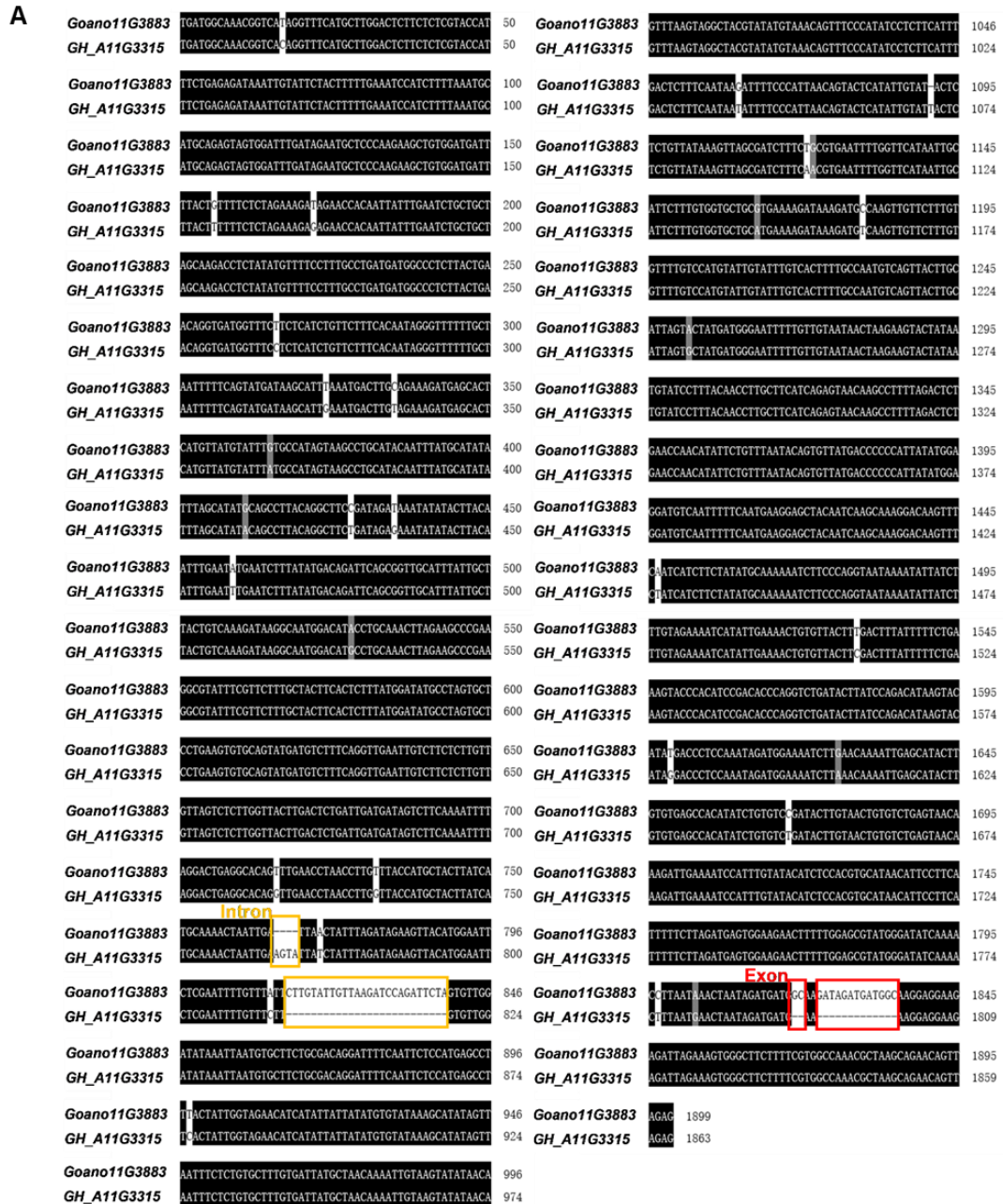
Supplemental Figure 19. The expression level of nine genes in fibers at 20 DPA of CSSL59 and Su8289. The left y-axes show the relative expressions according to qRT-PCR, and the right y-axes show the FPKM values obtained from RNA-seq data. $**P < 0.01$, Student's *t* test.



Supplemental Figure 20. Expression level of *Goano11G3883* in fibers at 20 DPA from Su8289, CSSL13, CSSL56, CSSL57, CSSL58, and CSSL60. ** $P < 0.01$, Student's *t* test.



Supplemental Figure 21. (A and B) Structural and glucan_synthase domain variation of *Goano11G3883* and *GH_A11G3315* in *G. anomalum* and *G. hirsutum* TM-1, respectively.



Supplemental Figure 22. (A and B) Structural variation of *Goano11G3883* and *GH_A11G3315* by PCR amplification in CSSL59 and Su8289, respectively. Sequences highlighted in yellow and red boxes are structural variation sites in intron and exon, respectively (A).

Supplemental Table 1. Statistic of sequencing data from the PacBio Sequel and Illumina platform for *G. anomalum*.

Type of sequencing libraries	Insert size	Read length (bp)	Read number	Total data (Gb)	Sequence depth (×)
PacBio	40 kb	133,688 (Max) 9,561 (Mean) 16,309 (N50)	8,647,163	82.68	64.09
Illumina	230 bp	150	155,987,099	46.60	36.12
	350 bp	150	137,948,704	41.33	32.04
	500 bp	150	149,730,393	44.68	34.64
Total				132.61	102.80

The statistic was based on the filtered data in PacBio library and clean data in Illumina library. Sequence depth was calculated according to the genome size of 1.29 Gb.

Supplemental Table 2. Summary of genome assemblies from PacBio to Hi-C for *G. anomalum*.

Category	PacBio (Contig)	BioNano (Contig)	BioNano (Scaffold)	Hi-C (Contig)	Hi-C (Scaffold)
Contig/Scaffold number	611	687	396	685	364
Contig/Scaffold length (bp)	1,202,351,677	1,202,351,677	1,208,495,100	1,202,351,483	1,208,248,306
Contig/Scaffold Max (bp)	25,786,769	25,786,769	99,134,223	25,786,769	107,236,083
Contig/Scaffold N50 (bp)	7,783,093	6,738,719	73,503,624	6,738,719	99,188,525
Contig/Scaffold N90 (bp)	2,031,882	1,724,051	21,629,783	1,724,051	73,503,624
Gap size (bp)	0	0	6,143,423	0	5,896,823

Supplemental Table 3. Summary of BioNano data quality and assembly results for *G. anomalum*.

Category	<i>G. anomalum</i>
BioNano data quality	
Filtering threshold	150 kb
Enzyme	DLE-1
Molecule number	1,153,134
Total length (Mb)	291,883
Average length (kb)	253
Molecule N50 (kb)	255
Label density (/100 kb)	13.980
Genome coverage (×)	242.800
BioNano assembly results	
Number Genome Maps	144
Total Genome Map Length (Mb)	1,290.326
Mean Genome Map Length (Mb)	8.961
Median Genome Map Length (Mb)	0.746
Genome Map N50 (Mb)	58.216

Supplemental Table 4. Summary of Hi-C mapping data for *G. anomalum*.

Category	Number of reads	Percentage (%)
Unique paired alignments	249,816,916	55.27
Valid read pairs	240,410,680	53.19
Invalid read pairs	9,406,236	2.08
Dangling end pairs	6,689,797	1.48
Re-ligation pairs	2,410,771	0.53
Self-cycle pairs	303,540	0.07
Dumped pairs	2,128	0.00
Multiple pairs alignments	131,108,882	29.01
Pairs with singleton	50,686,398	11.21
Unmapped pairs	20,353,034	4.50
Total read pairs	451,965,230	100.00

Supplemental Table 5. Characteristics of the 13 pseudo-chromosomes in the final genome assembly of *G. anomalum*.

Pseudo-chromosome	Number of scaffolds ^a	Size (bp)
Chr.01	3	99,188,525
Chr.02	1	73,503,624
Chr.03	3	107,236,083
Chr.04	1	85,652,033
Chr.05	3	86,126,817
Chr.06	10	99,994,996
Chr.07	4	83,060,063
Chr.08	3	104,733,974
Chr.09	2	72,545,696
Chr.10	2	101,529,486
Chr.11	4	102,973,240
Chr.12	3	88,411,662
Chr.13	2	93,713,888
Total	41	1,198,670,087

^aThe scaffolds here were obtained from the BioNano assembly and some of them were truncated by others in the following Hi-C process.

Supplemental Table 6. Summary of genome base content for *G. anomalum*.

Base type	Number (bp)	Percentage of genome (%)
A	395,389,494	32.72
T	395,196,517	32.71
C	206,049,696	17.05
G	205,715,776	17.03
N	5,896,823	0.49
Total	1,208,248,306	100.00
G + C	411,765,472	34.25 ^a

^aGC content of the genome without N.

Supplemental Table 7. Evaluation of genome assembly integrity of *G. anomalum* using the BUSCO method.

BUSCOs	Number	Percentage (%)
Complete BUSCOs (C)	2,303	99.01
Complete single-copy BUSCOs (S)	2,086	89.68
Complete duplicated BUSCOs (D)	217	9.33
Fragmented BUSCOs (F)	10	0.43
Missing BUSCOs (M)	13	0.56
Total BUSCO groups searched	2,326	100

BUSCO: Benchmarking Universal Single-Copy Ortholog.

Supplemental Table 8. Evaluation of genome assembly integrity of *G. anomalum* using the CEGMA method.

	Complete + Partial CEGMAs		Total CEGMA groups searched	
	number	Percentage (%)	number	Percentage (%)
<i>G. anomalum</i>	242	97.58	248	100
<i>G. anomalum</i> (Grover et al., 2021)	243	97.98	248	100

CEGMA: Core Eukaryotic Genes Mapping Approach.

Supplemental Table 9. Summary of Illumina short reads mapping in *G. anomalum* genome.

	Category	Percentage (%)
Reads	Mapping rate	97.25
	Average sequencing depth	96.93
	Coverage	99.90
Genome	Coverage at least 4×	99.84
	Coverage at least 10×	99.74
	Coverage at least 20×	99.42

Supplemental Table 10. The sequence coverage of the *G. anomalum* genome by homologous search using RNA-seq data.

Dataset	Number	Total length (bp)	Bases covered by assembly (%)	Sequences covered by assembly (%)	with > 90% sequence in one scaffold		with > 50% sequence in one scaffold	
					Number	Percent	Number	Percent
> 500 bp	141,863	239,349,699	90.948	88.648	113,205	79.799	124,766	87.948
> 1,000 bp	91,314	203,490,609	93.068	93.668	75,296	82.458	85,040	93.129
> 2,000 bp	42,452	132,559,496	94.850	96.928	34,882	82.168	40,925	96.403
> 5,000 bp	2,683	16,839,815	95.370	98.658	2,091	77.935	2,626	97.876

Supplemental Table 11. Summary of gene structure annotation in *G. anomalum* genome.

	Gene set	Number	Average gene length (bp)	Average CDS length (bp)	Average exons per gene	Average exon length (bp)	Average intron length (bp)
De novo	Augustus	58,306	2,113.65	969.23	4.04	239.88	376.39
	GlimmerHMM	110,304	9,227.34	583.06	2.79	208.71	4,819.37
	SNAP	38,739	8,617.61	548	3.75	146.15	2,934.88
	Geneid	85,816	4,341.16	694.95	3.82	181.78	1,291.55
	Genscan	58,848	12,145.66	1,010.16	5.15	196.30	2,685.93
Homolog	<i>Arabidopsis thaliana</i>	75,480	1,294.09	679.65	2.50	271.49	408.71
	<i>Gossypium arboreum</i>	39,986	2,687.86	1,190.45	3.96	300.86	506.43
	<i>Gossypium hirsutum</i>	66,844	2,412.87	997.83	3.32	300.67	610.27
	<i>Gossypium raimondii</i>	70,338	1,622.10	791.99	3.07	258.21	401.56
	<i>Populus trichocarpa</i>	39,204	2,619.07	1,169.22	3.72	314.34	533.12
	<i>Theobroma cacao</i>	34,369	2,808.17	1,310.04	4.01	326.70	497.73
RNA-seq	PASA	82,914	2,728.24	1,001.98	4.89	204.72	443.28
	Cufflinks	54,828	4,768.84	2,110.71	6.42	328.77	490.43
EVM		64,660	2,266.69	906.12	3.84	235.89	478.87
Pasa-update*		64,373	2,236.80	907.45	3.82	237.49	471.23
Final set*		42,752	3,140.07	1,099.98	4.75	291.92	464.73

* It contains UTR region, others do not contain UTR region.

Supplemental Table 12. Summary of gene function annotation by using different databases.

	Database	Number	Percent (%)
Annotated		41,592	97.29
	Swissprot	30,288	70.85
	Nr	41,561	97.21
	KEGG	30,706	71.82
	InterPro	33,900	79.29
	GO	21,680	50.71
	Pfam	31,663	74.06
Unannotated		1,160	2.71

Supplemental Table 13. Summary of non-coding RNAs in the *G. anomalum* genome.

Type	Copy number	Average length (bp)	Total length (bp)
miRNA	262	129.67	33,974
tRNA	1,085	74.73	81,078
rRNA	774	296.19	229,250
18S	110	1,277.05	140,476
28S	307	138.80	42,613
5.8S	82	160.12	13,130
5S	275	120.11	33,031
snRNA	6,064	107.49	651,847
CD-box	5,872	106.47	625,211
HACA-box	52	125.73	6,538
splicing	140	143.56	20,098
Total	8,185		996,149

Supplemental Table 14. The summary of repetitive sequences.

Type	Number	Length (bp)	% (genome)
Class I: Retrotransposon	840,690	728,632,679	60.30
LTR retrotransposon	805,038	714,153,605	59.11
Copia	136,198	66,734,309	5.52
Gypsy	598,287	607,203,108	50.25
Unclassied	70,553	40,216,188	3.33
non-LTR Retroelement	35,652	14,479,074	1.20
LINE	35,566	14,415,724	1.20
SINE	86	63,350	0.0052
Class II: DNA transposon	32,627	13,910,223	1.15
TIR/MULE-MuDR	14,505	6,577,793	0.54
TIR/CMC	6,354	2,606,893	0.22
TIR/P	432	290,271	0.02
TIR/PIF	2,593	1,034,534	0.09
TIR/TcMar	175	69,345	0.0057
TIR/hAT	6,511	2,412,317	0.20
Helitron/Helitron	1,623	775,713	0.06
Unclassified	434	143,357	0.01
Other	2,172	1,620,171	0.13
Simple_repeat	2,172	1,620,171	0.13
unknown	20,680	12,118,599	1.00
Total	896,169	756,281,672	62.59

Supplemental Table 15. The summary of chromosomal rearrangements between *G. anomalum* and other extant diploid cotton genomes. (included as a separate EXCEL file)

Supplemental Table 16. Primers of 230 SSR markers. (included as a separate EXCEL file)

Supplemental Table 17. Population size for marker-assisted selection.

Chr.	BC ₃ F ₁	BC ₄ F ₁	BC ₄ F ₂	BC ₄ F ₃	BC ₄ F ₄
Chr.01	888 (86)*	774 (50)*	752 (132)*	145	127
Chr.02	495 (77)	464 (119)	487 (69)	117	155
Chr.03	243 (32)	696 (503)	227 (108)	20	55
Chr.04	165 (41)	348 (123)	240 (94)	145	210
Chr.05	170 (64)	318 (40)	347 (48)	113	104
Chr.06	299 (228)	869 (761)	347 (112)	136	214
Chr.07	121 (91)	443 (443)	207 (170)	47	98
Chr.08	275 (275)	392 (392)	183 (112)	58	121
Chr.09	209 (114)	588 (410)	235 (108)	66	181
Chr.10	250 (201)	550 (493)	259 (188)	245	293
Chr.11	827 (63)	1,377 (57)	706 (46)	267	395
Chr.12	128 (65)	795 (589)	247 (69)	73	33
Chr.13	261 (240)	926 (926)	306 (143)	101	239
Total	4,331 (1,577)	8,540 (4,906)	4,543 (1,399)	1,533	2,225

*The data in parentheses is the number of plants from alien addition lines.

Supplemental Table 18. The number of recombination types identified in each generation.

Chr.	BC ₂ F ₁	BC ₃ F ₁	BC ₄ F ₁	BC ₄ F ₂	BC ₄ F ₃	BC ₄ F ₄
Chr.01	3	4	9	8	8	13
Chr.02	4	5	6	3 (2)	3 (2)	3
Chr.03	1	1	3	1 (1)	1 (1)	1 (1)
Chr.04	1	5	3	2 (1)	2 (1)	3
Chr.05	4	6	6	6	7	7
Chr.06	2	2	3	5	5	6 (1)
Chr.07	1	0	1	1	1	1
Chr.08	1	0	3	1	1	2 (1)
Chr.09	3	2	2	3 (1)	3 (1)	3 (1)
Chr.10	1	2	2	1	1	3
Chr.11	11	11	11	13 (1)	14 (1)	17
Chr.12	3	2	3	3	3	3
Chr.13	1	0	4	4	4	4
Total	36	40	56	51 (6)	53 (6)	74* (4)

The data in the parentheses denotes the number of hybrid recombination types in the generations produced by selfing.

*Since some recombination types containing substitution segments from different chromosomes, the total number of recombination types was greater than the total number accumulated in chromosome units.

Supplemental Table 19. Summary of introgression segments. (included as a separate EXCEL file)

Supplemental Table 20. Genome coverage of *G. anomalum* substitution segments in the CSSL population.

Chr.	B ₁	B ₁ -introgression	Coverage (%)
Chr.01	176.40	176.40	100.00
Chr.02	191.50	156.14	81.54
Chr.03	118.70	71.10	59.90
Chr.04	101.60	101.60	100.00
Chr.05	263.90	116.90	44.30
Chr.06	167.80	146.10	87.07
Chr.07	195.40	119.60	61.21
Chr.08	183.50	183.50	100.00
Chr.09	172.60	157.50	91.25
Chr.10	165.50	29.60	17.89
Chr.11	216.20	216.20	100.00
Chr.12	159.50	53.25	33.39
Chr.13	198.10	140.80	71.08
Total	2,310.70	1,668.69	72.22

Supplemental Table 21. Summary of Illumina re-sequencing data for CSSLs. (included as a separate EXCEL file)

Supplemental Table 22. Descriptive statistics of nine traits in the *G. anomalum*-derived CSSL population in multiple environments. (included as a separate EXCEL file)

Supplemental Table 23. The detected segments/QTLs of the agronomic traits in the *G. anomalum*-derived CSSL population. (included as a separate EXCEL file)

Supplemental Table 24. Summary of RNA-Seq data for CSSL29 and Su8289 during PEG stress.

Sample	Raw reads	Clean reads	Clean base (Gb)	Error rate (%)	Q20 (%)	Q30 (%)	GC content (%)
CSSL29_0h_1	61,426,990	60,361,996	9.05	0.03	97.82	93.65	44.75
CSSL29_0h_2	44,191,544	43,628,714	6.54	0.03	97.73	93.43	44.47
CSSL29_0h_3	50,666,142	49,874,820	7.48	0.03	97.78	93.54	44.40
CSSL29_6h_1	52,910,090	51,782,160	7.77	0.03	97.73	93.49	44.81
CSSL29_6h_2	58,005,932	56,894,338	8.53	0.03	97.83	93.69	44.89
CSSL29_6h_3	47,752,394	47,012,056	7.05	0.03	97.86	93.77	44.97
CSSL29_12h_1	53,507,968	52,325,294	7.85	0.03	97.88	93.81	44.51
CSSL29_12h_2	55,945,848	54,851,274	8.23	0.03	97.86	93.76	44.52
CSSL29_12h_3	50,944,974	50,096,754	7.51	0.03	97.74	93.48	44.55
CSSL29_24h_1	49,578,464	48,538,146	7.28	0.03	97.06	91.96	43.86
CSSL29_24h_2	44,966,346	44,162,348	6.62	0.03	97.76	93.58	43.75
CSSL29_24h_3	46,933,152	45,592,854	6.84	0.03	97.74	93.49	43.78
CSSL29_72h_1	51,561,758	50,548,304	7.58	0.03	97.69	93.37	44.36
CSSL29_72h_2	39,450,540	38,676,436	5.80	0.03	97.69	93.34	44.48
CSSL29_72h_3	47,329,794	46,003,272	6.90	0.03	97.75	93.53	44.34
Su8289_0h_1	50,433,980	48,946,092	7.34	0.03	97.40	92.68	43.77
Su8289_0h_2	57,284,664	55,813,900	8.37	0.03	97.68	93.38	43.70
Su8289_0h_3	50,878,936	49,550,684	7.43	0.03	97.81	93.64	43.84
Su8289_6h_1	54,160,104	52,570,184	7.89	0.03	97.80	93.64	44.83
Su8289_6h_2	48,345,034	47,398,424	7.11	0.03	97.77	93.50	45.03
Su8289_6h_3	47,582,286	46,571,368	6.99	0.03	97.93	93.94	44.27
Su8289_12h_1	45,899,858	44,919,500	6.74	0.03	97.69	93.41	44.26
Su8289_12h_2	54,921,350	53,900,484	8.09	0.03	97.69	93.41	44.33
Su8289_12h_3	42,819,618	41,180,122	6.18	0.03	97.78	93.60	44.35
Su8289_24h_1	49,719,686	48,971,020	7.35	0.03	97.69	93.39	44.52
Su8289_24h_2	71,473,464	70,755,984	10.61	0.03	97.78	93.59	44.66
Su8289_24h_3	43,695,654	43,176,316	6.48	0.03	97.48	92.79	44.61
Su8289_72h_1	53,836,832	52,959,380	7.94	0.03	97.76	93.47	44.13
Su8289_72h_2	53,247,538	52,145,682	7.82	0.03	97.61	93.15	44.15
Su8289_72h_3	53,473,164	52,345,388	7.85	0.03	97.68	93.35	44.08

Supplemental Table 25. The annotation and expression level of 20 genes in CSSL29 and Su8289 during PEG stress. (included as a separate EXCEL file).

Supplemental Table 26. The qRT-PCR primers for nine candidate genes on the JAAS0803–JAAS5604 interval.

Gene ID	Forward PCR primer (5'–3')	Reverse PCR primer (5'–3')
<i>Goano05G0268</i>	AAGCTGCGAATATTGAACA	CAAGATGACCTCCGTAGATA
<i>Goano05G0164</i>	CTATGTACGCCGAGTTAATATG	CTTCTTCTTCTTCAGCATCC
<i>Goano05G0170</i>	AAAGTTCCCATTCATCATCAC	TCAAGCCTTAGACAAGTCAT
<i>Goano05G0207</i>	CACCAACAATAGCAACAATC	TTGAACTCATTAGCATCGTT
<i>Goano05G0222</i>	CTTTCCTTCCATTCTCCAAA	TCATCCATATCTTCATTCATAGAG
<i>Goano05G0235</i>	TGGATGGAGTGACCTCATACAA	ATCAAGAAGGAGATGTCCAAAGC
<i>Goano05G0236</i>	TTCTCAACTGTGCCTCCTAC	GTCCAGCATTATTAACACCATCTT
<i>Goano05G0301</i>	AGCAAGACAAGAAGAAGAAG	TCTCAGATGAGTTAGGTCC
<i>Goano05G0319</i>	TCTCAATCTCAAAGTAGAAAGAAG	CAACCATGAACAAGACCATAT

Supplemental Table 27. The VIGS primers for nine candidate genes on the JAAS0803–JAAS5604 interval.

Gene ID	Forward PCR primer (5'–3')	Reverse PCR primer (5'–3')
<i>Goano05G0268</i>	CGGGATCCGGTCTCCATACACTCCCTCG	CGAGTCATGACCTCCGTAGATAAAAAG
<i>Goano05G0164</i>	CGGAATTCTTCGTGAAAGCCGAGGAATA	CGGGATCCGAGATTGCGTCATTGGTCAT
<i>Goano05G0170</i>	CGGGATCCAAGTCCCATTTCATCATCAC	CGAGCTCACATATGGACTTCTTAACTC
<i>Goano05G0207</i>	CGGAATTCAGCAACAATCAGACGAGCCA	CGGGATCCCTCAAGTTACTAGCATACGC
<i>Goano05G0222</i>	CGGGATCCGCACCTCCTCCTCACTTCTG	CGAGCTCACCTAACCCTAAACCCTAAT
<i>Goano05G0235</i>	CGGGATCCAGGCTCTTGTTCTTGTTTCT	CGAGCTCTTTCATTGTTTCATCCATAT
<i>Goano05G0236</i>	CGGGATCCCACAAGGATGGCAAACCTGGC	CGAGCTCAGGATGGCATTGCTCTTTAT
<i>Goano05G0301</i>	CGGAATTCCTGCTCACCGCCATAAGCGAAAT	CGGGATCCCTTCTTGCTTCTTCACCTACAT
<i>Goano05G0319</i>	CGGGATCCCAGGAGCAGAAACAACCATC	CGAGCTCGCTAAGGTGGTGGGGAGAAT

Supplemental Table 28. The PCR primers of *Goano05G0268* and its orthologous gene *GH_A05G0249* in Su8289.

Gene ID	Sample	Forward PCR primer (5'–3')	Reverse PCR primer (5'–3')
<i>Goano05G0268</i>	CSSL29	CAACCGACTTACATCATCACCTTC	AACAAGATGACCTCCGTAGATAAA
<i>GH_A05G0249</i>	Su8289	CAACTGCCTTAGCAACCGACTT	TATTGCCATAACCATCAAGTGC

Supplemental Table 29. Structural variation statistics of *Goano05G0268* and its orthologous gene in other allotetraploid cotton species.

Genome	Assembly	Gene name	Deletion (bp)	Insertion-1 (bp)	Insertion-2 (bp)	Insertion-3 (bp)	SNP in exon
B ₁	<i>G. anomalum</i>	<i>Goano05G0268</i>					
(AD) ₁	<i>G. hirsutum</i> HAU v1.1	<i>Ghir_A05G002550</i>	408	2,544	159	2	10
(AD) ₂	<i>G. barbadense</i> ZJU v1.1	<i>GB_A05G0251</i>	408	2,548	162	2	9
(AD) ₂	<i>G. barbadense</i> HAU v2.0	<i>Gbar_A05G042520</i>	408	2,548	162	2	9
(AD) ₃	<i>G. tomentosum</i> HGS_v1.1	<i>Gotom.A05G027400</i>	408	2,550	161	2	10
(AD) ₄	<i>G. mustelinum</i> JGI_v1.1	<i>Gomus.A05G027200</i>	408	2,422	159	2	8
(AD) ₅	<i>G. darwinii</i> HGS_v1.1	<i>Godar.A05G025900</i>	408	2,549	163	2	9

Supplemental Table 30. The detected segments/QTLs of the trait of FS in the *G. anomalum*-derived CSSL population.

Environment	Marker interval	Chr.	Start (bp)	End (bp)	LOD	PVE (%)	ADD
E1	JAAS4769–NAU2152	Chr.11	91,616,161	99,990,495	4.96	40.49	2.39
E2	NAU1305–NAU3678	Chr.07	36,412,351	80,217,863	2.91	16.45	-2.79
E2	JAAS4769–NAU2152	Chr.11	91,616,161	99,990,495	3.66	21.39	1.48
E3	JAAS4769–NAU2152	Chr.11	91,616,161	99,990,495	5.91	43.97	1.96
E4	JAAS4769–NAU2152	Chr.11	91,616,161	99,990,495	3.24	20.51	1.72
Mean	JAAS2076–JAAS2022	Chr.04	27,206,433	79,551,098	2.71	12.72	2.28
Mean	JAAS4769–NAU2152	Chr.11	91,616,161	99,990,495	4.38	21.77	1.78

Supplemental Table 31. Primers of 19 SSR markers for fine mapping of the *qFS11*.

Marker name	Forward PCR primer (5'–3')	Reverse PCR primer (5'–3')
NAU3703	AACTCCCATCATCAGCAAGT	TATCAATCGGTTTCAGCAATG
JAAS8011	TGTGTGTGTGTTATTGGCTGC	GACCCAGTTGTGTCTAATGTTTTG
JAAS8027	TGCCCCACCATTCTATTGAT	GAAGCTGCCTTTCCTCACC
JAAS8033	CAATATGGATAAAGGTCAATTCCTTTT	GGGAAAATGGAGTTTGAGG
JAAS8034	TGACAAGAAATTCGGCAGTG	TGTCCAAAACACATGCTCGT
JAAS8036	TAGTTTGTTCCTCACGTCG	CGAATCGAGTTTTGCTCACC
JAAS8037	TGGTGTAGTTTAACCGTGCAA	TGATCGACTGATTCGACCTG
JAAS8040	CACATCATCAACCCATACTATGCT	TGAACTAAACACCTATTCACCTGC
JAAS8084	TGGCATAATAATGTCAAACCTTTT	TAAATCATTGCCTGGGCTTC
JAAS8099	TTCGGATAGGTCCGAAAGTG	ATGTTGCTTCACATCCAAGC
JAAS8103	CCTGCTGGTTTTTATGGCA	TCATTTGAAAAGGGAGCCA
JAAS8104	TTGTGGTGC GGTTTGTATGT	TGACAATTTTAAGTAAAGAGAGCAAG
JAAS8116	TCTCTTTCTTTCGCCTTGGGA	GTGCCCAGCAATATCGTTTT
JAAS8125	TGACTTTGCCTTATTTCCGC	ACACGTGACTGTGTGCTCGT
JAAS8129	TGCATGTCACAATCCTTGAC	TTTCTTGGTTAAGGCCAAGG
JAAS8143	CTGTACACGACTCTCCGCAA	GGGATAGCATCAGTTAAGCAGC
JAAS8144	AAATGGACCAAGTTGCTGCT	TGCCCAACTTGAGCTTGAAT
JAAS8157	GTGGGACCTTTGCTTTTGAA	TTTGGGGTCAAGTTTTGATTC
JAAS8164	GCCCATGCTCACCTCTAGTC	TGGAAGGGAAACAAACATGA

Supplemental Table 32. Summary of RNA-Seq data for CSSL13, CSSL59, and Su8289.

Sample	Raw reads	Clean reads	Clean base (Gb)	Error rate (%)	Q20 (%)	Q30 (%)	GC content (%)
CSSL13_20d_1	22,418,501	21,680,087	6.50	0.03	97.95	93.95	44.87
CSSL13_20d_2	26,870,022	26,001,940	7.80	0.03	98.00	94.09	44.68
CSSL13_20d_3	20,963,564	20,227,253	6.07	0.02	98.05	94.19	44.73
CSSL59_20d_1	25,673,966	24,568,436	7.37	0.03	97.95	93.73	44.54
CSSL59_20d_2	27,648,078	26,755,427	8.03	0.03	97.88	93.59	44.64
CSSL59_20d_3	25,127,994	23,966,272	7.19	0.03	98.05	93.95	44.74
Su8289_20d_1	26,678,116	25,693,401	7.71	0.03	97.91	93.65	44.75
Su8289_20d_2	22,309,720	21,487,496	6.45	0.03	97.92	93.69	45.02
Su8289_20d_3	31,491,960	30,147,965	9.04	0.03	98.00	93.81	46.11

Supplemental Table 33. The annotation and expression level of 12 genes at 20 DPA fibers in CSSL13, CSSL59, and Su8289. (included as a separate EXCEL file).

Supplemental Table 34. The sequence variants of nine genes between between *G. hirsutum* A₁-subgenome and *G. anomalum*. (included as a separate EXCEL file).

Supplemental Table 35. The qRT-PCR primers for nine candidate genes on the *qFS11* interval JAAS8037–JAAS8040.

Gene ID	Forward PCR primer (5'–3')	Reverse PCR primer (5'–3')
<i>Goano11G3880</i>	GATAAATTGGAGAAAGGAGGAA	TAAGAAGCAAACAAAGTAGGAA
<i>Goano11G3883</i>	AGATGATGGCAAGATAGATGA	TTCCTCTAACTGTTCTGCTTA
<i>Goano11G3885</i>	CTAAGTTTCCTTCTTCTCAAATG	ACTAGATATACGAGATAAGATGCT
<i>Goano11G3886</i>	AGATACGTTCTCAATCTTCAAT	TAAACATAACCTGTCTCCTCTA
<i>Goano11G3887</i>	GAAGATGAAAGGGAAATGTGTA	CAAGCGGATTCAAAGAAATTC
<i>Goano11G3888</i>	AAGATATGAGGTATGGCAAGAA	GTGTTTGTAGTACGAACTCTATG
<i>Goano11G3897</i>	CGGAATAGGGTTAAGTAAATCTTT	ATTGGAACAGCATAGCTCTAAA
<i>Goano11G3907</i>	ACCAGATGTCTCAGATAGAA	CTGTAGTTGGAGTTCGTTAT
<i>Goano11G3918</i>	ATAGCAAATGAATTGATCCATTC	CCATCTTGATTAACACTAACTCTA

Supplemental Table 36. The PCR primers of *Goano11G3883* and *GH_A11G3315* in CSSL59 and Su8289, respectively.

Gene ID	Sample	Forward PCR primer (5'–3')	Reverse PCR primer (5'–3')
<i>Goano11G3883</i>	CSSL59	AGAGGGTTGTATCAAACATCGTG	CTCTAACTGTTCTGCTTAGCGTTT
<i>GH_A11G3315</i>	Su8289	TGATGGCAAACGGTCACAGAGTA	CTCTAACTGTTCTGCTTAGCGTTT

Supplemental Table 37. The 130 *G. anomalum*-specific SSR markers for detecting recombinant individuals.

Chr.	SSR marker
Chr.01	JAAS1098, JAAS0006, NAU3690, NAU3615, JAAS1148, NAU2182, NAU5100, NAU3714, NAU2083, JAAS0392, JAAS3221
Chr.02	NAU2929, JAAS1489, NAU5421, NAU1190, JAAS0426, NBRI0092, JAAS2050, NAU3820, HAU1219
Chr.03	NAU2908, NAU1072, JAAS2579, JAAS4015, NAU895, NAU1167, JAAS4003, JAAS0861, JAAS4512, NAU3083
Chr.04	JAAS5943, JAAS5256, NAU2120, JAAS2076, NAU3508, JAAS2022, JAAS2977, DPL494, JAAS2662
Chr.05	JAAS0803, JAAS4908, JAAS1953, JAAS4815, DC40130, NAU3650, NAU5273, HAU1248, NAU911, JAAS3432, JAAS2949, JAAS0657
Chr.06	NAU2714, NAU4969, DPL101, JAAS6138, JAAS2590, NAU905, DPL365, NAU2397, JAAS6227, NBRI3941
Chr.07	JAAS4754, JAAS2966, NAU2686, NAU4956, NBRI0047, NAU1305, JAAS5041, JAAS0945
Chr.08	JAAS0199, JAAS1049, JAAS3476, JAAS4458, JAAS4933, JAAS4907, JAAS5813, JAAS5861, NAU1037, NAU1262, NAU1322, NAU2169, JAAS6420, NAU2914
Chr.09	JAAS3113, NAU3100, JAAS2010, JAAS5567, JAAS5248, JAAS4094, JAAS2567, JAAS0163, JAAS1469, JAAS0125, JAAS1923
Chr.10	JAAS1256, JAAS3070, NAU4881, NAU1236, JAAS2768, CGR6110, JAAS0321
Chr.11	NAU5192, JAAS4259, JAAS2330, JAAS3310, JAAS3820, JAAS3088, NAU1063, JAAS1048, NAU3703, JAAS0852, NAU2152, JAAS4829
Chr.12	NAU3109, NAU1274, NAU1119, JAAS2266, NAU3294, JAAS6372, JAAS4943, JAAS3735, JAAS6269
Chr.13	JAAS2956, JAAS3946, JAAS6264, JAAS5724, NAU2697, NAU3398, NBRI0431, NBRI0978

REFERENCES

- Chen, Z.J., Sreedasyam, A., Ando, A., Song, Q.X., De Santiago, L.M., Hulse-Kemp, A.M., Ding, M.Q., Ye, W.X., Kirkbride, R.C., Jenkins, J., et al. (2020). Genomic diversifications of five *Gossypium* allopolyploid species and their impact on cotton improvement. *Nat. Genet.* **52**:525-533. 10.1038/s41588-020-0614-5.
- Deng, X., Gong, J., Liu, A., Shi, Y., Gong, W., Ge, Q., Li, J., Shang, H., Wu, Y., and Yuan, Y. (2019). QTL mapping for fiber quality and yield-related traits across multiple generations in segregating population of CCRI 70. *J. Cotton Res.* **2**:13. 10.1186/s42397-019-0029-y.
- Diouf, L., Magwanga, R.O., Gong, W., He, S., Pan, Z., Jia, Y.H., Kirungu, J.N., and Du, X. (2018). QTL mapping of fiber quality and yield-related traits in an intra-specific upland cotton using genotype by sequencing (GBS). *Int. J. Mol. Sci.* **19**:441. 10.3390/ijms19020441.
- Guo, Y., Guo, X., Wang, F., Wei, Z., Zhang, S., Wang, L., Yuan, Y., Zeng, W., Zhang, G., Zhang, T., et al. (2014). Molecular tagging and marker-assisted selection of fiber quality traits using chromosome segment introgression lines (CSILs) in cotton. *Euphytica.* **200**:239-250. 10.1007/s10681-014-1150-0.
- Huang, C., Shen, C., Wen, T., Gao, B., Zhu, D., Li, X., Ahmed, M.M., Li, D., and Lin, Z. (2018). SSR-based association mapping of fiber quality in upland cotton using an eight-way MAGIC population. *Mol. Genet. Genomics.* **293**:793-805. 10.1007/s00438-018-1419-4.
- Jamshed, M., Jia, F., Gong, J., Palanga, K.K., Shi, Y., Li, J., Shang, H., Liu, A., Chen, T., Zhang, Z., et al. (2016). Identification of stable quantitative trait loci (QTLs) for fiber quality traits across multiple environments in *Gossypium hirsutum* recombinant inbred line population. *BMC Genomics.* **17**:197. 10.1186/s12864-016-2560-2.
- Jia, X., Wang, H., Pang, C., Ma, Q., Su, J., Wei, H., Song, M., Fan, S., and Yu, S. (2018). QTL delineation for five fiber quality traits based on an intra-specific *Gossypium hirsutum* L. recombinant inbred line population. *Mol. Genet. Genomics.* **293**:831-843. 10.1007/s00438-018-1424-7.
- Lacape, J., Nguyen, T., Courtois, B., Belot, J., Giband, M., Gourlot, J., Gawryziak, G., Roques, S., and Hau, B. (2005). QTL analysis of cotton fiber quality using multiple *Gossypium hirsutum* × *Gossypium barbadense* backcross generations. *Crop Sci.* **45**:123-140. 10.2135/cropsci2005.0123a.
- Li, C., Yu, H., Li, C., Zhao, T., Dong, Y., Deng, X., Hu, J., Zhang, Y., Zhang, F., Daud, M.K., et al. (2018). QTL mapping and heterosis analysis for fiber quality traits across multiple genetic populations and environments in upland cotton. *Front. Plant Sci.* **9**:1364. 10.3389/fpls.2018.01364.
- Liu, R., Gong, J., Xiao, X., Zhang, Z., Li, J., Liu, A., Lu, Q., Shang, H., Shi, Y., Ge, Q., et al. (2018). GWAS analysis and QTL identification of fiber quality traits and yield components in upland cotton using enriched high-density SNP markers. *Front. Plant Sci.* **9**:1067. 10.3389/fpls.2018.01067.
- Ma, L., Zhao, Y., Wang, Y., Shang, L., and Hua, J. (2017). QTLs analysis and validation for fiber quality traits using maternal backcross population in Upland cotton. *Front. Plant Sci.* **8**:2168. 10.3389/fpls.2017.02168.
- Rong, J., Feltus, F.A., Waghmare, V.N., Pierce, G.J., Chee, P.W., Draye, X., Saranga, Y., Wright, R.J., Wilkins, T.A., May, O.L., et al. (2007). Meta-analysis of polyploid cotton QTL shows unequal contributions of subgenomes to a complex network of genes and gene clusters implicated in lint fiber development. *Genetics.* **176**:2577-2588. 10.1534/genetics.107.074518.
- Saranga, Y., Jiang, C.X., Wright, R.J., Yakir, D., and Paterson, A.H. (2004). Genetic dissection of cotton physiological responses to arid conditions and their inter-relationships with productivity. *Plant, Cell Environ.* **27**:263-277. 10.1111/j.1365-3040.2003.01134.x.
- Shang, L., Wang, Y., Wang, X., Liu, F., Abduweli, A., Cai, S., Li, Y., Ma, L., Wang, K., and Hua, J. (2016). Genetic analysis and stable QTL detection on fiber quality traits using two recombinant inbred line populations and their backcross progeny in upland cotton. *G3 (Bethesda).* **6**:2717-2724. 10.1534/g3.116.031302.
- Shapley, Z.W., Jenkins, J.N., Zhu, J., and McCarty, J.C. (1998). Quantitative trait loci associated with agronomic and fiber traits of upland cotton. *J. Cotton Sci.* **2**:153-163.
- Shen, X., Guo, W., Zhu, X., Yuan, Y., Yu, J., Kohel, R., and Zhang, T. (2005). Molecular mapping of QTLs for fiber qualities in three diverse lines in Upland cotton using SSR markers. *Mol. Breeding.* **15**:169-181. 10.1007/s11032-004-4731-0.

- Tang, S., Teng, Z., Zhai, T., Fang, X., Liu, F., Liu, D., Zhang, J., Liu, D., Wang, S., Zhang, K., et al.** (2015). Construction of genetic map and QTL analysis of fiber quality traits for Upland cotton (*Gossypium hirsutum* L.). *Euphytica*. **201**:195-213. 10.1007/s10681-014-1189-y.
- Tan, Z., Zhang, Z., Sun, X., Li, Q., Sun, Y., Yang, P., Wang, W., Liu, X., Chen, C., Liu, D., et al.** (2018). Genetic map construction and fiber quality QTL mapping using the CottonSNP80K array in upland cotton. *Front. Plant Sci.* **9**:225. 10.3389/fpls.2018.00225.
- Wang, B., Guo, W., Zhu, X., Wu, Y., Huang, N., and Zhang, T.** (2007). QTL mapping of yield and yield components for elite hybrid derived-RILs in upland cotton. *J. Genet. Genomics*. **34**:35-45. 10.1016/S1673-8527(07)60005-8.
- Wang, H., Huang, C., Guo, H., Li, X., Zhao, W., Dai, B., Yan, Z., and Lin, Z.** (2015). QTL mapping for fiber and yield traits in upland cotton under multiple environments. *PLoS One*. **10**:e0130742. 10.1371/journal.pone.0130742.
- Wang, H., Jin, X., Zhang, B., Shen, C., and Lin, Z.** (2015). Enrichment of an intraspecific genetic map of upland cotton by developing markers using parental RAD sequencing. *DNA Res.* **22**:147-160. 10.1093/dnares/dsu047.
- Wang, M., Tu, L., Yuan, D., Zhu, D., Shen, C., L, J., Liu, F., Pei, L., Wang, P., Zhao., G., et al.** (2019). Reference genome sequences of two cultivated allotetraploid cottons, *Gossypium hirsutum* and *Gossypium barbadense*. *Nat. Genet.* **51**:224-229. 10.1038/s41588-018-0282-x.
- Yu, J., Zhang, K., Li, S., Yu, Y., Zhai, H., Wu, M., Li, X., Fan, S., Song, M., Yang, D., et al.** (2013). Mapping quantitative trait loci for lint yield and fiber quality across environments in a *Gossypium hirsutum* × *Gossypium barbadense* backcross inbred line population. *Theor. Appl. Genet.* **126**:275-287. 10.1007/s00122-012-1980-x.
- Yu, J.Z., Ulloa, M., Hoffman, S.M., Kohel, R.J., Pepper, A.E., Fang, D.D., Percy, R.G., and Burke, J.J.** (2014). Mapping genomic loci for cotton plant architecture, yield components, and fiber properties in an interspecific (*Gossypium hirsutum* L. × *G. barbadense* L.) RIL population. *Mol. Genet. Genomics*. **289**:1347-1367. 10.1007/s00438-014-0930-5.
- Zhang, K., Zhang, J., Ma, J., Tang, S., Liu, D., Teng, Z., Liu, D., and Zhang, Z.** (2012). Genetic mapping and quantitative trait locus analysis of fiber quality traits using a three-parent composite population in upland cotton (*Gossypium hirsutum* L.). *Mol. Breeding*. **29**:335-348. 10.1007/s11032-011-9549-y.
- Zhang, S., Feng, L., Xing, L., Yang, B., Gao, X., Zhu, X., Zhang, T., Zhou, B. and Jenkins, J.** (2016). New QTLs for lint percentage and boll weight mined in introgression lines from two feral landraces into *Gossypium hirsutum* acc TM-1. *Plant Breed.* **135**:90-101. 10.1111/pbr.12337.
- Zhang, Z., Ge, Q., Liu, A., Li, J., Gong, J., Shang, H., Shi, Y., Chen, T., Wang, Y., Palanga, K.K, et al.** (2017). Construction of a high-density genetic map and its application to QTL identification for fiber strength in upland cotton. *Crop Sci.* **57**:774-788. 10.2135/cropsci2016.06.0544.